Universidade de Lisboa

Faculdade de Farmácia

Disentangling the role of *Limosilactobacillus reuteri* D-lactate in lipid metabolism

"Confidencial"

Brian Nathan Saavedra Romero

Dissertation supervised by Dr. André Fernando Anastácio dos Santos and co-supervised by Professor Cecília Maria Pereira Rodrigues

Master course in Biopharmaceutical Sciences

2022

Universidade de Lisboa

Faculdade de Farmácia

Disentangling the role of *Limosilactobacillus reuteri* D-lactate in lipid metabolism

"Confidencial"

Brian Nathan Saavedra Romero

Dissertation supervised by Dr. André Fernando Anastácio dos Santos and co-supervised by Professor Cecília Maria Pereira Rodrigues

Master course in Biopharmaceutical Sciences

2022

Part of the results discussed in this thesis was presented in the following scientific meetings:

B. Romero, D. Pires, C.M.P. Rodrigues, and A. Santos. "Exploring the role of bacterial D-lactate in lipid metabolism". 1st edition of *Jornadas Científicas da ULisboa*. "A agenda 2030 para o Desenvolvimento Sustentável". June 28th, 2022. [ePoster presentation]

B. Romero, D. Pires, C.M.P. Rodrigues, and A. Santos. "Disentangling the role of *Limosilactobacillus reuteri* D-lactate in lipid metabolism". *13th iMed.ULisboa Postgraduate Students Meeting*. July 4th-5th, 2022. [Poster presentation]

This work was developed at the Research Institute for Medicines (iMed.ULisboa), Faculty of Pharmacy, University of Lisbon, and received funding support from PTDC/MED-FAR/3492/2021, CEECIND/04663/2017, and EXPL/MED-OUT/0688/2021 from Fundação para a Ciência e a Tecnologia (FCT).

ABSTRACT

Non-alcoholic fatty liver disease (NAFLD) comprises a wide spectrum of liver alterations from simple steatosis to hepatocellular carcinoma. Due to a westernized diet, NAFLD is becoming the most common chronic liver disease and its association with gut microbiota dysbiosis has been demonstrated. Currently, there is increasing interest in the use of probiotics to alleviate NAFLD outcomes. We have recently shown that mice supplemented with the probiotic *Limosilactobacillus reuteri* (*L. reuteri*) were protected from liver disease, partially via D-lactate production. Given the ability of *L. reuteri* to modulate gut homeostasis and dysbiosis, we hypothesized that its principal metabolite D-lactate may directly modulate liver lipid metabolism to ameliorate NAFLD. Firstly, we confirmed by GC-MS that Lactate is a major metabolite produced by *L. reuteri*. Subsequently, we aimed to unveil the role of D-lactate in hepatocyte and macrophage lipid metabolism and inflammation by exposing hepatocytes and macrophages to sodium palmitate (PA) 125 µM in the presence/absence of sodium D-Lactate or L-Lactate (control) 1 and 5 mM. Since both D- and L-lactate might share the same metabolic pathway, we silenced *D-ldh* gene expression in hepatocytes. We next assessed mRNA levels of genes related to fatty acid uptake (*Cd36* and *Cpt1*), lipid biosynthesis (*Lxr, Srebp1c*, *Chrebp*, *Acc1*, *Fasn*, *Dgat2*, and *Pparγ*), mitochondrial fission (*Fis1* and *Drp1*) and fusion (*Mfn2* and *Opa1*), and inflammation (*IL-8, Tnf-α,* and *Tgf-β*). The results showed that modulation with both concentrations of D-lactate reduced significantly mRNA expression levels of *Cd36, Cpt1, Srebp1c, Dgat2*, and *Pparγ* in PA-treated hepatocytes, but only mRNA expression of *Pparγ* in PA-treated macrophages. Further, protein production in hepatocytes was confirmed for CD36, CPT1, MFN2, and DRP1 by Western blot. In addition, a Nile Red assay demonstrated that D-lactate but not L-lactate protected against lipid accumulation. Moreover, we showed that the protective effect of D-lactate might be linked, in part, to the PDK4 pathway, as well as to cholesterol and/or PPARγ signalling. In conclusion, understanding the metabolic pathways behind D-lactate modulation in hepatocyte and macrophage response to lipid accumulation may unveil the role of *L. reuteri* in NAFLD improvement. We provide new insights into how microbiota-derived metabolites affect host metabolic homeostasis, focusing on the role of D-lactate in the regulation of liver metabolism while hinting at novel therapeutics.

Keywords: NAFLD; microbiota: *Limosilactobacillus reuteri*; D-lactate; *D-ldh*.

RESUMO

A doença de fígado gordo não alcoólico (do inglês NAFLD) compreende um amplo espectro de alterações hepáticas desde esteatose simples até carcinoma hepatocelular. Devido à globalização de uma dieta ocidentalizada, a NAFLD tornou-se a doença hepática crónica mais comum, tendo sido associada à disbiose da microbiota intestinal. Probióticos são bactérias com a capacidade de restaurar a homeostasia intestinal do hospedeiro, tendo o seu efeito benéfico já sido demonstrado no alívio da NAFLD. Recentemente mostrámos que ratinhos suplementados com *Limosilactobacillus reuteri* (*L. reuteri*) apresentam menor progressão da doença hepática num modelo de lesão hepática, em parte através da produção de D-lactato. Neste projeto, dada a capacidade de *L. reuteri* modular a doença hepática, prevemos que o metabolito D-lactato possa regular diretamente o metabolismo hepático, melhorando a patologia da NAFLD. Após confirmação de que o Lactato é o principal metabolito produzido por *L. reuteri*, determinámos a eficácia do D-lactato em modular o metabolismo lipídico e a inflamação em testes *in vitro* com linhas celulares de hepatócitos e macrófagos. Estas foram expostas a palmitato de sódio (PA) 125 µM na presença/ausência de 1 e 5 mM de D-lactato ou L-lactato (controlo). Uma vez que D- e L-lactato podem participar na mesma via metabólica, também silenciámos a expressão do gene D-lactato desidrogenase (*D-ldh*) nos hepatócitos e avaliámos os níveis de mRNA de genes relacionados com transporte de ácidos gordos (*Cd36* e *Cpt1*), biossíntese de lipídios (*Lxr*, *Srebp1c*, *Chrebp*, *Acc1*, *Fasn*, *Dgat2* e *Pparγ*), fissão e fusão mitocondrial (*Fis1*, *Drp1*, *Mfn2* e *Opa1*) e inflamação (*IL-8*, *Tnf-α*, e *Tgf-β*). Nos hepatócitos tratados com PA, o D-lactato reduziu significativamente os níveis de expressão de mRNA de *Cd36*, *Cpt1*, *Srebp1c*, *Dgat2* e *Pparγ*, bem como os níveis das proteínas CD36, CPT1, MFN2 e DRP1. Já nos macrófagos tratados com PA, o D-lactato afetou significativamente os níveis do mRNA de Pparγ. Por fim demonstrámos fenotipicamente que o D-lactato tem um efeito protetor contra a acumulação de lípidos nos hepatócitos. Assim, demonstrámos também que, o efeito protetor do D-lactato poderá estar relacionado com via de sinalização PDK4, colesterol e/ou o PPARγ. Desta forma, entender as vias metabólicas por trás da modulação do D-lactato na resposta de hepatócitos e macrófagos na acumulação de lípidos é essencial para desvendar o papel de *L. reuteri* na melhoria da NAFLD. Este trabalho expande o conhecimento sobre a forma como os metabolitos derivados da microbiota afetam a homeostasia metabólica do hospedeiro, destacando-se o papel do D-Lactato na regulação do metabolismo hepático, sugerindo novas abordagens terapêuticas.

Palavras-chave: DFGNA; microbiota: *Limosilactobacillus reuteri*; D-lactato; *D-ldh*.

ACKNOWLEDGMENTS

Em primeiro lugar quero agradecer a toda a equipa do laboratório "Cell function and therapeutic targeting" do iMED envolvida neste projeto, quer na parte experimental quer no feedback e dicas que me brindaram ao longo da sua realização. Principalmente, agradeço ao meu orientador o Dr. André Santos e à minha coorientadora a Prof. Dra. Cecília Rodrigues. Também agradeço ao Dr. David Pires, pelas ideias propostas e pelo tempo dedicado ao projeto. Igualmente um agradecimento ao grupo da Prof. Dra. Isabel Tavares de Almeida pelo apoio nas experiências relacionadas à cromatografia gasosa. Muito obrigado àqueles que foram os meus mestres no laboratório, Miguel Pinheiro, Vanda Marques, Marta Afonso e André Simão. Vocês sempre tiveram tempo disponível para resolver as minhas dúvidas e para me explicar com muita paciência as técnicas e a teoria detrás delas. Os momentos que passei ao lado de toda a equipa jamais serão esquecidos. Obrigado por me acompanharem nesta jornada!

Quero deixar uma mensagem de gratidão com muito carinho à Prof. Dra. Cecília já que sem o seu apoio e orientação eu não teria sido parte do seu maravilhoso grupo de investigação. Professora, muito obrigado por esta oportunidade e por acreditar em mim. Além, agradeço-lhe por nos motivar sempre e por aumentar em nós a vontade de darmos o nosso melhor em tudo o que fazemos. A professora para mim é um grande exemplo e inspiração.

Toda a aprendizagem que obtive ao longo deste percurso deixa-me muito satisfeito. Isto não teria sido possível sem a sua paciência e dedicação Exmo. Sr. Prof. Dr. André Fernando Anastácio dos Santos. Foi desafiante aprender a trabalhar contigo, mas acho que ao final conseguimos encontrar um equilíbrio no qual os dois estivéssemos a aprender e desfrutar do que fazíamos em equipa. Com certeza que toda a tua energia levar-te-á ainda mais longe. A tua paixão pelo que fazes e a tua maneira de transmitir o conhecimento é de admirar. O meu mais sincero agradecimento por tudo o que implicou ser parte da tua equipa de trabalho. Fico muito orgulhoso de ter participado neste o teu mundo da microbiota!

Com tudo o meu coração agradeço infinitamente aos meus pais portugueses, Dona Rosa e Luís Venâncio. Sem o seu carinho, preocupação e apoio eu teria demorado mais em atingir este objetivo e não o estaria a fazer desta maneira tão incrível. Vocês são e serão sempre um exemplo para mim, muito obrigado por me fazerem parte da sua família e por não me

deixarem nunca sozinho nos maus momentos. A minha família no México e eu vamos estar sempre agradecidos convosco.

A mi familia de México, les agradezco el amor y apoyo incondicional, son un pilar fundamental en mi vida y una parte importante en mis ganas de seguir cumpliendo mis metas. A mi mamá, a mis abuelos, a mis hermanos y hermana, a mis padrinos América y Chapo, muchas gracias por todo. Principalmente por el amor y motivación que siempre me han dado, y por recordarme siempre que están conmigo en cada camino que yo decida seguir. La distancia nos ha impedido un abrazo, un beso, una caricia, pero el amor siempre va a permanecer. Estoy muy orgulloso de cada uno de ustedes, vamos a seguir demostrando que los mexicanos somos bien chingones.

Agradezco a mis amigos de México que siempre me han apoyado y que a pesar de la distancia siempre se han preocupado por mí y se toman el tiempo para escuchar mis audios eternos de WhatsApp. Muchas gracias Andrea L. Rivera, Maggie Lanuza, Selene Villaseñor, Rosa Barrera, Julieta Badillo, Ximena, Citlali, Majo, Israel, Emmanuel Ledesma, Josselyn ¡Los amo un chingo! Siempre tendrán un lugar en mi corazón.

Aos meus colegas do laboratório que se tornaram nos meus amigos: Jan, Gonçalo, CardyA, Daria e Inês. Admiro-vos muito e estou super orgulhoso de vocês. Obrigado também por me ajudarem com as minhas dúvidas durante as experiências e por partilhar ideias que pudessem enriquecer o meu projeto. Além, fico muito contente de ter partilhado momentos convosco para além do trabalho no laboratório, aqueles jantarinhos e conversas a rir! Nunca me vou esquecer do show da Mônica! A vossa amizade é uma das melhores coisas que me deixa o mestrado e espero que se possa fortalecer ainda mais.

To my Italian artist Nicole Alesina! My partner in crime in the lab, thank you very much for listening to me and for worrying about my well-being, always pushing me for being better not only at work but also as a human being. I appreciated a lot all your kind words. I told you several times that you made me recover the light and energy that I had lost during my time in Portugal, I'm grateful to have met you.

¡Agradezco también a mi querida amiga Ana Villasana! Que suerte haber encontrado a una latinoamericana dentro del grupo, tuvimos una conexión especial desde el primer día. ¡Te quiero mucho Ana! A ti y a tu hermosa familia ¡Gracias por tu apoyo durante todo el primer año del curso!

A ti Rocío, me siento privilegiado de haberte conocido dentro del equipo del Dr. Santos. Gracias por tu cariño y motivación cuando estábamos juntos en el laboratorio. Por llevarme a almorzar con ustedes, aunque yo no quería porque era muy temprano. Tu alegría le dio un toque especial al grupo. Fue poco el tiempo que convivimos, pero tu amistad ha sido también un gran regalo que la maestría me ha dejado.

Estaré también siempre agradecido con la ex familia de Giant Creations ya que sin su comprensión y flexibilidad yo no habría podido cumplir con lo que la maestría me estaba exigiendo. Fue un grande desafío trabajar y estudiar al mismo tiempo, el apoyo y paciencia de ustedes me permitió culminar exitosamente esta fase profesional en mi vida. Muchas gracias Tani, David, Flavia, Marco, Ana Beatriz, Analys, Jeff y Myriam.

Por outro lado, quero agradecer à família Cunha Coelho e à minha querida amiga Julia pelo carinho, atenção e bons momentos que partilhámos até agora. Obrigado por me receberem sempre com muito carinho na sua família.

Tiago, em 2017 eu escrevia nos agradecimentos da minha tese de licenciatura “Este trabalho significa um passo mais para estar ao teu lado” Lembras-te? E 2 anos depois começávamos a nossa nova aventura juntos em Portugal. Hoje, agradeço-te pela paciência e motivação, por me dizeres sempre que sou o melhor para ti, pelo teu amor e dedicação neste crescimento mútuo. Não sabemos como será o futuro e como será a nossa história. No entanto, neste momento o que mais se passa pela minha mente é que este trabalho é uma prova de que não nos podemos esquecer dos nossos sonhos. Ainda que nalguns momentos achemos que o mundo e os outros são mais fortes, o segredo é não desistir. Ao final todo esforço e sacrifício tem a sua recompensa. Estou muito orgulhoso de mim e de ti, do que temos conseguido individualmente e em equipa. Muito obrigado Titão!

Eu não imaginava que a minha vida pudesse ser ainda mais extraordinária. Qualquer que seja o destino hoje é para vos dizer… muito obrigado a todos! Desejo-vos muito sucesso nos novos desafios!

Con mucho cariño para todos,

Brian Nathan.

LIST OF ABBREVIATIONS

ACC- Acetyl-CoA carboxylase

ACLY- ATP citrate lyase

ACOT12- Acyl-CoA thioesterase

ACSS- Acetyl-CoA synthetase

Ahr- Aryl hydrocarbon

AMPK- Monophosphate-activated protein kinase

AMPs- Antimicrobial peptides

APOB- Apolipoprotein B

BA- Bile Acids

CCL2- CC- chemokine ligand 2

CCR2- Chemokine receptor 2

ChREBP- Carbohydrate-responsive element-binding protein

CPT1- Carnitine palmitoyltransferase-1

DAG- Diacylglycerol

DGAT- Diglyceride acyltransferase

D-LDH- D-lactate dehydrogenase

DNL- De novo lipogenesis

DRP1- Dynamin-related protein 1

FAs- Fatty acids

FASN- Fatty acid synthase

FAT/CD36- Fatty acid translocase/ cluster of differentiation 36

FFAs- Free fatty acids

FGF19- Fibroblast growth factor transcription 19

FIS1- Fission protein 1

FMT- Faecal microbial transplantation

FXR- Farnesoid X receptor

GF- Germ-free

Glo- Glyoxalase

GLP-1R- Glucagon-like peptide-1 receptor

GPR43- G-protein-coupled receptor 43

GSH- Glutathione

HCC- Hepatocellular carcinoma

HDAC- Histone deacetylase

HFD- High-fat diet

HIF1- Hypoxia-inducible factor 1

HSCs- Hepatic stellate cells

IECs- Intestinal epithelial cells

IL- Interleukin

IMP- Imidazole propionate

IRS- Insulin receptor

KCs- Kupffer cells

LAB- Lactic acid bacteria

LCD- Lactoyl CoA dehydratase

LCFAs- Long-chain fatty acids

LDs- Lipid droplets

LPS- Lipopolysaccharides

LXR- Liver X receptor

MAFLD- Metabolic-associated fatty liver disease

MAMPs- Microbe-associated molecular patterns

MCD- methionine choline-deficient

Me2- Malic enzyme 2

MFN2- Mitofusin 2

MG- Methylglyoxal

MTTP- Microsomal triglyceride transfer protein

MUC2- Mucin

NAFLD- Non-alcoholic fatty liver disease

NASH- Non-alcoholic steatohepatitis

NEFA- Non-esterified fatty acids

NF-kB- Nuclear factor-κB

OA- Oleic acid

OAA- Oxaloacetate

Ocln- Occludins

OMM- Outer mitochondrial membrane

OPA1- Optic atrophy 1

PA- Palmitic acid

PAMPs- Pathogen-associated molecular patterns

PDH- Pyruvate dehydrogenase

PDK- Pyruvate dehydrogenase kinase.

PKC- Protein kinase C

PLA2- Protein phospholipase-A2

PLIN- Prepilin protein

PPAR- Proliferator-activated receptors

RNS- Reactive nitrogen species

ROS- Reactive oxygen species

SCFAs- Short chain fatty acids

SLG- S-D-lactoglutathione

SREBP-1c- Sterol regulatory element-binding protein 1

T2DM- Diabetes type 2

TCA- Tricarboxylic acid cycle

TG- Triglycerides

TGF- Transforming growth factor-β

TGR5- Takeda G-protein coupled receptor 5

Th2- Type 2 helper T

TLR- Toll-like receptor

TMA- Trimethylamine

TNF- Tumour necrosis factor

Trp- Tryptophan

VLDL- Very low-density lipoprotein

WD- Western diet

Zo1- Zonula occludin 1

INDEX

INDEX OF FIGURES

INDEX OF TABLES

1 Introduction

1.1 Non-Alcoholic Fatty Liver Disease (NAFLD): What is it and why do we need to be concerned about it?

The liver is a pivotal organ responsible for an array of physiological processes that help to support metabolism, immunity, blood volume regulation, detoxification, vitamin storage, and lipid and cholesterol homeostasis among other functions (Trefts et al., 2017). Despite the progress in the understanding of liver metabolism, disease status and repair, liver pathologies continue to have significant global morbidity and mortality burdens (Trefts et al., 2017). In this context, non-alcoholic fatty liver disease (NAFLD) has emerged as a major cause of chronic liver disease worldwide, becoming a recurrent indication for liver transplantation in Europe and the USA (Geier et al., 2021; Lazarus et al., 2022). Recently, it has been proposed to rename NAFLD to MAFLD (Metabolic dysfunction associated fatty liver disease) to categorize more accurately patients who have liver disease and metabolic dysfunction simultaneously (Herman, 2021). For instance, a patient with hepatic steatosis in combination with obesity and/or diabetes type 2 (T2DM) has at least two metabolic risk factors. Thus, this new and inclusive definition excludes the "non-cause" of the disease and provides a more specific diagnosis. Nevertheless, researchers who detract from the change highlight that understanding the molecular basis of NAFLD heterogenicity would be more appropriate (Herman, 2021). Notwithstanding the nomenclature change proposal, our study will refer to the pathology as NAFLD, as the issue remains under international debate.

NAFLD is characterized by an accumulation of triglyceride lipid droplets in liver cells (>5% of liver weight) caused by a disruption in lipid metabolism (X. Li & Wang, 2020). The increase of intrahepatic fatty acids (FAs) may lead to cell damage and inflammation, promoting fatty liver disease progression from simple steatosis (NAFL) to non-alcoholic steatohepatitis (NASH). Consecutively, NASH can progress to cirrhosis and hepatocellular carcinoma (HCC), the fourth-leading cause of cancer death worldwide (D. Q. Huang et al., 2021). Strikingly, the widespread presence of NAFLD is approximately 25% in adults (D. Q. Huang et al., 2021), with may have an increase of around 21% in its prevalence from 2015 to 2030 (Estes, Razavi, et al., 2018). This contributed to predicting that NASH will have increment up to 63%. Thus, the global NAFLD prevalence rate in adults will reach 33.5%, whilst NASH will be around 27% by 2030 (Estes, Razavi, et al., 2018). In line with this model, other studies forecasted an increase of up to 56% in NASH prevalence by the year 2030 in France, Germany, Italy, Spain,

China, Japan, the UK, and the USA (Estes, Anstee, et al., 2018). Furthermore, the global burden of the disease encompasses also extensive economic implications. In general, the NAFLD-related annual cost reaches $103 billion in the USA and €35 billion in Europe (Younossi et al., 2019). Importantly, most economic costs associated with NAFLD are implicated in the latter stages of the disease (Lazarus et al., 2022). In addition, it is known that NASH implications are underestimated which means that the costs could be even higher (Geier et al., 2021). Therefore, there is a need for early intervention efforts through the development of profitable therapeutic strategies, which contribute to the reduction of the NAFLD overall burden.

NAFLD pathogenesis is particularly complex since its aetiology involves the interplay between genetics and environmental factors (Bessoneet al., 2019). The development of this condition is intimately driven by the Western diet (WD) coupled with reduced physical activity and exercise (Hallsworth & Adams, 2019). WD is characterized by excessive consumption of calorie-dense food enriched in simple carbohydrates and saturated fats. This diet highly impacts the gut microbiota by altering its function and diversity. The gut microbiota is a highly dynamic and complex consortium of microorganisms including bacteria, archaea, fungi, and viruses. Coexistence of these microorganisms in equilibrium is known as eubiosis, whereas an imbalance in this ecosystem is referred to as dysbiosis (R. Wang et al., 2021). Dysbiosis of the gut community leads to adverse effects on host homeostasis (Safari & Gérard, 2019; Sharpton et al., 2021). For instance, the gastrointestinal ecosystem can ameliorate or aggravate NAFLD through several mechanisms within the gut-liver axis. Particularly, the overall homeostasis of this hub can be affected by changes in intestinal permeability, alteration of energy harvesting capacity, and production of microbial products that can alter signalling pathways in the liver (Aron-Wisnewsky et al., 2020; Safari & Gérard, 2019; M. Yao et al., 2021).

In the absence of approved drug therapy, lifestyle interventions are key in the clinical management of NAFLD. Nevertheless, the long-term sustainability of these interventions is poor. Interestingly, modulation of the gut microbiota has emerged as a novel strategy to ameliorate the disease. There are different directions for this approach including antibiotics, dietary factors, faecal microbial transplantation (FMT), miRNA modulation, and supplementation with probiotics, prebiotics, synbiotics, or postbiotics (Bi et al., 2020; Sharpton et al., 2021). Strikingly, growing evidence has shown crosstalk between the host and a broad reservoir of microbial metabolites. Therefore, beyond the changes in bacteria phyla, gastrointestinal dysbiosis leads to an imbalance in microbiota-derivative metabolites production including Short Chain Fatty Acids (SCFAs), secondary bile acids (BA), indoles, trimethylamine (TMA), ethanol, and lactate, among others. These effectors may be involved in the regulation

of multiple pathways in the liver through the gut−liver axis as substrates or signal molecules (Fernandez-Cantos et al., 2021; J. Wu et al., 2021; M. Yang et al., 2021; X. Zhang et al., 2021).

1.2 The gut-liver axis: A playground for NAFLD

The liver communicates with the intestine by releasing primary BAs, which are synthesized from cholesterol, into the biliary tract and the systemic circulation. In the gut, the microbiota is responsible for deconjugate and dehydroxylate primary BAs to form secondary BA, which can be reabsorbed and brought back to the liver by the portal flow (Tripathi et al., 2018)(Figure 1), thus contributing to the maintenance of the BA pool homeostasis via activation of the farnesoid X receptor (FXR) and the membrane Takeda G-protein coupled receptor 5 (TGR5) (Chávez-Talavera et al., 2017; Dawson & Karpen, 2015). FXR activation in enterocytes induces fibroblast growth factor transcription (FGF19) that is released into the portal circulation and transported to the liver. In the liver, FGF19 contributes to modulating primary BA production (Figure 1). Moreover, FXR and TGR5 integrate the homeostatic control of lipids and glucose (Gillard et al., 2022). Therefore, an impairment in the BAs signalling is tightly related to NAFLD pathogenesis.

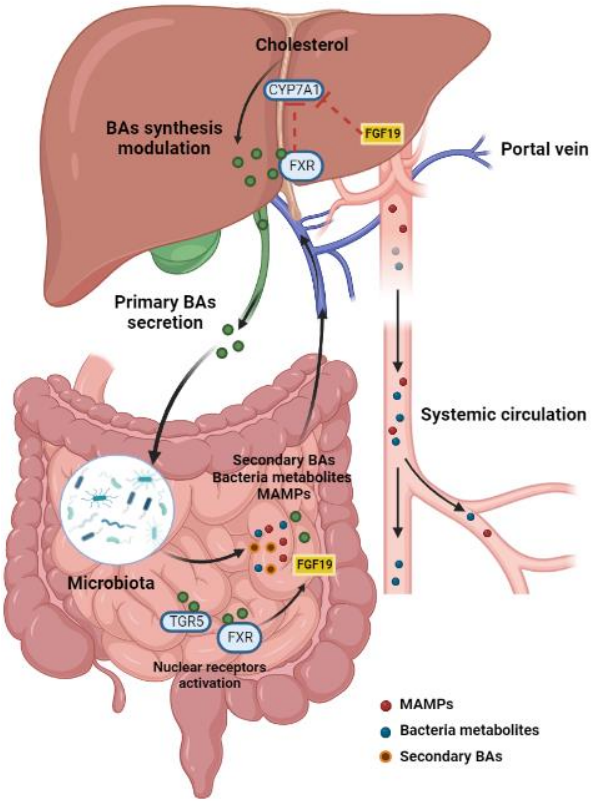

Figure 1. Gut-liver axis communication. Bile acids (BA) are synthesized from cholesterol in hepatocytes, secreted into the bile ducts and reach the intestine as conjugated primary BAs. In the gut, BAs interact with gut microbes and are converted into secondary BA. Moreover, BAs interact with cellular receptors such as Takeda G-protein-coupled receptor 5 (TGR5) and farnesoid X receptor (FXR). The binding of BA to FXR induces formation of fibroblast growth factor 19 (FGF-19), which serves as negative feed-back mechanism for BA synthesis in the liver. FGF-19 is secreted into the portal vein and proceeds to the liver, inhibiting hepatic bile acid synthesis via CYP7A1. Microbe-associated molecular patterns (MAMPs) and microbial metabolites can also reach the liver via the portal vein and influence liver function. Additionally, systemic circulation extends the gut-liver axis by transporting liver metabolites from dietary, endogenous, or xenobiotic substances to the intestine through the capillary system. Figure created with BioRender.

The intestinal mucosal barrier is a dynamic, stratified, and organized sieve that separates the resident microbes from the intestinal epithelial cells (IECs) (Figure 2). Importantly, the distribution of the epithelium has differences between the small and large intestine. In the small intestine, the epithelium extends over structures called villi, which are absent in the colon. The intestinal epithelium consists of cavities termed 'crypts of Lieberkühn' (Allaire et al., 2018). In this region, coexist multiple cell types with specialized functions. These IECs subtypes include enterocytes, goblet cells, paneth cells, brush cells, enteroendocrine cells, and stem cells (Allaire et al., 2018). Stem cells are located at the base of the crypts and give rise to several proliferative cells that differentiate and mature as they ascend through the transition zone, with the IECs eventually shedding into the lumen at the vertex of the crypts or villi (Allaire et al., 2018). Enterocytes are responsible for nutrient and water absorption whereas goblet cells sense the presence of bacterial products and secrete mucin (MUC2) contributing to the protective shield (Albillos et al., 2020). Paneth cells also contribute to the maintenance of the mucus layer by releasing antimicrobial peptides (AMPs), protecting nearby stem cells at the base of small intestinal crypts (Albillos et al., 2020; Hassan et al., 2020). Enteroendocrine cells are also secretory cells that produce several hormones and regulate gut physiology (Allaire et al., 2018). On the other hand, brush cells (also known as tuft cells) provide the epithelial source of IL-25. The production of IL-25 by injured epithelial cells is an important innate immune signal driving type 2 helper T (Th2) immune deviation in the subsequent adaptive immune response (Gerbe & Jay, 2016). Moreover, in specific areas of the epithelium, called Peyer's patches are localized specialized "M cells" that are capable of internalizing luminal antigens and presenting them to lymphocytes (Gerbe & Jay, 2016).

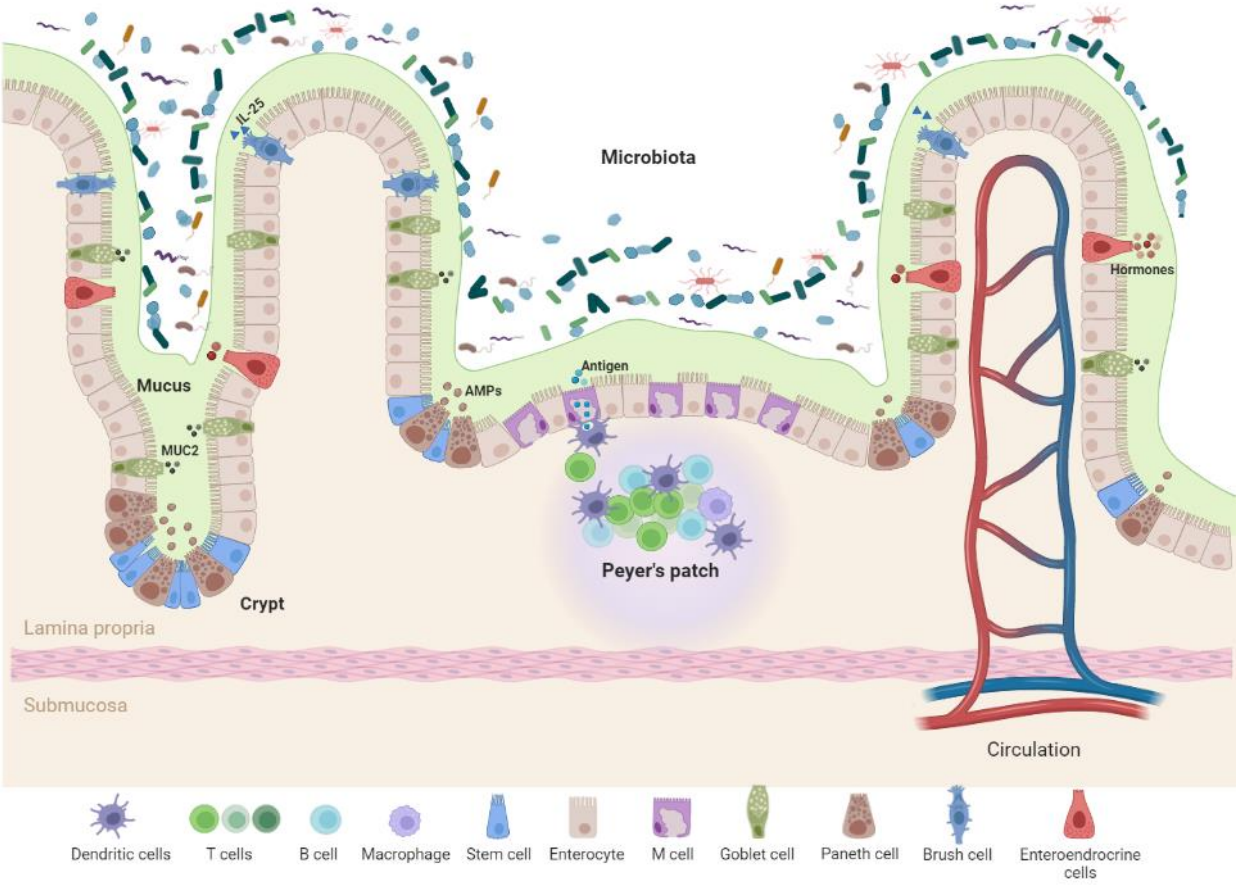

Figure 2. Small intestine barrier structure. Representative small intestinal epithelium. Enterocytes comprise the major cells type found in the crypt-villus axis and are capable of absorbing water and nutrients. Various secretory cells include goblet cells that secrete mucins, enteroendocrine cells that secrete hormones, and paneth cells that release antimicrobial factors to protect nearby stem cells at the base of small intestinal crypts. Brush cells are chemosensory cells and defence against parasites. M cells are localized to the follicle-associated epithelium overlying Peyer's patches and directly participate in antigen uptake and passage to underlying immune cells. Adapted from Allaire et al., 2018. Figure created with BioRender.

IECs are tightly attached to each other by junctional complexes such as desmosomes, tight and adherens junctions (Vancamelbeke & Vermeire, 2017). Tight junctions are a critical structure in restricting trans-epithelial permeability. Microbial signals, promote fortification of the epithelial barrier through upregulation of tight junctions and associated cytoskeletal proteins. The tight junctions consist of transmembrane proteins such as claudins and occludins, peripheral membrane proteins such as zonula occludens, and regulatory proteins. The adherens junctions are below the tight junctions and are required for their assembly. Together with desmosome, it is formed a complex with strong adhesive bonds to maintain the integrity of the epithelium (Thoo et al., 2019). In dysbiosis, these junctions can be disrupted, leading to increased mucosal permeability and translocation of pathogen-associated molecular patterns (PAMPs) such as lipopolysaccharides (LPS) (Vancamelbeke & Vermeire, 2017). Activation of

Toll-like receptors (TLRs) by bacterial LPS, especially TLR-4, in the Kupffer cells (KCs) leads to a pro-inflammatory response, which may contribute to hepatic fibrogenesis.

1.3 Liver lipid metabolism and alterations in NAFLD

Lipid metabolism support energy production and caloric storage processes essential for cellular structure and growth. In the liver, hepatic de novo lipogenesis (DNL) includes fatty acids (FAs) synthesized from acetyl-CoA and then esterified with 3-phosphoglycerol to generate triglycerides (TG). The rate-limiting enzymes of FAs synthesis are the enzymes Acetyl-CoA carboxylase (ACC), which carboxylates the acetyl-CoA to produce malonyl-CoA (Lu et al., 2021), and fatty acid synthase (FASN) which in turn catalyzes the production of long-chain fatty acids from malonyl-CoA. Insulin and glucose can regulate both enzymes by activating transcriptional factors sterol regulatory element-binding protein 1c (SREBP1c), and carbohydrate-responsive element-binding protein (CHREBP) respectively (X. Li & Wang, 2020). TG synthesis involves the enzymes stearoyl-CoA desaturase (SCD1) and diglyceride acyltransferase (DGAT). Of note, high free fatty acids (FFA) entry into hepatocytes triggers an imbalance in the function of these enzymes and lipogenic regulatory factors, further impairing hepatic lipid metabolism.

At the onset of the disease, NAFLD is characterized by intrahepatic TG accumulation, thereby tightly related to obesity. Indeed, in NAFLD and obese patients the major TG composition of the liver is reported to be from non-esterified fatty acids (NEFA), followed by DNL, and finally from the diet, being the NEFA pool the primary contributor to hepatic TG in NAFLD. Furthermore, obesity successively leads to insulin resistance, which in turn becomes a feature of NAFLD. Insulin is a pancreatic hormone required to keep blood glucose levels within a tightly controlled range (Sakurai et al., 2021). Under physiological conditions, insulin inhibits hepatic glucose production and increases fatty acid and triglyceride synthesis (Maude et al., 2021). Nevertheless, in several pathological states, peripheral tissues can lose their responsiveness to insulin and switch to a state known as insulin resistance (IR). IR promotes adipose tissue lipolysis leading to augmented FFAs levels in the blood, which are taken up by the liver in a concentration-dependent manner, causing hypertriglyceridemia (Sakurai et al., 2021).

In addition, the impairment of insulin uptake caused by impaired insulin sensitivity in extrahepatic tissues leads to an overload of glucose influx into the liver, causing hyperglycaemia, whereas hyperinsulinaemia triggers an overload of insulin into the hepatic tissue. Under such conditions, both insulin (through SREBP1c activation) and glucose (through

CHREBP activation) drive the increased hepatic conversion of carbohydrates into FAs through DNL, resulting in lipid accumulation which generates toxic compounds (Bessone et al., 2019). The accumulation of lipotoxic intermediates, such as diacylglycerol (DAG) or ceramides, can alter hepatic insulin signalling increasing hepatic glucose production (Ferguson & Finck, 2021). These toxic metabolites activate the protein kinase C-θ (PKCθ) which phosphorylates insulin receptor substrates 1 and 2 (IRS1/2), leading to its ubiquitination and further proteasomal degradation. This mechanism involves the interaction between lipopolysaccharide (LPS) from intestinal microbiota and the toll-like receptor 4 (TLR4), which induces, in turn, the ceramide/ PKCθ pathway. Furthermore, ceramides also activate protein phospholipase-A2 (PLA2) and inhibit insulin signalling by counteracting Akt phosphorylation (Bessone et al., 2019). Moreover, the accumulation of DAG within cytosolic lipid droplets induces translocation of protein kinase C (PKC)-ε to the plasma membrane and inhibits the intracellular kinase domain of the insulin receptor (X. Li & Wang, 2020; Sakurai et al., 2021).

Regarding FFAs uptake by the liver, fatty acid translocase (FAT/CD36) facilitates the uptake and utilization of long-chain fatty acids in hepatocytes. The upregulation of this gene has been associated with insulin resistance, hyperinsulinemia and increased hepatic TG storage and secretion (Abumrad et al., 2021). The TG synthesized in the liver can be stored in lipid droplets (LDs) or coupled to apolipoproteins and further secreted as very-low-density lipoprotein (VLDL), this is an important pathway for the mobilization of liver fat (X. Li & Wang, 2020). The synthesis of hepatic VLDL encompasses two main steps. First, it is carried out a partial lipidation of the large apolipoprotein B-100 (APOB100), a mechanism that requires the action of microsomal triglyceride transfer protein (MTTP), resulting in a small and dense VLDL precursor (Heeren & Scheja, 2021). The second phase comprises the expansion of this particle with lipids from LDs to form a mature and TG-rich VLDL, which will be secreted into plasma (Heeren & Scheja, 2021). Different disturbances in this process can contribute to NAFLD progression. For instance, the aggravation of liver insulin signalling inhibits the synthesis of apolipoprotein B (APOB), causing impairment in the exportation of hepatic lipids through the VLDL mechanism. In addition, when the TG incorporation into VLDL is blocked by microsomal MTTP deficiency or due to APOB mutations in patients, TG accumulates in the liver and consequently causes hepatic steatosis and NASH development (McCommis KS et al., 2017). Conversely, when this machinery is not affected it can generate an increase in VLDL production and secretion due to TG accumulation. However, these particles can carry toxic lipids and their structure can be altered which difficult their secretion. Hence, obese patients with NAFLD show increased secretion of VLDL-TG as a response to hepatocytes release of

excessive TG. Nevertheless, this release is not sufficient to normalize the intrahepatic TG content, contributing to the accumulation of liver fat (Fabbrini et al., 2016).

Besides VLDL secretion, the liver can eliminate FAs through a catabolic process, where mitochondrial β-oxidation is the main mechanism. This process includes three major steps: activation, transport, and oxidation. First, the activation of Long-chain fatty acids (LCFAs) to fatty acyl-CoA by acyl-CoA synthase in the outer membrane takes place. Subsequently, the enzyme carnitine palmitoyltransferase-1 (CPT1) works as a shuttle for long-chain fatty acids (LCFAs) to cross the mitochondrial membrane. The activity of CPT1 can be affected by malonyl-CoA, an intermediate of DNL, which acts as an allosteric inhibitor for this enzyme (Lu et al., 2021). Malonyl-CoA is produced from the tricarboxylic (TCA) cycle-derived citrate via conversion to acetyl-CoA by the ATP citrate lyase (ACLY) and further carboxylation by the enzyme ACC (Batchuluun et al., 2022). Of note, some transcription factors such as peroxisome proliferator-activated receptor α (PPARα) can enhance the expression of CPT1. As a consequence of FAs oxidation, reactive oxygen species (ROS) are generated. In response to intrahepatic FAs overload, there is an upregulation of the TCA cycle and mitochondrial respiratory chain. This dysregulation potentiates an increment in oxidative stress which induces lipid peroxidation, plasma intracellular membrane damage, and cell death (X. Li & Wang, 2020). In contrast, impairment of β-oxidation in NAFLD can occur via SREBP1c-mediated induction of ACC enzyme and overproduction of malonyl-CoA, which is an allosteric inhibitor of CPT1 (Batchuluun et al., 2022). Thus, liver mitochondrial dysfunction is considered a significant contributor to NAFLD pathogenesis. Interestingly, mitochondria might have a flexible behaviour translated into a compensatory and protective response in the early stages of NAFLD. In line with this statement, in both fatty liver mouse model and NAFLD patients, the expression of genes involved in hepatic mitochondrial β-oxidation such as PPARα, PGC1α, and CPT1 was elevated as expected (Lu et al., 2021; Kohjima et al., 2007). Theoretically, increased DNL should inhibit FAs oxidation due to the generation of malonyl-CoA (X. Li & Wang, 2020). Moreover, DNL can be raised via acetate conversion into acetyl-CoA through the enzyme Acetyl-CoA synthetase 1 (ACSS1) in the mitochondria, and ACSS2in the cytosol (Gao et al., 2016). Nevertheless, the mitochondrial enzyme ACSS3, responsible to produce propionyl-CoA from propionate, might decrease acetyl-CoA production and reduces DNL (Jia et al., 2022). Additionally, not only β-oxidation is still enhanced to coordinate the excess of FFA influx, other minor pathways, such as peroxisomal β-oxidation, and ω-oxidation can be upregulated (Kohjima et al., 2007).

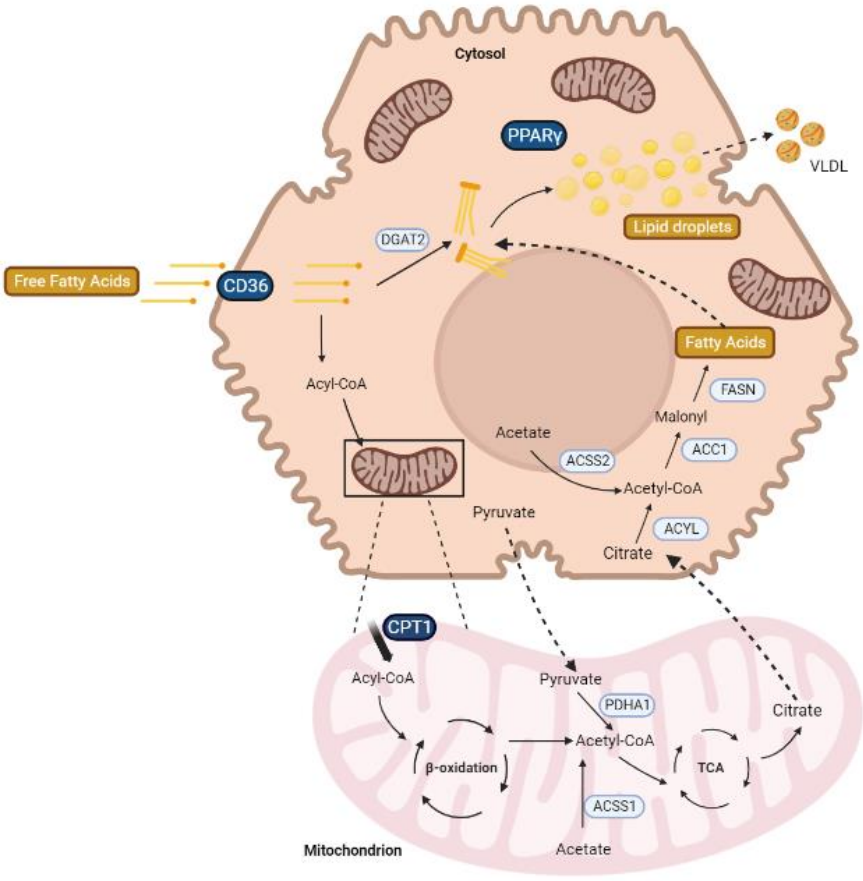

Figure 3. Overview of liver lipid metabolism. Free fatty acids (FFAs) are uptaken via CD36 transport into the cytosol. Within the cell, fatty acids (FAs) can be converted into triglycerides through the DGAT2 enzyme and stored in lipid droplets, where PPARγ contributes to the process. On the other hand, FAs can be oxidized in the mitochondria. The acetyl-CoA produced via β-oxidation can enter the tricarboxylic acid cycle (TCA) and generates citrate which is transported to the cytosol and participates in the lipogenesis pathway. Moreover, acetyl-CoA can be produced from pyruvate via PDHA1 or from acetate trough the enzymes ACSS1 (in the mitochondria) and ACSS2 (in the cytosol). Adapted from Batchuluun et al. 2022. Figure created with BioRender.

1.4 Macrophage role in NAFLD

Immunity has a critical role during NAFLD, as the inflammatory processes are key players in disease onset and progression. The immune landscape of the liver encompasses different cell populations, where tissue-resident macrophages are essential to preserving tissue homeostasis (H. Wang et al., 2021). In the liver, macrophages comprise resident Kupffer cells (KCs) and recruited monocyte-derived macrophages (Wculek et al., 2021). KCs are macrophages that exclusively reside in the liver sinusoids, where they interact closely with liver sinusoidal endothelial cells, hepatic stellate cells (HSCs), and hepatocytes to acquire their tissue-imprinted signature as well as the signals that enable self-maintenance (Huby & Gautier, 2021). On the other hand, infiltrating macrophages are derived from circulating monocytes developed from bone marrow-resident hematopoietic stem cells (H. Wang et al., 2021). Though presumably

some recruited macrophages differentiate into KCs, studies have suggested that infiltrating macrophages and KCs are morphologically different and transcriptionally diverse, emphasizing the presence of two major hepatic macrophage subsets in NAFLD.

Upon liver injury, KCs recruit monocytes that differentiate into activated macrophages (M1-like type), which are characterized by their phagocytic activity and secretion of pro-inflammatory cytokines as well as ROS (Figure 4) (Kazankov et al., 2019). Conversely, when inflammation is followed by reparative phases, as is common in NASH, macrophages can differentiate into an M2-like type that has an immune-suppressive but pro-fibrogenic phenotype (Figure 4) (Kazankov et al., 2019). In particular, the specific molecular switches behind macrophage-change phenotype or polarization are still to be clarified and validated.

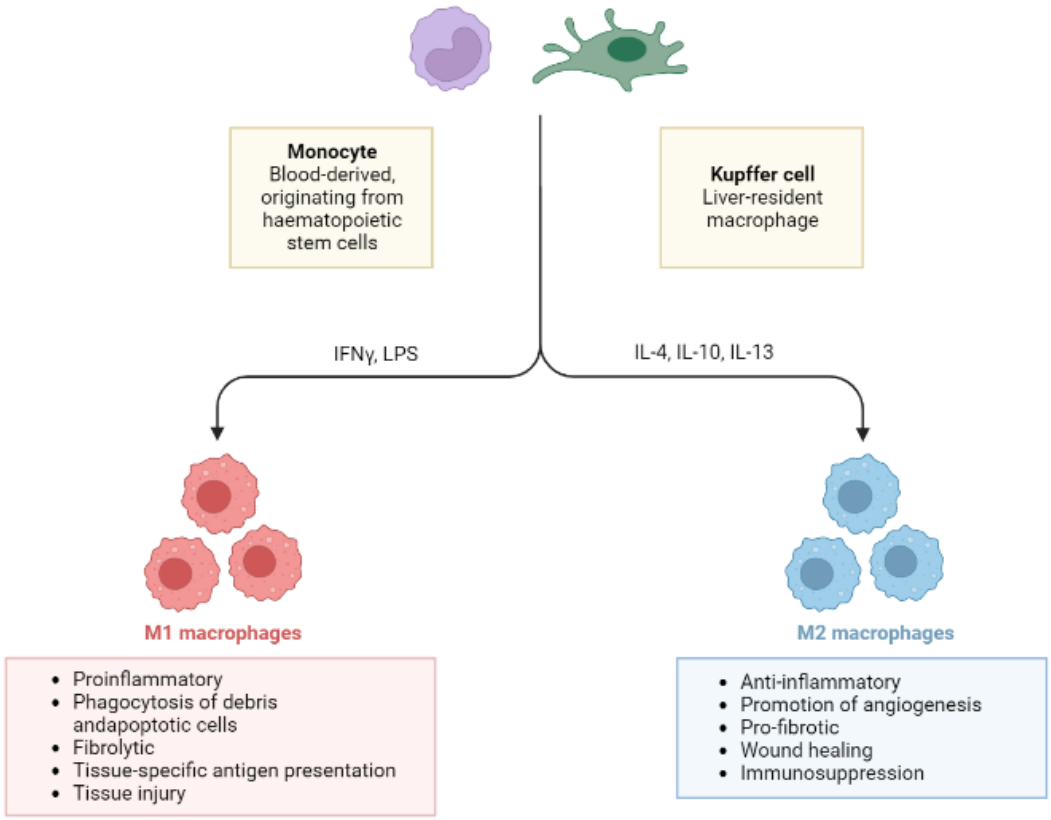

Figure 4. Macrophage polarization and phenotype in liver inflammation. Liver macrophages derive from resident Kupffer cells or recruited circulating monocytes. Monocytes can be polarized towards M1- or M2-type macrophages. M1 macrophages drive inflammation, whereas M2-type have anti-inflammatory and pro-fibrotic properties. LPS, lipopolysaccharides; IFNγ, interferon- γ; IL-4, interleukin-4; IL-10, interleukin-10, IL-13, interleukin-13. Adapted from Kazankov et al., 2019. Figure created with BioRender.

In NAFLD, macrophages of a pro-inflammatory phenotype seem to contribute to disease severity whereas macrophages with an anti-inflammatory and reparative phenotype have been

associated with attenuated hepatic injury and improved insulin sensitivity (Kazankov et al., 2019). Liver macrophages can be activated by various stimuli such as lipopolysaccharide (LPS) entering the circulation owing to enhanced intestinal permeability and acting through the TLRs; via fatty acids (FAs) through TLRs and adipokines from adipose tissue and via cholesterol and their metabolites acting through CD36 and scavenger receptor A (SRA). Subsequently, KCs secrete pro-inflammatory cytokines such as tumour necrosis factor (TNF), IL-1β and IL-6 to help recruit neutrophils and circulating monocytes via the CC- chemokine ligand 2 (CCL2)–CC- chemokine receptor 2 (CCR2) interaction (Figure 5) (H. Wang et al., 2021). In addition to their contribution to the KCs pool, monocytes also follow a classical pathway of differentiation in NAFLD progression, leading to the generation of monocyte-derived inflammatory macrophages to further amplify hepatic inflammation and contribute to fibrogenesis. This occurs via stimulation of HSCs through transforming growth factor-β (TGF-β), which facilitates their transformation into activated myofibroblasts with extracellular matrix deposition (Figure 5) (Huby & Gautier, 2021; Kazankov et al., 2019)

Under pathological settings, the self-renewal of KCs by proliferation is disturbed, gradually lost, and then replaced by monocyte-derived KCs (T. Wang & Ma, 2021). Although the generation of monocyte-derived KCs maintains the macrophage pool in the liver, their gene expression spectrum differs from that of embryonically derived KCs. In particular, monocyte-derived macrophages have been reported to show a more pronounced inflammatory profile (Tran et al., 2020). These features imply a different impact on the liver response to lipid-mediated stress. In fact, monocyte-derived KCs limit hepatic triglyceride storage but promote liver injury to a greater extent than embryonically derived KCs (Tran et al., 2020).

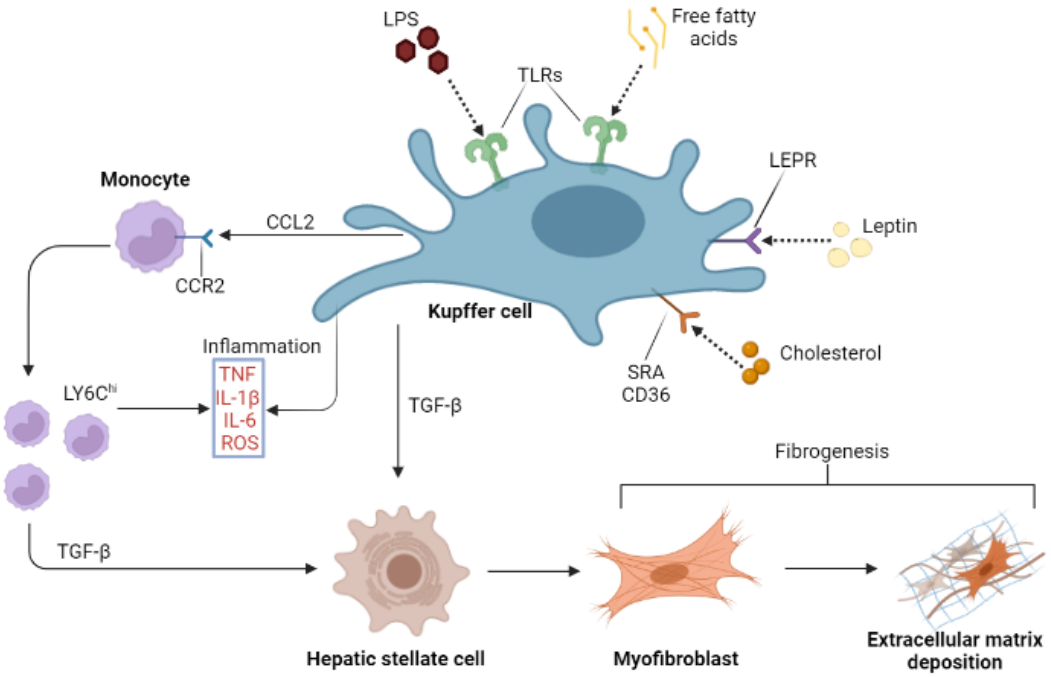

Figure 5. Factors contributing to macrophage activation in NAFLD. There are several main pathways for Kupffer cell activation in NAFLD: via gut- derived endotoxins such as lipopolysaccharide (LPS) acting through the Toll- like receptors (TLRs); via free fatty acids (FFAs) through TLRs and adipokines (leptin via the leptin receptor (LEPR)) from adipose tissue; and via cholesterol and its metabolites acting through CD36 and scavenger receptor A (SRA). Kupffer cells then secrete pro-inflammatory cytokines such as tumour necrosis factor (TNF), IL-1β and IL-6 to help recruit circulating monocytes via the CC- chemokine ligand 2 (CCL2)–CC- chemokine receptor 2 (CCR2) interaction. Monocytes differentiate into pro- inflammatory macrophages to further amplify hepatic inflammation and contribute to fibrogenesis via stimulation of hepatic stellate cells by transforming growth factor- β (TGFβ), facilitating their transformation into activated myofibroblasts with extracellular matrix deposition. Adapted from Kazankov et al., 2019. Figure created with BioRender.

1.5 Gut microbiota modulation: Probiotics as a strategy to restore the gut-liver axis

In recent years, the gut microbiota has attracted increased attention in the field of metabolic diseases. Diet is a direct modulator of the gut microbiota, contributing to altering not only bacterial Phyla relative abundance but also bacterial metabolite production. Remarkably, the use of probiotics in line with lifestyle modifications has enhanced the outcomes in NAFLD treatment. Probiotics refer to live microorganisms that are beneficial to the host when administered in sufficient amounts (Suez et al., 2019) and have demonstrated potential for restoring gut homeostasis and attenuating NAFLD (M. Yao et al., 2021). These microorganisms encompass several lactic acid bacteria (LAB) strains which have been demonstrated to confer health-promoting effects to the host such as intestinal barrier restoring, antimicrobial activities, anti-inflammatory effects, antioxidant activities, and lipid metabolism improvement (H. Li et al., 2021). Table 1 summarizes different examples of probiotics used to treat liver injury. In

this context, through different meta-analyses, probiotic mixes composed of three or more species, including *Bifidobacterium breve, Bifidobacterium longum, Streptococcus salivarius,* and *Lactobacillus* such as *Lactobacillus delbrueckii, Lactobacillus acidophilus* (*L. acidophilus*), and *Lacticaseibacillus casei* (*L.casei*) have reported improvements in glucose control and insulin function in type 2 diabetic subjects as well as in liver enzymes in patients with fatty liver disease (Koutnikova et al., 2019). Particularly, *Lactobacillus* strains comprise a large heterogeneous group of gram-positive, non-sporulating, and facultative anaerobic bacteria and have been reported to be modulators in reducing fat liver content. Recently, it was reported a reduction in Triacylglycerol (TG) levels and enhance in antioxidant capacity in the liver with a supplementation mixture of *Lactiplantibacillus plantarum (L.* plantarum) and *L. acidophilus* in a mouse model with liver injury (H. Li et al., 2021). In line with these studies, a human origin probiotic cocktail composed of 5 *Lactobacillus* and 5 *Enterococcus* strains prevented glucose metabolism dysfunctions, improved insulin sensitivity, and attenuated hepatic steatosis in older mice fed with a high-fat diet (HFD). Moreover, this 10 probiotics mixture increased the mRNA expression of tight junction proteins such as *Zo1 and Ocln* in the intestinal tissues, which restored the intestinal barrier (Ahmadi et al., 2020). Intriguingly, not only the use of multi-strain mixture but also single-strain probiotics have also been reported as a good approach to attenuate liver pathologies. In that regard, it was shown that administration of *Limosilactobacillus fermentum (L. fermentum)* in HFD-fed mice has a protective effect translated into amelioration of glucose clearance and fatty liver (Yoon et al., 2020). *L. fermentum* treatment was able to stimulate brown adipocyte tissue (BAT)-mediated energy expenditure by increasing serum levels of BA. Furthermore, under this probiotic treatment, hepatic genes related to gluconeogenesis, lipogenesis, and lipid sequestration were downregulated. Similarly, the administration of *Lacticaseibacillus rhamnosus* GG (*L. rhamnosus* GG) has also demonstrated a protective mechanism against hepatic steatosis. To start with, the research group identified that *L. rhamnosus* GG consumes palmitic acid (PA) and oleic acid (OA), both common dietary fatty acids in the western diet, as its substrates during cultivation in an *in vitro* experiment. Subsequently, using a tracer-labelled [^{14}C]-OA (or PA) in *in vivo* models, they found that even under short-term periods, *L. rhamnosus* GG reduces intestinal fatty acid absorption and decreases body fat accumulation (Jang et al., 2019). Of note, the effect was not associated with gut permeability or systemic inflammation which implies that this strain can protect against the initial stage of NAFLD. In addition, *L. rhamnosus* GG reduces the mRNA expression of genes related to TG synthesis *Dgat1* and *Dgat2* under HFD-long-term. Likewise, *L. casei* and *Limosilactobacillus reuteri* (*L. Reuteri)* have also shown positive outcomes when administrated

individually in animal models for liver damage. Specifically, *L. casei* strain Shirota reduced hepatic and intestinal damage in mice with acute liver injury via PPAR signalling, retinol, and pyruvate metabolism (R. Yan et al., 2021), whereas the supplementation of *L. Reuteri* contributed to decreasing liver fibrosis in experimental acute cholestasis (Santos et al., 2020). The probiotic potential of *L. reuteri* strains is linked to their metabolite production profile. Of particular significance, most *L. reuteri* strains can produce and excrete reuterin, a well-known antimicrobial compound (Mu et al., 2018). Besides reuterin, a reservoir of metabolites including lactic acid, acetic acid, ethanol, reutericyclin, histamines, exopolysaccharides, folate, and cobalamin have been determined as products of some *L. reuteri* strains (Mu et al., 2018). Although the beneficial effects of this bacteria in NAFLD have been reported, the underlying mechanisms have not been fully elucidated. Moreover, despite this genus being correlated with fat liver reduction, we should consider that each species may have its own physiological functions in regulating gut-liver axis signalling and, thereby, controlling host homeostasis in a species-dependent manner. Therefore, identifying the pivotal pathways implied in hepatic lipid metabolism not only paves the way to understanding the mechanisms but will also provide opportunities to further improve their therapeutic potential. Specifically, exploring the interaction between specific commensal bacterial species and their metabolites is a research opportunity to identify new therapeutic targets to ameliorate NAFLD.

Table 1. Examples of probiotics used to treat liver injury

Probiotic	Experimental model	Probiotic Effect	Mechanisms of action	Reference
Lactiplantibacillus plantarum and *Lactobacillus acidophilus*	Mice with chronic alcoholic liver injury	Improvement of intestinal epithelial permeability and reduction in serum LPS levels. Inhibition of lipid accumulation, oxidative stress, and inflammation	AMPK, Nrf-2, and TLR4/NF-κB pathway	H. Li et al., 2021
A cocktail composed of 5 *Lactobacillus* and 5 *Enterococcus* strains	HFD-fed older mice	Prevent glucose and insulin metabolism dysfunctions. Reduction in hepatic steatosis and inflammation. Increased mRNA levels of tight junction proteins	Increase in bile salt hydrolase and decrease in taurine in the gut	Ahmadi et al., 2020
Limosilactobacillus fermentum	Diet-induced obesity (HFD-fed mice)	Amelioration of glucose clearance and fatty liver. Reduction in inflammation	Increase in intestinal FXR/FGF15 signalling. Inhibition of adipocyte differentiation and inflammation	Yoon et al., 2020
Lacticaseibacillus rhamnosus GG	Diet-induced hepatic steatosis (HFD-fed mice)	Reduction in intestinal fatty acid absorption	Competition for fatty acid absorption in the intestine	Jang et al., 2019
Lacticaseibacillus casei	Mice with acute liver injury	Attenuation of hepatic and intestinal damage	PPAR signalling and upregulation of pyruvate metabolism	R. Yan et al., 2021
Limosilactobacillus reuteri	Acute bile duct-ligated mice	Reduction in liver fibrosis	Modulation of macrophage anti-inflammatory response	Santos et al., 2020

1.6 The interplay between macrophages and gut microbiota

The local microenvironment interactome is critical to imprinting tissue-specific functions of macrophages. Gut microbes are a key factor capable of modifying the profile of these innate immune cells. In fact, germ-free (GF) animals are broadly impaired in many aspects of the development of early immune response (Kamada et al., 2013), highlighting the pivotal crosstalk between macrophages and gut microbes. It has been studied that GF mice are more susceptible to infection than conventionally raised mice (Kamada et al., 2013). This indicates that an important function of the commensal microbiota might be to protect the host from infection by enhancing innate immunity. Of note is the fact that also the gut microbial metabolites might influence not only intestinal cells but also liver cells such as resident-macrophages (Zheng et al., 2020). Hence, recent research started to shed light on the relationships between monocytes, macrophages, and the commensal microbiota. Okubo and colleagues reported that altered gut microbiota may affect not only the barrier function of the gut but also the amount of microbe-associated molecular patterns (MAMPs) produced in the gut, such as LPS (Okubo et al., 2016). The study strengthened the hypothesis that LAB metabolites might modulate the KCs by lowering the LPS levels in the serum, alleviating the formation of NASH. LPS is an inflammatory signal activating TLR on hematopoietic stem cells. These activate pro-inflammatory pathways leading to the secretion of cytokines and chemokines from various cell types in the liver. All known human TLRs are expressed by hematopoietic stem cells, bolstering the importance of their interaction with the gut microbes (Okubo et al., 2016; Wallace et al., 2022). In addition, a large LPS produced by *Helicobacter hepaticus* has been shown to induce an anti-inflammatory gene signature via TLR2/CREB pathway in murine intestinal macrophages (Danne et al., 2017). Moreover, in the intestine, monocytes undergo final differentiation in the lamina propria, in close proximity to commensal bacteria and its metabolites such as SCFAs. Besides providing energy for the host, SCFAs exhibit anti-inflammatory effects via binding to G-protein-coupled receptor 43 (GPR43), which is expressed in immune cells, including macrophages (J. Wang et al., 2020). In this context, Julie Schulthess and colleagues assessed a possible effect of SCFAs on macrophage differentiation. The authors isolated human peripheral blood-derived CD14+ monocytes and incubated these with macrophage colony-stimulating factor and the SCFAs butyrate, acetate, or propionate (Schulthess et al., 2019). The results demonstrated that butyrate can drive monocyte-to-macrophage differentiation through histone deacetylase 3 (HDAC3) inhibition, thereby amplifying antimicrobial host defence. This report supports a model in which butyrate imprints a non-inflammatory antimicrobial program in gut macrophages, which is consistent with the

concept that butyrate produced by the microbiota shape host-microbial crosstalk to promote gut-liver homeostasis (Schulthess et al., 2019).

Also, other SCFAs such as propionate and acetate modulate macrophage activity. For example, propionic acid, a major SCFA, prevents obesity-related inflammation partially by acting on macrophages (J. Wang et al., 2020). Moreover, the circulating acetate level was increased by antibiotic use in HFD-fed mice, reducing macrophage infiltration via activating Adenosine Monophosphate-Activated Protein Kinase (AMPK)(Carvalho et al., 2012). Strikingly, it was detected that the use of antibiotics led to the increase in Proteobacteria. Even with the prevalence of this gram-negative bacteria, it was reported a reduction in circulating LPS, which diminished inflammation. Further, it was described that acetate could have a role in this effect (Carvalho et al., 2012). Likewise, trimethylamine N-oxide (TMAO), a soluble microbiome-derived metabolite, has also an effect on macrophage polarization toward the M1 features in an NLRP3 inflammasome-dependent manner (K. Wu et al., 2020). Regulation of NRLP3 inflammasome signalling is required to maintain intestinal homeostasis (Zheng et al., 2020). Upon intestinal injury, certain members of the microbiota such as *Proteus mirabilis* and *Escherichia coli* stimulate monocytes to induce NLRP3-dependent IL-1β release, which elicits intestinal inflammation (Seo et al., 2015). Particularly, it was reported that *P. mirabilis* harbours the virulence gene *hpmA* (Hemolysin), which might induce K^+ efflux. This activity is sensed by host macrophages to activate the NLRP3 inflammasome (Seo et al., 2015). Due to the reported variation in the ability of different intestinal bacteria to activate the NLRP3 inflammasome, it is expected that mice with different microbiota compositions will differ in the intestinal activation of the inflammasome under disease state. Thus, the identification of immunomodulatory metabolites produced by commensal or pathogen bacteria requires a multidisciplinary approach. Therefore, gut-liver axis integrative research could provide new preventive and therapeutic strategies for NAFLD.

1.7 The role of gut microbiota-derived metabolites in lipid metabolism

Microbial metabolites are produced from the metabolism of dietary input, environmental factors, and xenobiotics as well as from host-derived molecules, such as bile acids (Sharpton et al., 2021). These molecules have been included in the postbiotics definition. Although the international community is still building a consensus on the term's exact definition (Aguilar-Toalá et al., 2018; Salminen et al., 2021), postbiotics have been defined as a preparation of inanimate microorganisms and/or their components that confers a health benefit on the host (Salminen et al., 2021). Postbiotics comprise bacteria metabolites that can enter the portal

circulation and facilitate the gut-liver axis crosstalk. Therefore, the function and biochemical output of the gut microbiota it is being more relevant than the underlying composition. The microbiota metabolites involved in these interactions include short-chain fatty acids (SCFAs), lactic acid, bile acids (BA), bacteriocins, adhesins, aryl hydrocarbon (Ahr) ligands, indole derivatives, branched-chain fatty acids, among others (Salminen et al., 2021).

Emerging evidence suggests that microbial-derived metabolites may be of significance in the NAFLD spectrum. Zhao et al., investigated whether acetate, the most abundant SCFA, is a key microbial product supporting DNL in mice subjected to a bolus or a gradual fructose consumption. The study demonstrated that in both situations, fructose provides a signal and substrate to trigger hepatic DNL. Particularly, it was reported that fructose catabolism in hepatocytes acts as a signal to induce induces DNL genes including *Acss2*, whereas fructose metabolism by the gut microbes provides acetate as a substrate for the DNL, which is mediated by ACSS2(S. Zhao et al., 2020). Thus, causing an increase in lipid production rate. By contrast, acetate can cross the blood-brain barrier and increase satiety which in turn might reduce lipids intake and decrease lipid liver storage (Koh et al., 2016).

The role of propionate in liver lipid metabolism has also been studied related to the administration of prebiotics. Prebiotics are substrates that are selectively utilized by host microorganisms conferring a health benefit (Salminen et al., 2021). A randomized controlled trial study showed that dietary supplementation with the prebiotic inulin is mainly metabolized into acetate in the colon and increases intrahepatic lipids. In contrast, dietary supplementation of a designed inulin-propionate ester attenuated the acetate-mediated increase in intrahepatocellular lipids by impairing hepatic acetate metabolism (Chambers et al., 2019). The mechanism involves the enzyme ACSS3, present in the mitochondria of hepatocytes and for which propionate is the preferred substrate over acetate(Yoshimura et al., 2017). This enzyme generates propionyl-CoA, therefore high levels of propionate would increase competition with acetate for conversion into their CoA products, which in turn may reduce the cytosolic acetyl-CoA available for DNL.

Butyrate, which is also an SCFA produced by the microbial fermentation of dietary fiber in the large intestine, has shown beneficial effects in mammals. In NAFLD, the administration of sodium butyrate attenuated HFD-induced steatohepatitis by modulating gut microbiota and intestinal barrier function in mice (D. Zhou et al., 2017). Subsequently, Zhou et al. reported that sodium butyrate prevents NAFLD progression in HFD-fed mice by increasing glucagon-like peptide-1 receptor (GLP-1R), which has been reported to protect hepatocytes against the

progression of NAFL to NASH (D. Zhou et al., 2018). The treatment with sodium butyrate upregulated hepatic GLP-1R expression by inhibiting histone deacetylase 2 (HDAC2), thus improving hepatic GLP-1 sensitivity and ameliorating NAFLD (D. Zhou et al., 2018). In accordance with the positive correlation between sodium butyrate and liver lipid metabolism, it was demonstrated that butyrate improves liver lipid metabolism in HFD-fed mice. When administrated, sodium butyrate decreased the expression of hepatic steatosis-associated genes. Moreover, the activity of the central metabolic sensor AMPK was upregulated in response to the treatment in the animal model as well as in human HepG2, and primary mouse hepatocytes (Z. H. Zhao et al., 2021). In contrast, Prins et al. highlighted that butyrate can be also a precursor for DNL. In this study was reported that butyrate did not decrease, but rather increased TG accumulation in precision-cut liver slices (PCLSs). Additionally, butyrate reduced mRNA levels of proteins involved in β-oxidation. The fact that butyrate has been reported to elicit a decrease in steatosis in *in vivo* experiments, but not in PCLSs, suggests that the regulatory role of this metabolite can be a consequence of organ interplay (Prins et al., 2021). Thus, depending on the mechanisms or signalling pathways that SCFAs activate alone or in synergy, appear to both prevent or promote the development of NAFLD.

Besides SCFA, the gut microbiome can produce different small molecules by metabolizing tryptophan (Trp). Trp is an essential aromatic amino acid acquired through common diet sources, including oats, poultry, fish, milk, and cheese. The gut microbes can metabolize Trp into indoles and its derivatives, with some of them acting as Ahr ligands. Indole and its derivatives participate in the maintenance of liver homeostasis and benefit intestinal permeability and immune function, which might inhibit liver inflammation (Agus et al., 2021). In line with these statements, a recent study reported that administration of the phytochemical sulforaphane (SFN) in HFD-fed mice increased the level of the microbial metabolite indole-3-acetic acid (IAA) and the protein content of Ahr in liver tissues whilst protein levels of SREBP-1C, ACC1, and FAS were reduced compared with the HFD control (Xu et al., 2021), implying that IAA regulates liver lipid metabolism by activating Ahr. Nonetheless, Ahr can encompass different effects when activated by various ligands in different cell types. For instance, the activation of the Ahr/CD36 pathway was reported to promote hepatic steatosis in mice (L. Yao et al., 2016).

1.8 D-Lactate: villain or ally?

It is difficult to accurately categorize bacterial metabolites in a short spectrum comprised only of two sides: “beneficial” or “detrimental” for health. Different microbial metabolites might have a dual role in regulating liver lipid metabolism or could be pleiotropic molecules that play a role in many cellular processes, such as D-Lactate. Interestingly, this organic anion has also been involved in health benefits and harms. This lactate isoform is produced in minimal quantities by human cells, where the plasma D-lactate concentration normally is maintained at around 0.01 mM (Levitt & Levitt, 2020). This right-handed form of lactate is exclusively converted into pyruvate in mammal cells by the mitochondrial D-lactate dehydrogenase (D-LDH), being this reaction not bidirectional. Thus, D-LDH does not catalyse the conversion of pyruvate to D-lactate and other sources give rise to this enantiomer. Endogenous D-lactate can be formed through the methylglyoxal pathway in nanomolar concentrations but increases under pathophysiological conditions in humans, such as short-bowel syndrome, severe colitis, fatigue syndrome, diabetes mellitus and neuropathological conditions (Manosalva et al., 2022). Nonetheless, it is unknown whether this increase in D-lactate is related to defective D-LDH. Interestingly, it has been reported that patients harbouring deleterious enzymatic variants producing poor metabolizers of D-lactate result in increased blood levels of the metabolite (Monroe et al., 2019). In fact, *D-ldh* mutations have been associated with mild cerebellar ataxia, hypotonia, and mitochondrial complex IV deficiency (Kwong et al., 2021). Monroe and colleagues suggested that as no clear correlation between D-lactate concentrations and the neurological phenotype has been demonstrated, the neurological symptoms may be caused by other specific metabolic products of bacterial overgrowths, such as neurotoxin mercaptans, aldehydes, or others that may function as false neurotransmitters (Monroe et al., 2019). Moreover, although the pKa for lactic acid is lower than some SCFAs, lactate may help to inhibit the growth of some pathobionts with poor tolerance for lower pH.

On the other hand, most of the D-lactate present in humans is derived from bacterial production, particularly by LAB such as Lactobacillaceae strains, which exert health-promoting functions. Despite the negative link associated between higher concentration levels of this D-lactate (>3mM) (Levitt & Levitt, 2020; Manosalva et al., 2022) and pathological conditions, it has been demonstrated that supplementation with *Lactobacillus*-based probiotics is safe and contributes to attenuating liver diseases. In addition, D-lactate-associated pathologies might be linked to both the metabolic activity of microbiota and the ability of the host to metabolize D-lactic acid (Levitt & Levitt, 2020). Furthermore, in the colon, many commensal bacteria produce D-lactate as a result of anaerobic glycolysis. Under physiological circumstances, D-

lactate can be metabolized by lactate-utilizing bacteria, which use lactate to form acetate, propionate, or butyrate (Koh et al., 2016), thus, preventing the accumulation of D-Lactate in the gut. Indeed, Sheridan and colleagues examined the regulation of genes involved in lactate utilization in *Anaerobutyricum soehngeni* and *Coprococcus catus*, microorganisms characterized as lactate-utilizing species from the human gut. The study identified a specific cluster for each bacterium (the *lct* cluster in *A. soehngenii* and the *lap* cluster in *C. catus*) whose transcriptional expression is highly upregulated in response to lactate. Consecutively, there were proposed mechanisms of butyrate formation from D- or L-lactate in *A. soehngeni* as well as mechanisms of propionate and acetate formation from both lactate isoforms in *C. catus* (Sheridan et al., 2022). Thereby, this evidence demonstrates that D-lactate produced in the intestinal tract does not significantly contribute to the levels of D-lactate in the systemic circulation under physiological circumstances (Koh et al., 2016; Scheijen et al., 2012).

Recently, it has been reported that supplementation with *L. reuteri* doubled the amount of D-lactate in the small intestine tissue and increased four times liver *D-ldh* mRNA expression. Additionally, D-lactate reduced macrophage TGF-β production, contributing to attenuating liver damage (Santos et al., 2020). Interestingly, our preliminary data demonstrate that preventive supplementation with *L. reuteri* in methionine choline-deficient diet (MCD)-fed mice zddiminished hepatocellular vacuolization and liver ROS. Moreover, a reduction in both inflammatory *tnf-α* and liver *tfg-β* mRNA was observed. In addition, the histological differences in liver fat accumulation led us to investigate mRNA markers of lipid metabolism. In that regard, *L. reuteri* supplementation stabilized *Dgat2*, *Nr1h3,* and *Rxr* (transcriptional control of lipid metabolism) and *Cd36* mRNA levels. These results support the idea that probiotics might go beyond gut microbiome modulation. Nevertheless, the precise mechanism of action by which D-Lactate reduces lipid accumulation and the signalling pathways involved in such effects remain largely unknown.

It is being a major challenge to identify the exact role of each microbial effector in host metabolism and to pinpoint their precise mechanisms in health and disease, which can differ between tissues and even within the same tissue, depending on the cell type. Thus, the characterization of new and potential microbial metabolites can provide therapeutics to ameliorate liver-related diseases either as a single small molecule or in combination. Importantly, NAFLD therapies have to proceed with caution due to the different conditions presented in each stage.

2 Hypothesis

Considering that one of the main metabolites produced by *L. reuteri* is D-lactate and that D-lactate may be involved in mitochondrial activity, we hypothesize that D-lactate modulates hepatocyte and macrophage mitochondrial activity and ameliorates steatosis-induced liver damage.

3 Aims

This project aims to identify the mechanisms by which D-lactate alters liver lipid metabolism.

Specific objectives:

a) To identify extracellular *Limosilactobacillus reuteri* (*L. reuteri*) metabolites in culture medium;
b) To explore the mechanisms through which D-lactate alters lipid metabolism, in both hepatocyte and macrophage cells using an *in vitro* steatosis model;
c) To assess gene expression in hepatic steatosis-associated pathways under D-lactate modulation.

4 Methods

4.1 Cell cultures and treatment conditions

Immortalized murine hepatocytes (cell line AML12) were grown in Dulbecco's Modified Eagle´s Medium (DMEM/F-12, HEPES; Thermo Fisher Scientific, no. 11330057) supplemented with 10% of fetal bovine serum (FBS; Thermo Fisher Scientific, no. A4766801), 1% of antimycotic (Thermo Fisher Scientific, no. 41400045), 1% insulin transferrin selenium (IST; Thermo Fisher Scientific, no. 41400045) and 40 ng/mL of dexamethasone, and kept at 37°C, 95% humidified air/5% CO_2.

For the gene assessment in hepatocytes, the cells were cultured in 12-well plates for 48h with an initial seeding density of $2x10^5$ cells/mL prior to starting the treatment. After reaching 85%-90% of confluency the hepatocytes were subjected to the following treatment: 125 µM of sodium palmitate (PA; Sigma-Aldrich, no. P9767) conjugated with BSA (Sigma-Aldrich, no. A6003) for steatosis induction. After the addition of PA, the cell cultures were modulated with 1 or 5 mM of L- or D-Lactate (Sigma-Aldrich; no. 71718-10g and no. 71716-1g respectively). Once the induction started, the cell cultures were incubated for 6h or 24h at 37°C, with 95% humidified air/5% CO_2.

In order to evaluate our hypothesis in macrophages, the mouse macrophage cell line J774A.1 was grown in Dulbecco's Modified Eagle´s Medium supplemented with 1% A/A and 10% FBS. The cells were cultured in 12-well plates for 24h and treated with lipopolysaccharides (LPS; Sigma-Aldrich, no. 93572-42-0), PA, or with a mixture of both and, with D- or L-lactate 1 or 5 mM. The macrophage cultures experiments were performed in collaboration with David Pires at iMED. In parallel, for the western blot, only the cell line AML12 was analysed. The hepatocytes were plated at $2x10^5$ in 6-well plates for 72h former the treatment. Subsequently, after 85%-90% of confluency, the cells underwent the treatment described below: PA 125 µM conjugated with BSA and modulated with 1 or 5 mM of L- or D-Lactate. Afterward, the cultures were incubated for 24h at 37°C, with 95% humidified air/5% CO_2. Eventually, in the three experimental designs, subgroups were formed considering the controls for each condition and the different concentrations of both isoforms of lactate.

It is important to mention that L-lactate was used as an internal control in order to investigate if all the alterations could be attributed to lactate itself regardless of the isoform or if the effects were specific to D-lactate.

4.2 MTS assay

To analyse the mitochondrial activity was performed an MTS assay using the CellTiter 96® AQ_{ueous} (Promega, no. G3582) which uses the compound 3-(4,5-dimethylthiazol-2-yl)-5-(3-carboxymethoxyphenyl)-2-(4-sulfophenyl)-2H-tetrazolium (MTS) in conjunction with 1-methoxy phenazine methosulfate (PMS). The PMS compound acts as an intermediate electron acceptor and transfers electrons from NADH in the cytoplasm to reduce MTS in the culture medium into an aqueous soluble formazan, which can be quantified at 490 nm. Here, hepatocytes were cultured in a 48-well plate for 48h with an initial density of $0.5x10^5$ cells/mL. Cells were then subjected to the following treatment: PA 125, 250, and 500 µM with 1, 5, 10, 50, or 100 mM of D- or L-lactate. Importantly, subgroups were formed considering the controls for each condition and the different concentrations of both isoforms of lactate and PA. Prior to starting the assay, the MTS and PMS reagents were thawed in a water bath at 37°C. Then a master mix with 95% of MTS and 5% of PMS was prepared. To obtain the volume of the master mix it is needed to consider the volume of culture medium in each well, which in our case was 200 µL, and next applied the formula:

$$Volume = \frac{number\ of\ samples\ x\ 200\ \mu L}{5}$$

The respective amount for MTS (95%) and PMS (5%) was calculated considering the final volume and then mixed in the remaining 4/5 parts with culture medium. To start the assay, the culture medium of each well was aspirated and then 200 µl of the master mix were added to each well. The plates were incubated at 37°C in a CO_2 incubator for 30 minutes. Afterward, the absorbance was measured at 490 nm using a Varioskan™ LUX multimode microplate reader (Thermofisher).

4.3 D-lactate colorimetric assay

To analyse the consumption of D-Lactate in each group condition, we performed a colorimetric assay using a D-Lactate Assay kit (Abcam No. Ab83429). For this experiment 2 time points were set, 0h (aliquot taken right away after the treatment starts) and 24h (aliquot taken at the end of the treatment). This assay is based on the conversion of D-lactate to pyruvate in the presence of nicotinamide-adenine dinucleotide (NAD+) and D-lactate dehydrogenase (D-LDH) and monitored by a spectrophotometric technique. D-Lactate is specifically oxidized by D-LDH and generates a proportional colorimetric product measured at 450 nm. The useful concentration range in samples is 0.1-10 mM D-Lactate. To run the protocol, first, we prepared a standard curve following the manufacturer´s protocol. Then, samples were prepared and incubated with the reaction mix for 30 min. The optical density was measured at 450 nm using Varioskan™ LUX multimode microplate reader (Thermo fisher Scientific). and the D-Lactate amount was calculated with the standard curve equation:

$$La = \frac{(Corrected\ absorbance - (y - intercept))}{Slope}$$

The concentration of the metabolite (nmol/µL) was calculated as:

$$D - Lactate = \left(\frac{La}{Sv}\right) * D$$

Where:

La= Amount of D-lactate in the sample well (nmol)

Sv= Sample volume added into the reaction well (µL)

D= Sample dilution factor.

4.4 Nile red staining

In order to investigate if D-lactate has a protective role against fatty acid accumulation in hepatocytes, we used the Nile red fluorometric quantification to assess intracellular fat accumulation after the treatment strategy. Hepatocytes were plated in a 96-well plate following the same group distribution as described in section 4.1. Subsequently, the culture medium was aspired and then cells were incubated with 5 µg/mL Nile red (Sigma-Aldrich, no. 72485-100mg) diluted in 100 µL of culture medium per well, at 37ºC in a CO_2 incubator for 90 min. Cells were then washed with PBS to remove the excess of dye. Finally, the fluorescence was measured (excitation/emission at 552/636nm respectively) using Varioskan™ LUX multimode microplate reader (Thermo fisher Scientific). The fluorescence values were corrected with total protein content using the Bicinchoninic Acid Assay (BCA) method, using the Pierce™ BCA Protein Assay Kit (Thermo Fisher Scientific; no. 23227), according to the manufacturer's specifications, using BSA as standard. After Nile red assay, the PBS was aspired and 25µL of Radio-Immunoprecipitation Assay (RIPA) buffer (Sigma-Aldrich, no. R0278) were added per well. The cells were then homogenized and 5 µL per sample were transferred to a new 96-well plate and diluted in 35 µL of water. Lastly, 400 µL of BCA mix per well were added and then the cells were incubated at 37ºC for 30 min. After the incubation period, 300 µL were transferred to a 96-well plate and the absorbance was measured at 562 nm. A standard curve was also prepared.

4.5 siRNA transfection in hepatocytes

Hepatocytes were grown in 12-well plates following the protocol described in section 4.1. After 24h of confluency, cells were transfected with short interference RNA (siRNA) against *D-ldh* (silencer select pre-designed siRNA; Invitrogen, no. 4790771) or a siRNA control (siControl; Silencer™ Select Negative Control No. 1; Thermo Fisher Scientific) using the Lipofectamine™ 3000 reagent Protocol. Firstly, Lipofectamine™ 3000 (Thermo Fisher Scientific, no. L3000015) was diluted in Opti-MEM medium (Thermo Fisher Scientific, no. 31985062) (Tube 1). In tubes apart was prepared a dilution of siRNA for *D-ldh* (Tube 2) and siRNA control (Tube 3) in Opti-MEM medium. Afterward, the 3 tubes were incubated for 5 minutes and then the diluted Lipofectamine™ 3000 was added to each siRNA tube (ratio 1:1). Later, the tubes were incubated for 5 min, and then 100 µL of the transfection mix were added to each well considering the plate distribution. Finally, the transfected cells were incubated at 37°C, with 95% humidified air/5% CO_2. After 24h post-transfection cells were treated with PA 125 µM and subjected to the treatment strategy with D- or L-lactate as described in section 4.1.

4.6 Cell harvest

The cells were recovered using a scrapper and thereafter were transferred to a 1.5 mL microtube and centrifuged at 20°C, 500 rpm for 5 min. Afterward, the pellet was recovered and resuspended in 0.5 mL TRIzol (Thermo Fisher Scientific, no. 15596018). The pellet was frozen at -80°C for further RNA isolation.

4.7 Total RNA isolation

Before the RNA extraction, the harvested cells were re-suspended in 0.5 mL of Trizol and then frozen at -80°C. For total RNA isolation was carried out the next protocol (Adapted from TRIzol Reagent User Guide): Samples were thawed, homogenized, and then incubated for 5 minutes at room temperature (RT). Then, 0.2 mL of chloroform was added per 1 mL of TRIzol™ and subsequently the samples were mixed by shaking for 15 seconds using vortex and then incubated for 2–3 min at RT. Next, the samples were centrifuged for 15 min at 12,000 × g at 4°C and afterward, the aqueous phase containing the RNA was transferred to a nuclease-free microcentrifuge tube by angling the tube at 45° and pipetting the solution out. Once the aqueous phase was transferred to the microtubes, 0.5 mL of isopropanol was added per 1 mL of TRIzol™ used for lysis and mixed by immersion. Then, samples were incubated for 20 min at RT and after that time centrifuged for 10 min at 12,000 × g at 4°C. The pellet was recovered and resuspended in 0.8 mL of 75% ethanol per 1 mL of TRIzol™ used for lysis. Next, samples were centrifuged for 5 min at 7500 × g at 4°C, the supernatant was discarded and the final pellet was dried at RT. Lastly, the pellet was resuspended in 20–50 µL (considering pellet size) of RNase-free water and incubated in a heat block at 55°C for 10 minutes. The extracted RNA was quantified using the Qubit RNA assay kit (Invitrogen, Thermo Fisher Scientific), according to the manufacturer's instructions. Lastly, samples were frozen at -80ºC, until further use.

4.8 RT-qPCR

The complementary DNA (cDNA) was synthesized using NZY Reverse Transcriptase (NZYTech, no. MB12402) and the VWR® thermal cycler XT96, following the protocol shown below.

1. On ice, in a sterile and nuclease-free microcentrifuge tube was prepared the next reaction mix per sample:

Table 2. Reaction mixture for cDNA (step 1)

Reagent	Volume (µL) per sample
Total RNA	5
Random Hexamer Mix	2
dNTPs Mix	1
Nuclease free-water	9

2. Next, the mix was centrifuged briefly and incubated at 65 °C for 5 min. Then, samples were incubated for 1 min on ice and next were added the following reaction components:

Table 3. Reaction mixture for cDNA (step 2)

Reagent	Volume per sample
10x Reaction buffer	2
NZY Reverse Transcriptase	1

3. The final volume for each sample was 20 µL. Before continuing with the protocol in the thermocycler, each tube was mixed gently and centrifugated briefly. Afterward, the next temperature cycle was carried out:

Table 4. cDNA temperature cycle

Temperature (°C)	Time (min)
25	10
50	50
85	5

4. Lastly, the cDNA product was stored at -20°C until further use.

The cDNA product was amplified using the 2x SensiFAST SYBR Hi-ROX kit (Bioline, Meridian Bioscience, Inc., no. BIO-92020). The assay was performed on a 384-well QuantStudio™ 7 Flex Real-Time PCR System (Applied Biosystems, Thermo Fisher Scientific). In each well were added 2 µL of the sample and 3 µL of the master mix. Primer sequences for qPCR are listed in Table A, whereas the master mix composition needed for each gene is described in table 5 and the PCR run method is shown in Table 6. Fold change expression was calculated using the threshold cycle ($2^{-\Delta\Delta Ct}$) method or with standard curves, both methods normalized to the level of the *Hprt* gene as an endogenous control.

Table 5. Primer sequences for qPCR

Gene	Forward sequence (5´--» 3´)	Reverse sequence (5´ --» 3´)
Hprt	GGTGAAAAGGACCTCTCGAAGTG	ATAGTCAAGGGCATATCCAACAACA
D-ldh	GAGGCTCTGAAGGCAGTTGT	GGAGGTTGACACCTGTGCAT
Cd36	GTCTATCTACGCTGTGTTCG	ACAGGCTTTCCTTCTTTGC
Pparγ	CTCACAATGCCATCAGGT	GCTGGTCGATATCACTGG
Dgat2	AGTTTCCTGGCATAAGGCCC	TGGGAACCAGATCAGCTCCAT
Cpt1	TGGACCCAAATTGCAGTGGT	GCATCTCCATGGCGTAGTAGT
Opa1	AGAAGTTTCTGAGGCCCTTCTCTT	TTCTTTGTCTGACACCTTCCTGT
Fis1	GACTGTGGCCCAGTAGAGAC	TCAAAATTCTTCAGATCCTCCACA
Drp1	GCTCAGTGCTGGAAAGCCTA	TCCATGTGGCAGGGTCATTT
Acss2	GCTTCTTTCCCATTCGGT	CCCGGACTCATTCAGGATTG
Il-8	GCTACGAACTGCCTGACGG	GCTGTTATAGGTGGTTTCGTGGA
Tnf-α	AGGCACTCCCCCAAAAGATG	TGAGGGTCTGGGCCATAGAA
Srebp1c	GCAGGACACTGAGAGACCCC	GTACCCACTGGCCTTCTCAC
Pdk4	ATCTAACATCGCCAGAATTAAACC	GGAACGTACACAATGTGGATTG
Fasn	AAGTTGCCCGAGTCAGAGAAA C	ACTCATAGAGCCCAGCCTTCCATC
Glo1	CCCTCGTGGATTTGGTCACA	ACGCTGTTTCTTTTCCACGC
L-ldh	AACTTGGCGCTCTACTTGCT	GGACTTTGAATCTTTTGAGACCTTG
Mfn2	CAGAGCAGAGCCAAACTGCT	AACATGTTGAGTTCGCTGTCC
Me2	CGTCCGGGGAGAGAAGATGT	CGTAAACGCCATTCCCTTGT
Hif1a	AGGATGAGTTCTGAACGTCGAAA	CTGTCTAGACCACCGGCATC
Tgf-β	CTGCTGACCCCCACTGATAC	GTCAGCGCTGAATCGAAAGC
Acc1	GGACACCAGTTTTGCATTGA	AGTTTGGGAGGACATCGAAA
Lxr	TGTGCGCTCAGCTCTTGTC	CTCCGTTGCAGAATCAGGAGAA

Hypoxanthine Phosphoribosyltransferase (*Hprt*), D-lactate dehydrogenase (*D-ldh*), Cluster of differentiation 36 (*Cd36*), Peroxisome Proliferator-Activated Receptor Gamma (*Ppar-γ*), Diacylglycerol O-Acyltransferase 2 (*Dgat2*), Carnitine palmitoyltransferase 1 (*Cpt1*), OPA1 Mitochondrial Dynamin Like GTPase (*Opa1*), Fission Mitochondrial 1 (*Fis1*), Dynamin-related protein 1 (*Drp1*), Acyl-CoA Synthetase Short Chain Family Member 2 (*Acss2*), Interleukin-8 (*Il-8*), Tumour necrosis factor alfa (*Tnf-α*), Sterol-regulatory element binding protein-1C (*Srebp1c*), Pyruvate Dehydrogenase Kinase 4 (*Pdk4*), Fatty Acid Synthase (*Fasn*), Glyoxalase I (*Glo1*), Lactate Dehydrogenase (*L-ldh*), Mitofusin 2 (*Mfn2*), Malic Enzyme 2 (*Me2*), Hypoxia Inducible Factor 1 Subunit Alpha (*Hif1a*), Transforming Growth Factor Beta (*Tgf-β*). Acetyl-CoA carboxylase 1 (*Acc1*), Liver X receptor (*lxr*).

Table 6. SYBR Green master mix composition for each sample

Component	Volume (µL)
Sybr green	5
Primer Forward	0.4
Primer Reverse	0.4
Nuclease free water	0.2

4.9 Total protein extraction

After the 24h of treatment and incubation, the hepatocytes were collected in a 1.5 mL microtube and centrifuged at 500 g for 5 min at 4ºC. Then, the pellet was resuspended in 500 µL phosphate-buffered saline (PBS; Thermo Fisher Scientific, no. 70011-036) and centrifuged at 500 g for 5 min at 4°C. Subsequently, cells were resuspended and homogenized in 60 µL of total protein buffer and incubated for 30 min on ice. Later, samples were sonicated for 30 seconds in ultrasounds and centrifuged at 3200 g for 10 min, 4ºC. The pellet was discarded, and the supernatant was collected. Protein concentration was quantified by the Bradford method.

A BSA calibration curve was performed. Then, 2 µL for each sample was diluted into 798 µL H_2O and mixed using a vortex for 5 sec. A 96-well plate was used to prepare the reaction mix using one well per sample. In each well was mixed 240 µL of the sample with 60 µL of BioRad assay dye. The absorbance was measured at 595 nm using a Varioskan™ LUX multimode microplate reader (Thermo Fisher Scientific). The protein concentrations were determined by using the linear regression of the standard curve. Finally, samples were frozen at -80ºC until further use.

4.10 Western blotting

Steady-state levels of selected proteins were determined by immunoblot analysis. Briefly, 40 µg of total protein extracts were separated in a discontinuous gel system of a 4% stacking gel and 8%, 10%, or 14% sodium dodecyl sulfate-polyacrylamide electrophoresis gel (SDS-PAGE), comprised of 30% (w/v) protogel (Panreac Applichem, no A1672), mili-Q water, upper and lower buffers, ammonium persulfate (APS) and tetramethyl ethylenediamine (TEMED; Merck Millipore, no. 1.10732.0100). The electrophoresis was performed first at a constant voltage of 100 V for 20 min and then at 130 V for approximately 1 h, until the bromophenol blue reached the end of the gel. The PageRuler™ Plus Prestained Protein Ladder (Thermo Fisher Scientific; no. 26620) was used as a molecular weight marker. The gels were then

transferred onto nitrocellulose membranes (Transfer Kit, Bio-Rad), using Trans-blot Transfer System (Bio-Rad) following the manufacturer's instructions. Then, the membranes were blocked with 5% (w/v) no-fat dry milk in TBS-tween-20 (0.5% v/v; Sigma-Aldrich, no. P1379) for 30 minutes and next washed with TBS-tween-20 for 10 min, 3 times. Afterward, the membranes were incubated at 4°C overnight with different primary rabbit or mouse polyclonal antibodies (Table 7).

Table 7. Primary antibodies for Western blot

Antibody against	Class/Host	Reference
CPT1A	Polyclonal/Rabbit	PA5-106270 Invitrogen Scientific Thermo Fisher
DGAT2	Polyclonal/Rabbit	PA5-103785 Invitrogen Scientific Thermo Fisher
D-LDH	Recombinant monoclonal/Rabbit	MAS-36153 Invitrogen Scientific Thermo Fisher
CD36	Polyclonal/Rabbit	PA1-16813 Invitrogen Scientific Thermo Fisher
Phospho-DRP1	Polyclonal/Rabbit	3455 Cell Signaling Technology
DRP1	Polyclonal/Rabbit	SC-32898 Santa Cruz Biotechnology, Inc
PPARα	Polyclonal/Rabbit	Ab-8934 Abcam
PPARγ	Monoclonal/Mouse	Ab-41928 Abcam
MFN2	Monoclonal/Mouse	AB-56889 Abcam
FASN	Monoclonal/Rabbit	C20G5 Cell Signaling Technology
NRF2	Polyclonal/Rabbit	Ab-31163 Abcam
β-Actin	Monoclonal/Mouse	A5541 Sigma-Aldrich Merck

Carnitine palmitoyltransferase 1A (CPT1A), Diacylglycerol O-Acyltransferase 2 (DGAT2), D-lactate dehydrogenase (D-LDH), Cluster of differentiation 36 (CD36), Dynamin-related protein 1 (DRP1), Peroxisome proliferator-activated receptor alpha (PPARα), Peroxisome proliferator-activated receptor

gamma (PPARγ), Mitofusin 2 (MFN2), Fatty acid synthase (FASN), Nuclear factor erythroid 2-related factor 2 (NRF2), Beta-actin (β-Actin).

Before the incubation with the secondary antibody, the membranes were washed with TBS-tween-20 (0.5% v/v) for 10 min, 3 times, and then incubated respectively with the goat anti-mouse IgG (H+L) or goat anti-rabbit IgG (H+L)-HRP secondary antibody (Bio-Rad, no. 170-6516 and no. 1706515 respectively) for 1 h and 30 min at room temperature (RT). Finally, the total levels of proteins were detected by Immobilon TM Western Chemiluminescent HRP Substrate (Merck Millipore, no. WBKLS0500) or Super SignalTM West Femto substrate (Thermo Fisher Scientific, no. 34096) using the ChemiDocTM MP System (Bio-Rad). Ponceau (Sigma-Aldrich, no. P7170) was used to assess loading control. β-actin was used as a loading control. The relative density of protein bands was analysed using the Image Lab Version 5.0 densiometric analysis program (Bio-Rad).

4.11 *L. reuteri*-metabolites analysis

The *Limosilactobacillus* strains *L. reuteri* DSM 17938 and *L. reuteri* ATCC PTA 6475 (BioGaia Probiotics) were grown aerobically in a centrifugate tube with 10 mL of De Man, Rogosa, and Sharpe broth (MRS; Merck, no. MC1106600500) for 48 h at 37°C. After the incubation period, the bacteria cultures were centrifugated for 15 min, 20°C, and 3000 rpm. 5 mL of the supernatant were recovered and then analysed by Gas Chromatography coupled with Mass Spectrometry (GC-MS) in the Shimadzu gas chromatograph GC-2010 and the gas chromatograph mass spectrometer GCMS-QP2010 Plus. MRS medium without inoculating was used as a control. The internal standard (IS) method was used for quantification and data were expressed as relative area to the internal standard. The technique was carried out by Professor Isabel Tavares de Almeida laboratory group at iMED.

4.12 Data analysis

All experiments were performed at least in triplicate and experimental data were displayed as the standard error of the mean (SEM). The statistical analysis was performed with GraphPad Prism 8.0 software (GraphPad Software, Inc., USA). The statistical methods used in each experiment is described in the respective figure legend.

5 Results and discussion

5.1 Lactic acid is the major metabolite *of L. reuteri*

To identify the major metabolites produced by *L. reuteri* two strains were analysed: *L. reuteri* DSM 17938 and *L. reuteri* ATCC 6475. Annex 1a, 1b, and 1c depict one of the chromatograms for the culture medium without inoculate, *L. reuteri* ATCC 6475 and *L. reuteri* DSM 17938, respectively. The GC-MS chromatogram shows the relative area of each detectable metabolite. Table 8 shows the average of the peak area ratio (analyte/IS) for each analyte. The GS-MS results substantiate that lactic acid is the major metabolite produced by both *L. reuteri* strains, whereas succinic, valeric, and isocaproic acids were detected in lower amounts compared with the control (Table 8). Particularly, in *L. reuteri* DSM 17938 the relative area for lactic acid was 19,90 and for the *L. reuteri* ATCC 647 strain 22,81, while in the control the value was 0,89. This highlight that Lactate is the major detectable metabolite in both strains. Nevertheless, we should not discard a role for the minor detectable metabolites, as they can still impact on host metabolism.

Since *L. reuteri* produces both lactate isoforms in the same proportion (Vitetta et al., 2017), we may suggest that supplementation with this probiotic increases the amount of D-lactate in the gut-liver axis. This result is consistent with our previous report in an animal model in which hepatic *D-ldh* mRNA levels were a fourfold increase in probiotic-treated mice. Moreover, increased D-lactate levels in the small intestine tissue also suggested an increase in gut D-lactate production (Santos et al., 2020). Although we demonstrated that D-lactate is one of the main effectors of this probiotic, we identified other metabolites in the *in vitro* experiment, which might have a role in the reduction of hepatic lipids. In particular, both strains showed increased abundance of succinic acid, 2-OH-isocaproic acid, 2-OH-3-methyl-valeric acid, 3 and 3-OH-propionic acid when compared with the control.

Table 8. Relative areas of detected metabolites were determined by GC-MS

Metabolite	Relative area		
	Culture medium (control)	***L. reuteri* DSM 17938 supernatant**	***L. reuteri* ATCC 6475 supernatant**
Lactic acid	0,89	19,90	22,81
3-phenyl lactic acid	0	0,26	1,54
2-OH-isocaproic acid	0	0,70	1,94
2-OH-3-methyl-valeric acid	0	0,06	0,01
3-OH-hexanoic acid	0,06	0,07	0,06
5-OH-hexanoic acid	0,16	0,13	0,14
Succinic acid	1,18	1,59	2,00

Data was collected after 48h of growth.

Intriguingly, succinic, valeric, and isocaproic acids have also been reported to ameliorate gut-liver axis disorders. Wang et al. reported that the commensal bacteria *Parabacteroides distasonis* (*P. distasonis*) alleviates obesity and metabolic dysfunctions via succinate production (K. Wang et al., 2019). It was observed that mice treated with *P. distasonis* enhanced the level of succinate in the gut, along with the activation of intestinal gluconeogenesis and reduction of food intake. Indeed, the study reported that succinate significantly reduced food intake by 37.5% and activated gluconeogenesis in the intestine. The activation of this pathway led to an increase in the concentration of glucose in the portal vein. This increment detected by a hepatoportal glucose sensor generates signalling to the brain by gastrointestinal nerves to control food intake (K. Wang et al., 2019). Succinate is also an intermediate in propionate synthesis (Fernández-Veledo & Vendrell, 2019), which may explain the augmentation in 3-OH propionic acid in both strains contrasted with the control (Annex 1b). Besides succinic acid, isocaproic acid and methyl-valeric acid were detected in *L. reuteri* DSM 17938 and ATCC 6475. Valeric acid and caproic acid also provide energy for intestinal epithelium and exert anti-inflammatory effects in cholestasis (B. Li et al., 2021). In fact, by modulating endogenous bile acids through cholestyramine in PBC-patients, were identified potential links between SCFAs, valeric acid, caproic acid, and bile acids dynamics. It was disclosed that elevations of these metabolites mediated, in part, the anti-cholestatic and anti-inflammatory effects of cholestyramine (B. Li et al., 2021). Despite the values of these metabolites being lower in both strains compared with lactic acid, we cannot rule out their putative effect on lipid metabolism. In addition, lactic acid can be converted into propionate, butyrate, or acetate. These molecules,

along with D-lactate, may cause beneficial effects against NAFLD (J. Wu et al., 2021). In fact, to the best of our knowledge, the role of D-lactate in lipid metabolism has not been examined. Therefore, further studies to determine their individual and/or synergistic effects are needed. Hence, focusing on these results represents a new approach to underlying a new readout of its function.

5.2 *L. reuteri* D-Lactate has a protective role against fatty acid accumulation in hepatocytes

The use of probiotics is associated with their ability to restore host homeostasis. Recent data described that some *Lactobacillus* species have the capability to diminish host intestinal fatty acid absorption under HFD feeding conditions, through the consumption of dietary fat, reducing the amount of fat absorbed by the liver (Jang et al., 2019). Our preliminary results demonstrated that preventive supplementation with *L. reuteri* DSM 17938 in a NASH animal model reduced hepatocellular vacuolization (Figure 6). This raises the question of whether the probiotic effect could be in part due to its metabolites production which, in turn, modulates lipid metabolism. Since we confirmed that D-lactate is a major metabolite of *L. reuteri* DSM17938, we speculate that this metabolite could have role in liver lipid metabolism.

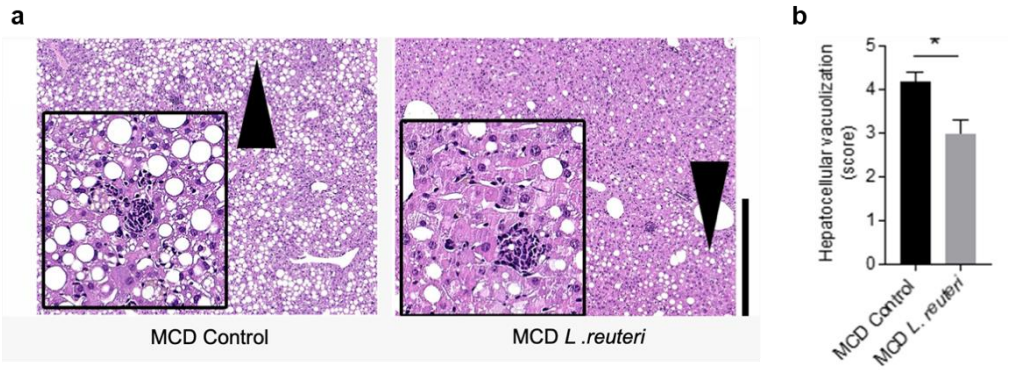

Figure 6. *L.reuteri* protects against liver fat accumulation. Representative images of hematoxylin and eosin (H&E) stained liver sections from MCD control and supplemented with *L. reuteri* DSM 17938. Scale bar = 100 µm. (b) Hepatocellular vacuolization score in MCD-control and *L. reuteri* supplemented mice. For hepatocellular vacuolization statistical analysis was performed using t-test *$p < 0.05$.

In order to explore the role of D-lactate in an *in vitro* experiment, we induced lipid accumulation with PA, one of the most abundant FAs present in the Western diet and whose excessive levels lead to hepatic steatosis (Eynaudi et al., 2021). For the treatment strategy, the minimum concentrations of D-Lactate and PA that resulted in a robust induction of steatosis

without loss of viability were identified. Upon preliminary optimization, only 1 and 5 mM of D- and L-lactate as well as 125 µM of PA showed more consistent results regarding the MTS assay. Moreover, despite not showing significant differences between groups, the groups subjected to 1 and 5 mM of D-lactate and PA 125 µM caused less loss of mitochondrial viability (Annex 1d). Therefore, these concentrations were used in the following experiments. Additionally, to our knowledge, D-lactate adverse effects have been mostly based on measurements of D-lactate concentrations in plasma (Levitt & Levitt, 2020). To reach more than 3 mM of D-lactate in plasma implies that the liver may be exposed to higher concentrations of the metabolite

To evaluate our hypothesis, after the induction of FAs accumulation and the treatment strategy with D- or L-lactate, we performed a Nile Red staining assay to detect intracellular lipids. The Nile red fluorometric quantification showed that after 24h, the PA treatment causes a significant increase in lipid accumulation compared with the control untreated as expected ($p = 0.0020$) (Figure 7a-b). The hepatocytes treated with 24h PA and subjected to 1 mM of D or L-lactate, did not show significant differences compared with the PA control group (Figure 7a). While the use of 5 mM of D-lactate showed significantly less accumulation of FAs when compared with PA alone ($p = 0.0097$) or L-lactate ($p = 0.0455$) (Figure 7b).

To investigate the consumption rate of D-lactate during the *in vitro* assays we used a colorimetric assay that specifically detects D-lactate isoform. For that purpose, we performed the test at two time points, immediately after the treatment started and at the end of the incubation period, 6h (data not shown) or 24h. Clearly, both D-lactate initial concentrations decreased after 24h, either in the presence or absence of PA (Figure 7c-d), suggesting that the metabolite is being consumed by the cells. This brings into question whether the cells switch their metabolism to metabolize the D-lactate first due to its potential toxicity. Furthermore, to provide a better understanding of the cell dynamics under the established conditions, we calculated the D-lactate consumption rate per hour. Overall, with 5 mM, the consumption rate was notably higher in both time conditions compared with 1 mM (Figure 8). This could be indicative that AML12 D-lactate maximum metabolization rate is ~100 µM/h. Although accordingly to MTS assays, 5 mM of D-lactate did not show toxicity we show that the cells were under higher physiological stress with 5 mM than with 1 mM of D-lactate.

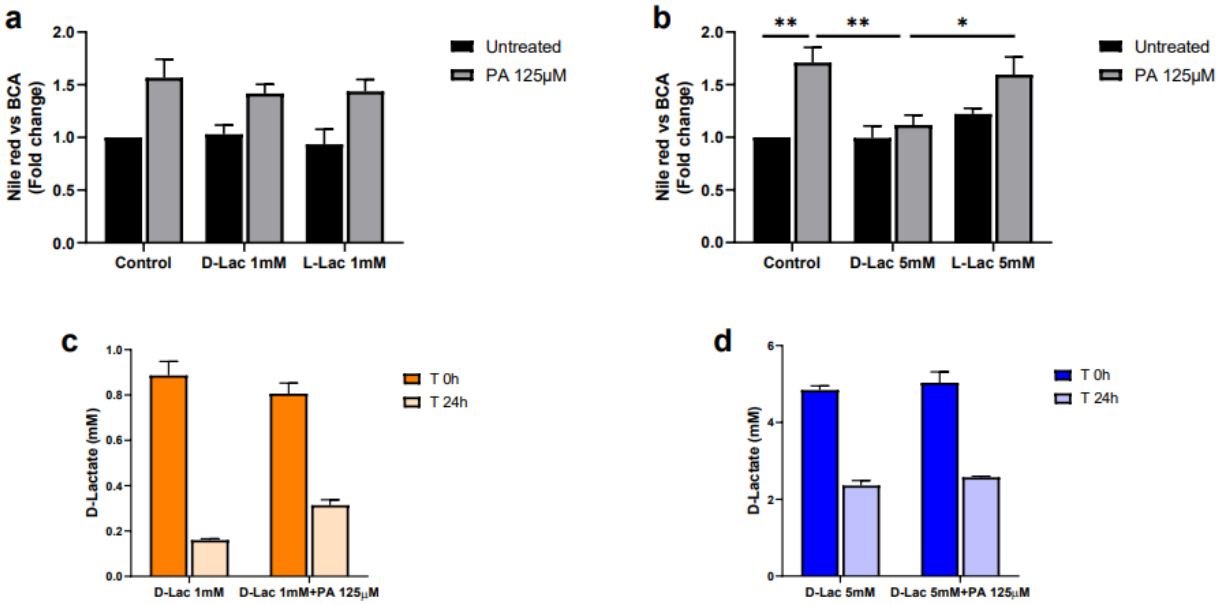

Figure 7. D-Lactate has a protective role against fatty acids accumulation in AML12 murine hepatocytes. Fluorometric measurement of Nile red staining normalized for total protein content after 24h treatment with palmitic acid (PA) 125µM and D or L-lactate 1mM (a) or 5Mm (b). D-Lactate colorimetric assay after 24h treatment with PA 125µM and D-Lactate 1mM (c) or 5Mm (d). For Nile Red assay mean values were calculated as fold change versus controls with error bars ± SEM of 4 individual experiments. Statistical analysis was performed with ANOVA Tukey's multiple comparisons test. *p< 0.05 and **p < 0.01. For the D-lactate colorimetric assay were performed 2 individual experiments.

Our preliminary *in vivo* results suggest that amelioration of liver injury might be in part via decreased liver uptake of long chain fatty acids, triglycerides production, and reduced lipogenesis. We should take into account that the effects could also be attributable to the LAB strain and its interactome, rather than D-lactate alone. Nevertheless, our *in vitro* data show that this molecule might have a protective role against hepatic lipid accumulation (Figure 7b). In addition, in figure 8 we can observe that 5mM induces maximal turnover of D-lactate in cells in contrary to 1mM. Indeed, D-lactate can be metabolized into pyruvate and subsequently into acetyl-CoA, which may be used in several biological pathways including lipogenesis (Ipsen et al., 2018). However, we did not observe an increase in DNL in treated cells, but rather a decrease (see section 5.3). A plausible explanation for the consumption rate in the 5 mM concentration could be explained by an attempt of the cells to eliminate the potential toxic amounts of D-lactate from the surrounding environment. Future work should focus on PA concentration measurement in both time points as well as on the evaluation of cellular stress markers.

Here we show that the consumption rate is dependent on the D-lactate concentration. We speculate that cells subjected to 5 mM of D-lactate are in constant stress to eliminate it, whereas

under 1 mM the consumption rate could indicate a reduction in cellular stress. Our results provide the framework for future studies to assess *in vivo* the beneficial effects of D-lactate 1 mM. In fact, after 24h the beneficial effect against FAs storage is perceptible when D-lactate levels in the culture medium reach less than 2.5 mM.

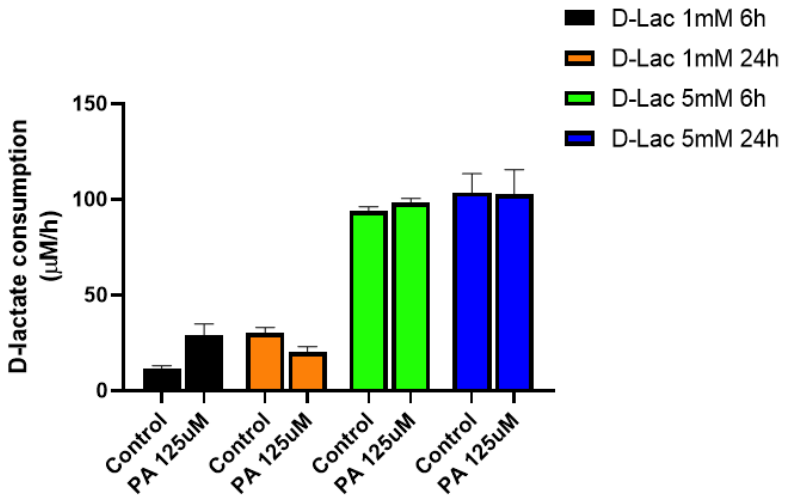

Figure 8. D-Lactate consumption rate per hour. The consumption rate was calculated considering the remained amount of D-lactate in the culture medium after 6h (black and green bars) and 24h (orange and blue bars). Results correspond to 2 individual experiments.

5.3 D-Lactate alters the expression of genes related to lipid metabolism

According to our previous study, supplementation with *L. reuteri* doubled the amount of D-lactate in the small intestine tissue and increased four times mRNA levels of liver *D-ldh* (Santos et al., 2020), which can only be found in mitochondria. Interestingly, our *in vitro* experiment showed that after 6h, 5 mM of D-lactate but not L-lactate can significantly increment hepatic *D-ldh* mRNA expression in the condition without PA ($p = 0.037$) (Figure 9a). Upon 24h, mRNA expression of *D-ldh* was significantly upregulated in cells treated with D-lactate 1 and 5 mM alone ($p < 0.0001$ and $p = 0.0005$, respectively) as well as in D-lactate with PA conditions ($p < 0.0001$ for both concentrations) (Figure 9b). This result resembles our *in vivo* model and validates that D-lactate rises the expression of the enzyme *D-ldh* in the liver.

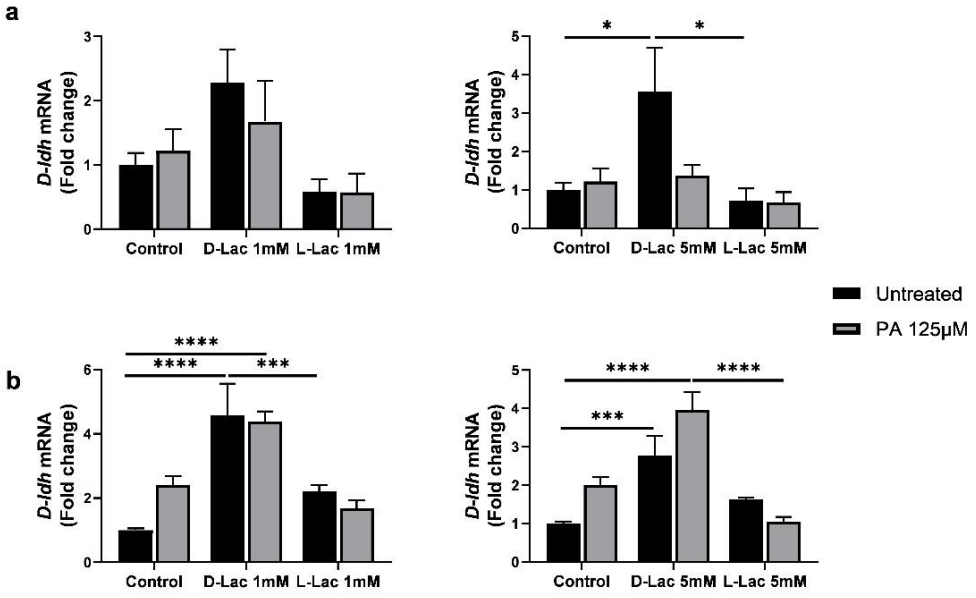

Figure 9. D-lactate increases hepatic D-ldh expression. Quantitative RT-PCR analysis of *D-ldh* after 6h (a) or 24h (b) under D or L-lactate 1 or 5mM in murine hepatocytes with and without palmitic acid (PA) treatment. Mean values were calculated as fold change versus control untreated with error bars ± SEM of 7 to 8 individual experiments. Statistical analysis was performed with ANOVA Tukey's multiple comparisons test. *$p < 0.05$, ***$p < 0.001$ and ***$p < 0.0001$.

The liver is critical for digestive absorption and performs the uptake, synthesis, accumulation, and secretion of lipids and lipoproteins (Trefts et al., 2017). The histological differences observed in liver fat accumulation of the MCD-induced mice supplemented with *L. reuteri* (Figure 6a), led us to investigate whether D-lactate treatment alters liver lipid metabolism. Since steatosis could be attributed to a combination of DNL, fatty acid uptake, and reduced fatty acid oxidation (Ipsen et al., 2018), we assessed mRNA markers of these mechanisms. First, we determined levels of the transcription factors *Chrebp* and *Srebp1c*, responsible for the coordinated induction of glycolytic and lipogenic genes respectively (Batchuluun et al., 2022). Additionally, we evaluated gene expression of *Lxr* (transcriptional control of lipid metabolism), *Cd36* (long-chain fatty acid transport), *Cpt1* (long-chain fatty acid mitochondrial uptake), *Dgat2* (triglycerides synthesis), *Pparγ* (lipid droplets formation), *Acc1* and *Fasn* (fatty acid synthesis). Besides D-lactate, we established a treatment with L-lactate as an internal control to corroborate whether the alterations in the metabolic pathways were dependent of the lactate enantiomer or not. Of note, we identified specific changes related only to D-lactate and we focused on those alterations.

After 6h treatment, modulation with D-lactate 1 mM in hepatocytes exposed to PA, significantly decreased mRNA levels of *Cd36*, *Srebp1c*, and *Dgat2* when compared to the cells subjected to PA alone (*Cd36*, $p = 0.0016$; *Srebp1c*, $p = 0.0016$; and *Dgat2*, $p < 0.0001$) (Figure

10 a, c and f). Although no statistical difference was reported for *Cpt1* and *Pparγ* between these groups, their expression levels tended to decrease slightly in the PA-treated cells modulated with D-lactate 1 Mm compared with the PA group (Figure 10 b and g). On the other hand, the treatment with 5 mM of D-lactate in the cells subjected to PA significantly diminished the levels of *Cd36, Cpt1,* and *Srebp1c* in contrast with PA control (*Cd36, p*<0.0001; *Cpt1, p*= 0.0209; and *Srebp1c, p*= 0.0005) (Figure 10 a-c). Albeit no significant differences were reported for *Dgat2* and *Pparγ* between PA control and 5 mM D-lactate treated groups, it can be observed from figure 10 (f-g) that the patterns are essentially the same as in the lowest concentration. Interestingly, *Fasn* levels showed an opposite result among both concentrations of D-lactate in the PA-induced steatosis conditions. With D-lactate 1 mM, *Fasn* levels were significantly upregulated in D-lactate and PA treatment compared with PA control (*p*=0.0164), whereas under 5 mM the mRNA levels decreased (Figure 10e). For the 6h treatment, results from *Acc1* and *Lxr* genes were not consistent between experiments (data not shown).

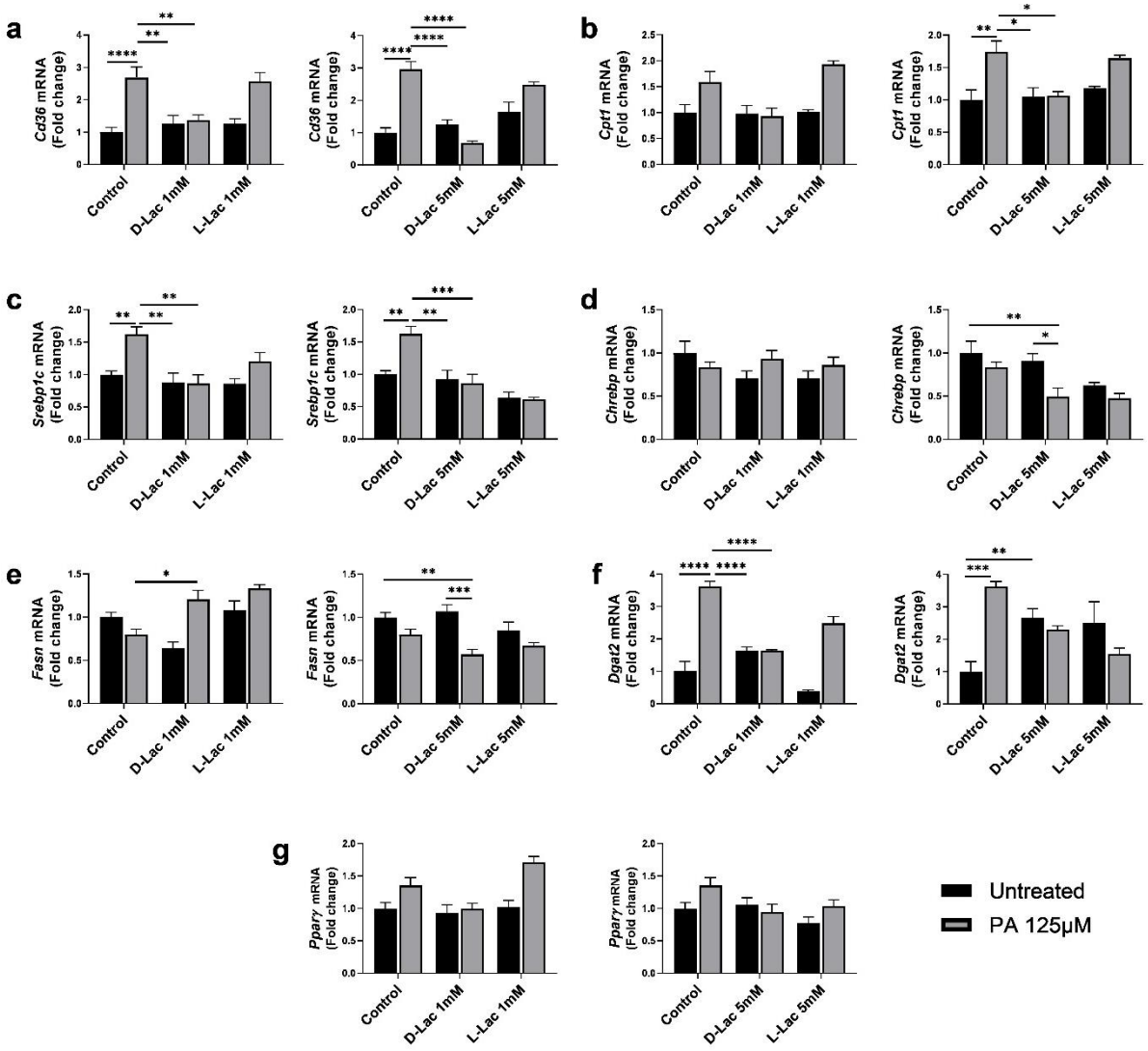

Figure 10. D-lactate alters the expression of hepatic-steatosis-associated genes. Quantitative RT-PCR analysis for (a) *Cd36* (fatty acid uptake), (b) *Cpt1* (fatty acid mitochondrial uptake), (c) *Srebp1c* (d) *Chrebp* (e) *Fasn* related to De Novo Lipogenesis, (f) *Dgat2* (triglycerides synthesis) and (g) *Pparγ* (lipid droplets formation), in mouse hepatocytes treated with palmitic acid (PA) 125 µM and 1 or 5mM of D or L-lactate for 6h. Mean values were calculated as fold change versus control untreated with error bars ± SEM of 7 to 8 individual experiments. Statistical analysis was performed with ANOVA Tukey's multiple comparisons test. *$p < 0.05$, **$p < 0.01$, ***$p < 0.001$ and ****$p < 0.0001$.

Overall, figure 10 reveals that L-lactate can diminish FAs biogenesis but not the uptake neither to the cytosol nor to the mitochondria, whereas D-lactate restores to control levels FAs transport in both sites. In fact, Nile red assay demonstrated that D-lactate, but not L-lactate, decreases FAs influx. Therefore, it can be inferred that L-lactate does not alter FAs transport after 6h. Interestingly, upon 24h treatment, we can have a beneficial effect from L-lactate either in lipid transport or lipid synthesis (Figure 11a-g). This could be explained by the fact that L-lactate is metabolized faster than D-lactate (Levitt & Levitt, 2020). Cells might equilibrate L-

lactate levels, while D-lactate is still present and can cause cellular stress. Particularly, after 24h treatment mRNA expression of *Cpt1* was significatively diminished either with 1 or 5 mM of D-lactate in the PA-treated cells compared with PA control ($p<0.0001$), reaching levels of the control untreated, whereas mRNA levels related to FAs transport to the cytosol did not report statistical significance (Figure 11 a-b). Moreover, the gene expression of *Srebp1c*, *Fasn*, and *Acc1* were not significantly different between PA-induced steatosis groups modulated with D-lactate and PA control (Figure 11 c, e, and h). Nevertheless, we observed that when contrasting PA control with the PA-groups modulated with D-lactate, it is clear that the metabolite may contribute to restoring mRNA levels of *Cd36*, *Srebp1c*, and *Acc1* (Figure 11 a, c, and h). As can be seen in figure 11 (i), *Lxr* is upregulated in all PA treated cells compared with control cells ($p = 0.0048$), as expected (Schulman, 2017). LXR induces the expression of several genes implicated in the regulation of lipid metabolism (Schulman, 2017). Here, we observed an upregulation of the LXR targets *Srebp1c* and *Acc1* exclusively in the PA-control compared with the control untreated, which is in line with *Lxr* levels in this condition. On the other hand, although there are no significant differences between groups treated only with PA and the groups treated with PA and D-lactate together, our data show a reduction in *Srebp1c* and *Acc1* expression whereas no alterations in *Fasn* mRNA levels. In fact, the transcriptional regulation of *Acc1* and *Fasn* is governed by the three transcription factors SREBP1c, CHREBP, and LXR. Although *Lxr* mRNA levels are upregulated in both treatment strategies and also the mRNA levels of *Chrebp* in the lowest concentration, *Srebp1c* expression diminishes in both cases which might explain the mRNA stabilization for *Acc1* and *Fasn*. Moreover, under the highest concentration of D-lactate, the mRNA expression of *Chrebp* was not altered.

Additionally, it has been demonstrated that SREBP1c contributes to NAFLD through increased DNL (Linden et al., 2018). For instance, liver *Srebp1c* mRNA levels exhibited net increases of 70 and 62% in obese patients with steatosis and steatohepatitis over control values, respectively (Pettinelli & Videla, 2011). DNL can increase endogenous PA as well as the formation and release of VLDL enriched with PA and cholesterol esters. This raises the question of whether D-lactate modulates the PA intake. Therefore, it is crucial that new experiments should be performed to evaluate the PA uptake when cells are treated with D-lactate.

The final step of liver TG biosynthesis is catalysed by the enzyme DGAT2, which is responsible for incorporating endogenously synthesized monounsaturated FAs into TGs. In accordance with the shortest incubation period, mRNA levels of *Dgat2* were also diminished after 24h in hepatocytes subjected to PA and treated with D-lactate (Figure 11f). Particularly,

significant differences were reported between PA with D-lactate 5mM and PA control (p = 0.0177). This is in accordance with the *in vivo* mice model in which *Dgat2* mRNA was also downregulated in the liver tissue of probiotic-treated mice. Indeed, it has been reported that inhibition of *Dgat2* results in a downregulation of multiple genes encoding proteins involved in lipogenesis, including *Srebp1c* (Sabnis, 2021). Also, DGAT2 inhibition suppresses hepatic VLDL secretion and leads to a reduction in circulating cholesterol levels (McLaren et al., 2018; Sabnis, 2021). This led us to hypothesize that in our *in vitro* model cholesterol levels might be at lower levels in the cells treated with PA and D-lactate together since *Srebp1c* and *Dgat2* expression is downregulated compared with PA control. Finally, this is supported by the Nile Red assay, in which a higher amount of D-lactate shows a significant reduction in lipid accumulation. Therefore, we demonstrated that D-lactate is able to reduce TG synthesis under steatosis conditions. Nevertheless, future work should explore cholesterol pathways under D-lactate treatment.

On the other hand, it has been reported that DGAT2 is one of the targets of CHREBP (Shin et al., 2016). However, in our model this association is not clearly evident (Figure 11 d, f). Of note, D-lactate can be converted to pyruvate which, in turn, can be made into glucose and activate CHREBP. In our experimental model, it is unlikely that D-lactate metabolization can contribute to gluconeogenesis and CHREBP activation. This conclusion is supported by the observation that in most of the cases 1 and 5 mM of D-lactate did not upregulate *Chrebp* expression.

FAs from adipose tissue, diet, and DNL are stored within LDs in hepatocytes. In agreement with the reduction in TG synthesis in the steatosis groups under D-lactate treatment, figure 11 (g) illustrates a significant reduction in mRNA levels of *Pparγ* under both D-lactate treatments. Evidence indicates that PPARγ modulates liver lipid metabolism through the uptake of FAs from circulation and storing them in lipid droplets (LDs) (Lee et al., 2018). Moreover, it has been reviewed that overexpression of PPARγ1 and PPARγ2 may induce LDs accumulation in the liver, which is the initiation step in NAFLD progression (Lee et al., 2018). Hepatic PPARγ expression is maintained at a low level in normal conditions, which allows the liver to release VLDL proteins to peripheral tissues as an energy source. An excess of saturated fatty acids in the cytoplasm would trigger the formation of harmful bioactive lipids, causing lipotoxicity. Therefore, TG synthesis and LDs formation should protect the liver from damage induced by these molecules (Filali-Mouncef et al., 2022). This would be a normal process for combating against abnormal FAs flux on circulation. In line with this, the mRNA levels reported in our model for *Pparγ* in PA-treated hepatocytes are significantly upregulated compared with the

control untreated (Figure 11g). Interestingly, the treatment with both concentrations of D-lactate in the steatosis conditions significantly lowered *Pparγ* expression, compared with the steatosis control group. Likewise, both D-lactate concentrations diminished the expression of *Cd36* in the steatosis condition compared with PA control (Figure 11a) but no statistical significance was reported. However, mRNA levels revealed a considerably decrease with the D-lactate treatment. The fatty acid translocase CD36 exerts pleiotropic actions regulating liver lipid homeostasis and is a direct target of PPARγ (Rada et al., 2020). Increased PPARγ upregulates the expression of *Cd36* for FFAs uptake and contributes to lipid accumulation in the liver. In addition, prolonged exposure to FFAs increased not only total expression of CD36, but also triggered its translocation to the plasma membranes in rat hepatocytes (Rada et al., 2020). Our results reinforce this crosstalk since mRNA expression of *Cd36* and *Pparγ* demonstrate a similar trend in the presence of PA. Further, the D-lactate treatment in the PA condition abrogated the upregulation of both genes in the two timepoints as well as in both lactate concentrations (Figures 10a and 11a). This effect was significant in both D-lactate concentrations after 6h for *Cd36* whilst for *Pparγ* was markedly different after 24h. Thereby, the assumption that D-lactate might have a putative role in PPARγ signalling and in consequence a modulator of CD36 translocation, is a plausible hypothesis that should be explored. Further studies are warranted to confirm a possible indirect link between PPARγ and D-lactate in liver lipid metabolism.

LDs also interact with mitochondria when nutrients are scare, in order to maintain metabolic energy. This communication might facilitate the transfer of FAs for β-oxidation (Filali-Mouncef et al., 2022). Interestingly, it has been reported a dysregulation of β-oxidation throughout NAFLD progression (Lu et al., 2021). Therefore, we sought out to understand if D-lactate metabolite is able to modulate fatty acid oxidation. As expected, similar to the shortest timepoint, after 24h treatment *Cpt1* expression was significantly upregulated in the PA-treated hepatocytes when compared with control untreated (Figure 11b) ($p<0.0001$). This suggest that the cells should increase this mechanism in compensation to the FAs overload. Additionally, this increase is consistent with the increment of *Pparγ* and *Cd36* mRNA levels which confirm an interaction between FAs transport and LDs formation and catabolism (Figures 11a and 11g). Likewise, when hepatocytes underwent steatosis induction and D-lactate treatment, *Cpt1* mRNA expression dropped compared with PA-control, significantly upon 24h treatment ($p<0.0001$) (Figure 11b). This implies that D-lactate is capable of restoring the FAs (or LD) shuttle to the mitochondria and perhaps subsequently β-oxidation process. In fact, since we

observed a decrease in *Cd36*, which means less transport of FFAs from the extracellular matrix to the cytoplasm, it was also expected that FAs transport from the cytoplasm to the mitochondria would be downregulated. Moreover, the decrease in both transporters is concordant with the Nile red assay observed previously, where in the steatosis groups the presence of D-lactate diminished FAs accumulation. Nevertheless, an important question for future studies with the same *in vitro* model and treatment strategy, is to unveil if exist significant gene alterations within the four steps of the oxidation process: dehydrogenation, hydration, oxidation and thyolisis.

Overall, these results led us to infer that D-lactate could have an indirect role in PPARγ activity. Future work should validate this hypothesis, either *in vitro* or *in vivo* experiments, broadening the assessment of downstream target genes for PPARγ as well as its upstream regulators. Importantly, we need to take in consideration that signalling pathways involved in NAFLD spectrum are not always positively correlated. For instance, fat accumulation and expression of DNL-associated genes, such as *Srebp1c*, *Fasn*, *Acc1* and *Dgat2*, have been negatively correlated with NASH progression and fibrosis stage (Nagaya et al., 2010), which demonstrates that liver lipid metabolism is NAFLD-stage dependent. Moreover, besides the fact that not all the genes involved in the same pathway are altered in the same direction, our data support the hypothesis that D-lactate may have different roles between reactions of the same signalling pathway. In particular, the gene expression of *Cd36*, *Cpt1*, *Dgat2* and *Ppary* decreases when D-lactate is present in the PA-induced cells. Thereby, it is reasonable to assume that D-lactate restores the transcription of these genes in steatosis *in vitro* models. Nevertheless, the mechanism behind should be explored.

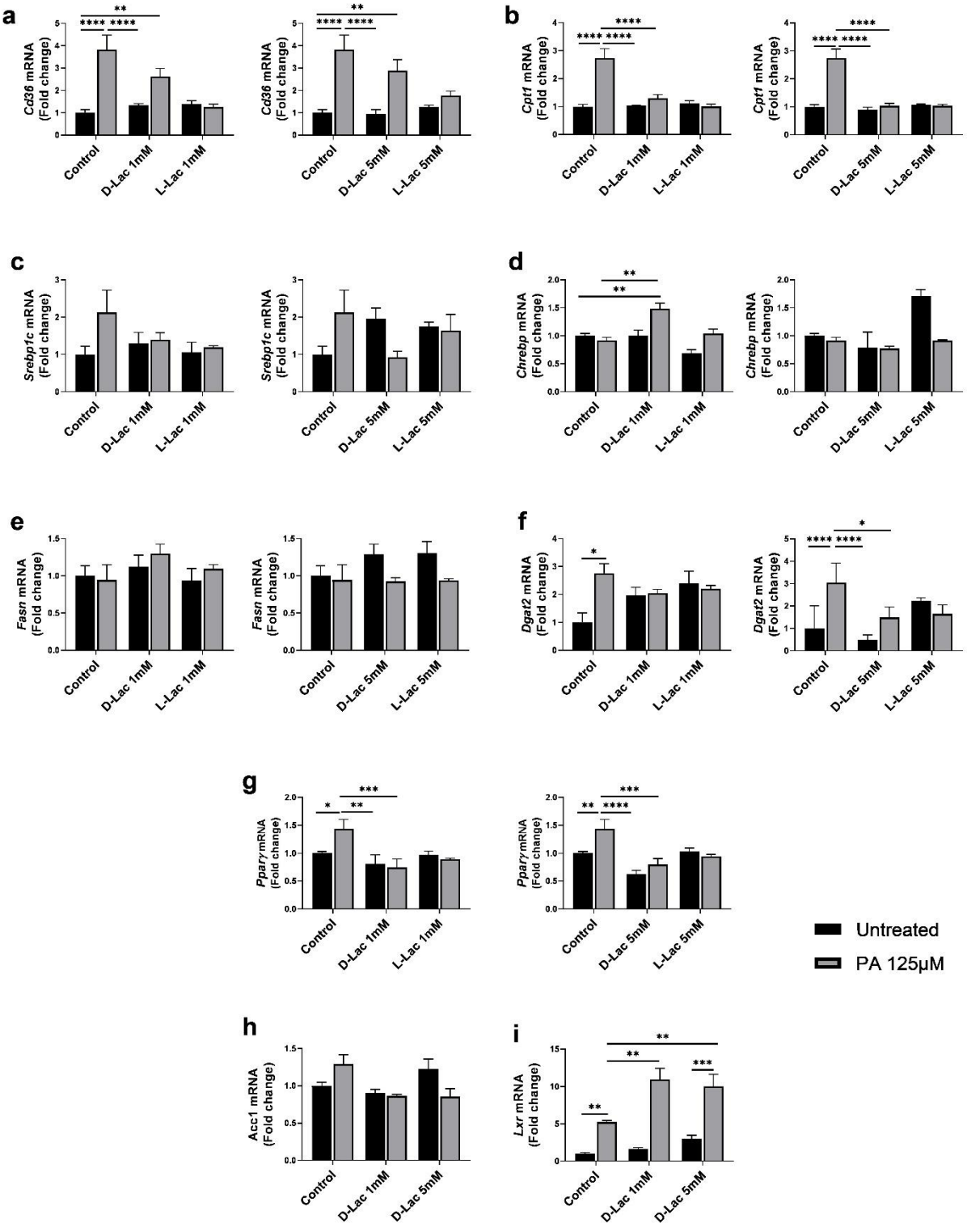

Figure 11. D-lactate alters the expression of hepatic-steatosis-associated genes. Quantitative RT-PCR analysis for (a) *Cd36* (fatty acid uptake), (b*) Cpt1* (fatty acid mitochondrial uptake), (c) *Srebp1c* (d) *Chrebp* (e) *Fasn* related to De Novo Lipogenesis (DNL), (f) *Dgat2* (triglycerides synthesis), (g) *Pparγ* (lipid droplets formation), in mouse hepatocytes treated with palmitic acid (PA) 125 µM and 1 or 5mM of D or L-lactate for 24h. Of note, for Acc1 and *Lxr* (both related to DNL), the conditions with L-lactate are not shown (h, i). Mean values were calculated as fold change versus control untreated with error bars ± SEM of 7 to 8 individual experiments. Statistical analysis was performed with ANOVA Tukey's multiple comparisons test. *$p < 0.05$, **$p < 0.01$, ***$p < 0.001$ and ****$p < 0.0001$.

Lactobacillaceae strains are able to ameliorate liver inflammation and fibrosis (Bajaj et al., 2022; Liu et al., 2020; Ritze et al., 2014). Recently, our research group discovered that *L. reuteri* supplementation reduced liver fibrosis in acute bile duct-ligated (BDL) mice, and that its metabolite D-lactate decreases macrophage TGF-β production that may link to reduced liver fibrosis (Santos et al., 2020). Therefore, besides alterations of lipid metabolism, *L. reuteri* and its metabolites might also influence other host metabolic pathways.

The increase in the TG concentration inside hepatocytes can produce toxic free radicals like ROS, reactive nitrogen species (RNS) and lipid free radicals. Free radicals activate several apoptotic and necrotic pathways which upregulates different cytokines like tumour necrosis factor alpha (TNF-α), transforming growth factor beta (TGF-β) and interleukins (IL) inside the necrotic liver cells (Nair & Nath, 2020). Here, we sought to understand the effect of D-lactate on inflammatory characteristic markers of NAFLD, including IL-8, TNF-α and TGF-β (Bessone et al., 2019; X. Li & Wang, 2020). In our *in vitro* model, the *IL-8* gene was found to be significantly lower after 6h treatment with D-lactate 1 or 5mM in the presence of PA compared with PA control ($p = 0.0110$ and $p = 0.0039$, respectively) (Figure 12a). The mRNA level of this interleukin was not dissimilar between these conditions in the 24h experiment. Nonetheless, *IL-8* expression was significatively different sole with the lowest concentration ($p = 0.0004$) (Figure 12b). Excessive FFAs influx in liver may induce upregulation of TNF-*α* (Tiegs & Horst, 2022). Based on data in figure 12 (c-d), upon 6 or 24h treatment, the mRNA expression of *Tnf-α* was not statistically significant between PA-treated cells and PA-treated cells modulated with D-lactate. Nonetheless, in the 6h experiment, it is considerable higher the mRNA level when D-lactate and PA are both present in the culture medium compared with the other groups (Figure 12c). Apparently, both molecules generate a pro-inflammatory signal, however, it could be associated with PA toxicity and not with the presence of D-lactate since there are no significant differences between the PA-treated hepatocytes exposed to D-lactate and PA-control. Indeed, it is well-known that PA augments TNF-α-induced cytotoxicity trough the activation of TLR4-dependent signalling pathways (Oh et al., 2012; Tiegs & Horst, 2022). The same effect was observed after 24h treatment in the hepatocytes subjected to PA and treated with 1 or 5 mM of D-lactate (Figure 12d).

In particular, palmitate serves as building lipid blocks and can be elongated and unsaturated to form more complex lipids, such as phospholipids, diacylglycerol and ceramides, who may have critical cell signalling functions in inflammation (Korbecki & Bajdak-Rusinek, 2019). Here we confirmed that PA induced AML12 murine hepatocytes toward a pro-inflammatory state, possibly through the activation of the TLR4.

TGF-β escalates the progression of acute liver damage to chronic condition. This cytokine not only fastens the progression but also activates the quiescent HSCs and differentiates them into fibroblasts (Nair & Nath, 2020). After 24h treatment, we observed a significant decrease in *Tgf-β* expression in the condition with PA and D-lactate 1 mM contrasted with PA control (p= 0.0167) (Figure 12f). Nevertheless, *Tgf-β* mRNA levels did not show significant differences between PA control and control untreated. In contrast, hepatocytes exposed to PA for 6h significantly augmented *Tgf*-β expression (p= 0.0001) (Figure 12e). Surprisingly, at this timepoint it was reported an opposite result between the two concentrations of D-lactate either in the presence or absence of PA. While with 1 mM of D-lactate alone does not dysregulate the cytokine expression, the highest concentration causes a significant augmentation of *Tgf-β* mRNA levels compared with the control untreated (p<0.0001). In addition, D-lactate 5 mM alone reflects a more pro-inflammatory profile rather than the effect observed in the group in which PA and D-lactate 5 mM are present. However, after 24h, the cytokine expression is restored under this condition. Although it is difficult to ascertain the reason for these controversial results, our study suggests that with respect to inflammation, D-lactate can switch its effect in a concentration-dependent manner, which is not observed in hepatic-steatosis-related genes. Nevertheless, it is needed to investigate other inflammatory signalling-associated components.

It has been reported that exogenous lactate does not affect the expression of pro-inflammatory genes and that plays an anti-inflammatory role through the stimulation of histone lysine lactylation (D. Zhang et al., 2019). Moreover, it was reported that lactate activates the G-protein-coupled receptor 81 (GPR81) in its physiological concentration range of 1–20 mM (Ranganathan et al., 2018). The gastrointestinal mucosa is exposed to high levels of lactate (~10 mM) from diet and bacterial fermentation. So, it is conceivable that lactate concentrations in the colon are sufficient to activate GPR81 (Ranganathan et al., 2018). In addition, under inflammatory environment lactic acid can also activate the GPR81-mediated pathway and inhibits the activation of the Nuclear Factor-κB (NF-kB), which upregulates the expression of pro-inflammatory cytokines such as TNF-α, TGF-β and IL-8 (H. cun Zhou et al., 2022). A recent *in vitro* experiment demonstrated that hepatocytes exposed to total cellular fluids from lactic acid bacteria (LAB) downregulate the expression of TLR and the NF-κB pathway, decreasing the expression of inflammatory cytokines (Kanmani & Kim, 2018). Hence, we speculate that D-lactate can be the active molecule responsible for those alterations since our results showed that D-lactate alters *IL-8* and *Tgf*-β mRNA levels.

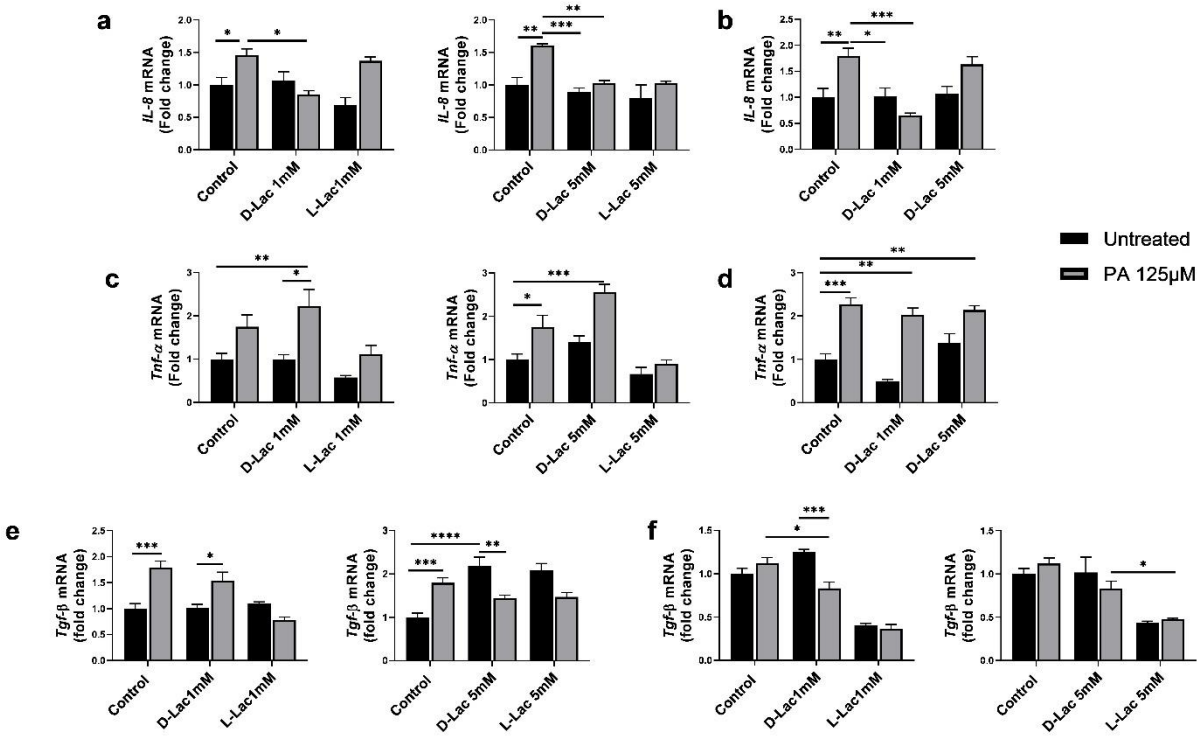

Figure 12. **D-lactate alters mRNA levels of inflammation markers in mouse hepatocytes**. Quantitative RT-PCR analysis for *IL-8* after 6h (a) and 24h (b) of D or L-lactate treatment. Quantitative RT-PCR analysis for *Tnf-α* after 6h (c) and 24h (d) of D or L-lactate treatment. (c) qPCR mRNA expression levels of *Tgf-β* upon 6h (e) and 24h (f) treatment of D or L-lactate treatment. For *IL-8* and *Tnf-α* the conditions with L-lactate are not present on figure 11. Mean values were calculated as fold change versus control untreated with error bars ± SEM of 5 to 6 individual experiments. Statistical analysis was performed with ANOVA Tukey's multiple comparisons test. **p* < 0.05, ***p*< 0.01, ****p* < 0.001 and *****p* < 0.0001.

Since D-lactate is exclusively metabolized in the mitochondria (Levitt & Levitt, 2020; Manosalva et al., 2022) we proposed that this metabolite could alter mechanisms of mitochondria dynamics, mainly fusion and fission processes. To test our hypothesis, we analysed markers for mitochondrial fission: Fission Protein 1 (FIS1) and Dynamin-Related Protein 1 (DRP1), as well as Optic Atrophy 1 (OPA1) and Mitofusin 2 (MFN2) for mitochondrial fusion (Giacomello et al., 2020). MFN2 regulate outer mitochondrial membrane (OMM) fusion, while OPA1 orchestrates inner mitochondrial membrane fusion. Both proteins act together to repair the dysfunctional mitochondria by mixing their contents with those of healthy mitochondria (Giacomello et al., 2020). On the other hand, fission process is mainly regulated DRP1 and FIS1 proteins. DRP1 can assemble into a ring-like structure that squeezes cellular membranes to divide mitochondria into two parts. FIS1 is anchored to the OMM, and its function is to recruit DRP1 from the cytoplasm to the OMM. In this process, the mitophagy

programme is initiated to eliminate bad mitochondria, and the mitochondrial biogenesis signal is activated to renew mitochondrial production (Giacomello et al., 2020).

Based on Figure 13, after 6h of modulation with D-lactate 1 mM in PA-treated cells, it was evident a significant reduction in *Drp1* mRNA compared with PA control (p= 0.0105) whereas no differences were reported for *Fis1*. Furthermore, the same result was observed with D-lactate 5 mM (p<0.0001). However, after 24h treatment, neither *Drp1* nor *Fis1* significantly changed (Figure 13a-b). In regard to mitochondrial fusion markers, *Opa1* and *Mfn2* expression were significantly decreased in hepatocytes treated with PA and D-lactate 5 mM together, compared with hepatocytes only treated with PA in the shortest timepoint (*Opa1*, p<0.0001; and *Mfn2*, p= 0.0117) (Figure 13c-d). Under 1 mM the result was not dissimilar, however, only *Mfn2* showed significant differences between PA-treated cells and PA-treated cells exposed to D-lactate 1 mM (p= 0.0022). Interestingly, similar to fission markers after 24h treatment, no significant alterations were detected for *Opa1* and *Mfn2* between hepatocytes exposed to PA alone and hepatocytes treated with PA and modulated with D-lactate.

It has been demonstrated that PA treatment in hepatocytes enhances mitochondrial fragmentation, increasing the number of mitochondria per cell and reducing mitochondrial volume (Eynaudi et al., 2021). This effect reveals the maintenance in the total size of the mitochondrial network, mainly suggesting changes in the mitochondrial fusion/fission equilibrium. Nevertheless, we observed an identical pattern in all the genes and conditions which would imply that fusion and fission follow the same trend. Particularly, our results in the PA-treated groups demonstrated increased *Drp1* levels as well as *Mfn2* and *Opa1* expression when compared with the control untreated. On the other hand, the genes related to the fusion process were downregulated in the treatment strategy group after 6h treatment, compared with PA-control. Further, after 24h there are no significant alterations. It is apparent that under FAs overload, D-lactate might be involved in restoring mitochondria dynamics in an early stage. Interestingly, in a recent study was reported that lactate can regulates mitochondrial fission. Specifically, lactate exacerbated Drp1-mediated mitochondrial fission via the NR4A1/DNA-PKcs/p53 pathway, causing mitochondria swelling (Zhu et al., 2020). Intriguingly, this signalling mechanism has been reported in the regulation of mitochondrial fission in NAFLD (H. Zhou et al., 2018). Notwithstanding the lack of evidence of D-lactate within this mechanism, our results did not show an upregulation of fission markers under D-lactate treatment. Continuing research should complement these results with assays for detecting and monitoring changes in mitochondrial function on imaging and flow cytometry platform.

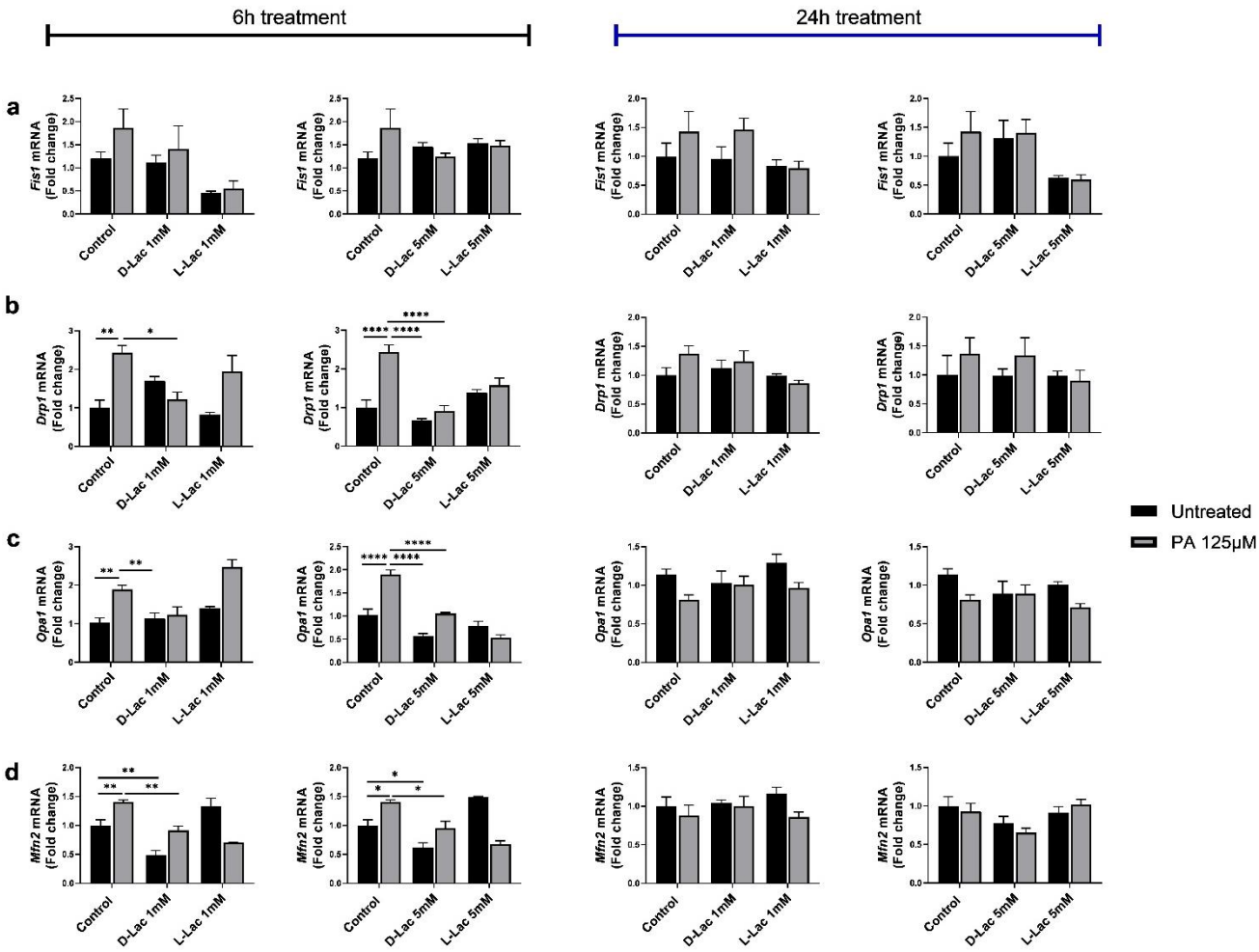

Figure 13. D-lactate downregulates markers of mitochondrial fission and fusion. Quantitative RT-PCR analysis of markers for mitochondrial fission *Fis1* (a) and *Drp1* (b) and markers for mitochondrial fusion *Opa1* (c) and *Mfn2* (d), after 6h (right) and 24h (left) in murine hepatocytes treated with palmitic acid (PA) and modulated with D or L-lactate 1 and 5mM for 6h. Mean values were calculated as fold change versus control untreated with error bars ± SEM of 7 to 8 individual experiments. Statistical analysis was performed with ANOVA Tukey's multiple comparisons test. *$p < 0.05$, **$p < 0.01$ and ****$p < 0.0001$.

In summary, the mRNA levels demonstrate in most of the cases the same effect with D-lactate in both time points. This indicates that in *in vivo* experiments it would be convenient to establish a regime with 1 mM of D-lactate every 6h instead of ingesting 5 mM per day. Moreover, *in vitro* experiments could be focused on continuous systems for the administration of D-lactate. With both models, we could expect to have protective effects against fat accumulation without cellular stress since we observed the same effect after 6h with 1 mM and with 5 mM after 24h.

Overall, we have disentangled some cues of how does D-lactate alter liver lipid metabolism. In the liver, D-lactate might trigger a protective cascade to avoid dysregulation of lipid metabolism and mitochondria dynamics. Although, the involvement of multiple complex factors including several metabolites or microbes in the gut cannot be ruled out. In fact, it is noteworthy that in most of the cases our results provide a clear distinction between both the levorotatory and dextrorotatory lactate molecules. While it is observed the same effect with D-lactate treatment either with 1 or 5 mM in the steatosis condition, the L-lactate effect presents more variations and inconsistencies among genes, timepoints and conditions within the same gene. Additionally, since D-lactate can be converted into pyruvate and pyruvate into L-lactate, but not D-lactate (Manosalva et al., 2022), it is reasonable to assume that in the L-lactate groups there could be an alteration in its production rate. This turns incompatible the comparison between both isoforms and difficult the use L-lactate as a control. Of note, the effect of bacterial L-lactate in NAFLD is not within the scope of this study. Nevertheless, we cannot preclude that the releasing of other metabolites produced by commensals other than *L. reuteri*, some of which might be uncultivable, could be involved in regulating inflammatory signalling and lipid metabolism *in vivo*.

Since mRNA levels do not always reflect phenotypic variations, we evaluated by Western blot the relative level expression of key proteins. Here we sought to understand whether the D-lactate-associated gene alterations result in similar variations in protein steady-state levels. Nevertheless, we were not able to generate reasonably robust results for Western blotting due to the project timeline. Therefore, at a first approach, we only evaluated the 5 mM condition after 24h with the respective controls. Despite this, preliminary results displayed in figure 14 suggest that D-lactate diminish protein production of CD36 and CPT1 in the PA-treated cells compared with PA control which is in accordance with our results from Nile red assay. However, only CD36 protein levels showed a considerably increase in the PA group compared with the control untreated (Figure 14 a-b). On the other hand, the remarkable effect observed in *Dgat2* mRNA levels differs from the immunoblotting experiment, where apparently L-lactate treatment reduces DGAT2 protein production in the PA-treated cells rather than D-lactate. Nevertheless, DGAT2 does not seem to be overexpressed at protein levels in the steatosis group which differs from mRNA expression. Conversely, the relative levels for FASN protein are consistent with the mRNA levels where no significance differences were reported. This led us to speculate that since hepatocytes are exposed to an excess of PA in our model, the cells do not need to produce FASN protein as this enzyme is involved in palmitate production.

In regard to mitochondria fusion, D-lactate reduced MFN2 protein expression after 24h in the PA-treated cells (Figure 14e), but it had no influence on *Mfn2* mRNA expression. This observation agrees with the reported by Eynaudi et al., where it was shown that hepatocytes exposed to PA treatment did not alter MFN2 protein levels (Eynaudi et al., 2021). In respect of the fission marker DRP1, while in mRNA levels no significant alterations were reported, at the protein level there is a slight decrease in the PA condition modulated with D-lactate compared with the PA control. Albeit the results are not aligned precisely with the observed at mRNA levels, it has been studied that changes in gene expression level are frequently not reflected at the protein level (Liu et al., 2016). Indeed, it is important to consider the aspects of translation regulation by other small molecules, such as microRNAs (miRNAs). Still, it was not possible to state final conclusions owing to the small sample size. Future work should therefore include robust results and examine at protein levels, in both timepoints, all the genes in which were observed significant differences in the qPCR results.

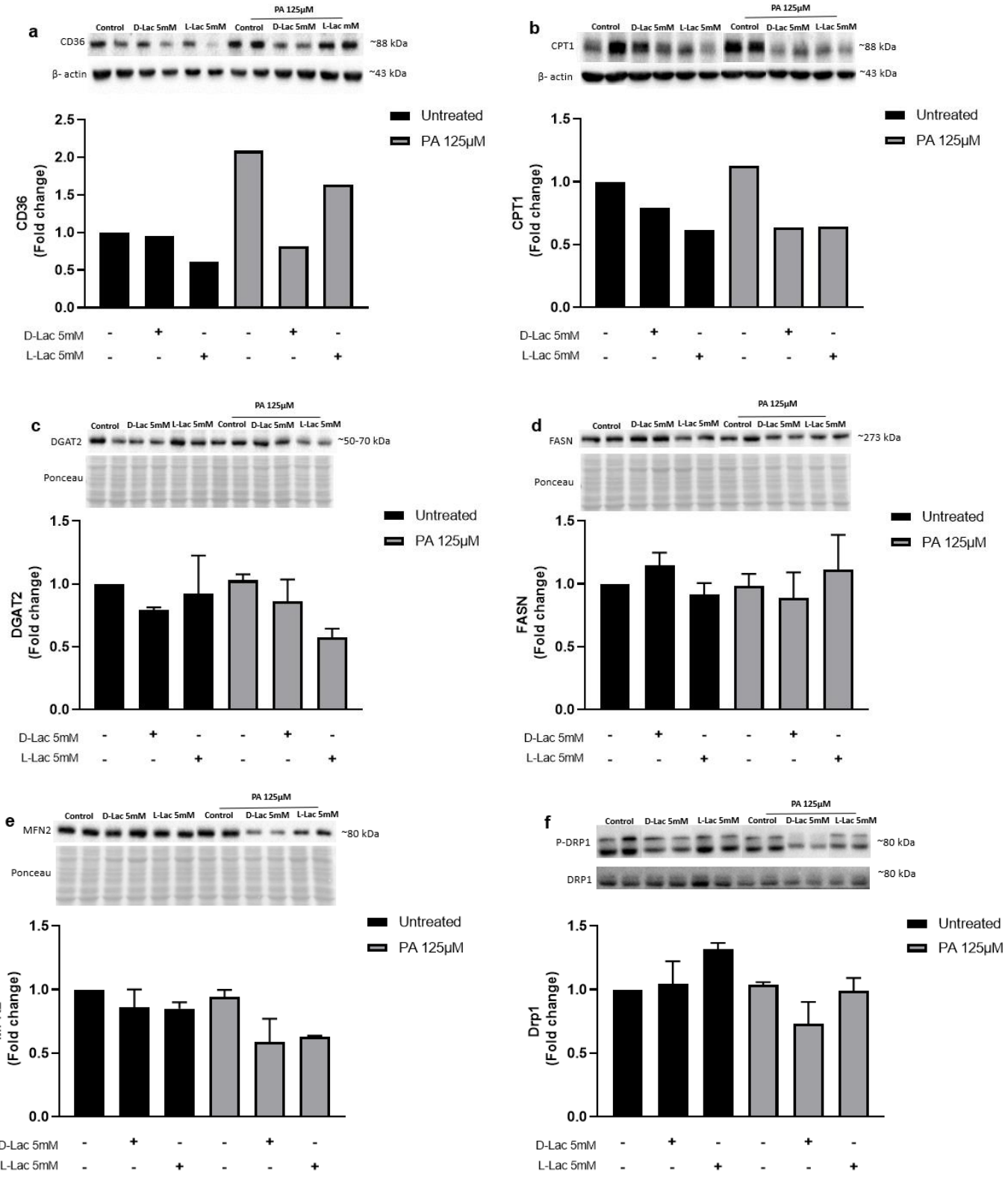

Figure 14. D-lactate affects transcriptional profiles of fatty acids transport and mitochondrial-associated proteins. Immunoblotting of CD36, CPT1, DGAT2, FASN, MFN2 and DRP1 in mouse hepatocytes subjected to 24h treatment with palmitic acid (PA) and D-lactate 5mM. Blots of CD36 and CPT1 were normalized to endogenous β-actin, whereas DGAT2, FASN and MFN2 were normalized to ponceau. P-DRP1 was normalized to DRP1. Representative immunoblots are shown.

5.4 D-lactate might play a dual role: as a substrate and a signalling molecule

Since both D- and L-lactate might share the same metabolic pathway in pyruvate production, and pyruvate is at the crossroads of multiple metabolic pathways, we arise the question of whether the observed effect at mRNA levels is owing to D-lactate catabolism or not. Hence, to substantiate the role of D-lactate in the regulation of the evaluated genes regarding lipid metabolism, inflammation and mitochondria dynamics, we silenced *D-ldh* gene expression in AML12 cells. We then assessed gene expression of the hepatic steatosis-associated genes in which we observed more significant differences. First, we confirmed that mRNA expression of *D-ldh* was diminished in the siRNA-transfected cells (Figure 15e and 16e). Furthermore, the effect of D-lactate 1 mM observed in the PA-induced steatotic hepatocytes in decreasing mRNA levels of lipogenic genes was confirmed in the PA negative control, with significative differences for *Cd36* ($p < 0.0001$), *Dgat2* ($p < 0.0001$) and *Pparγ* ($p = 0.016$) (Figure 15a-d). In the *D-ldh* siRNA transfected group exposed to PA and subjected to D-lactate 1 mM treatment, the mRNA expression of *Cd36*, *Dgat2* and *Pparγ* were similar to the *D-ldh* siRNA control groups with or without D-lactate as well as to the negative controls treated or not with D-lactate. Whereas for *Cpt1*, *D-ldh* silencing recapitulates the D-lactate restoring effect in the transfected hepatocytes treated with PA compared with the transfected hepatocytes treated with PA alone (Figure 15b). Likewise, in the treatment with D-lactate 5 Mm, the siRNA control did not abrogate the observed effect in reducing mRNA expression of the genes related to lipid metabolism in the palmitate-induced steatotic hepatocytes as expected compared with PA negative control ($p < 0.0001$ for *Cd36* and *Dgat2*; and $p = 0.0022$ for *Pparγ*) (Figure 16a-e). Although it is difficult to interpretate the results, a close inspection for figure 15 and 16 led us to infer that albeit *D-ldh* is diminished, D-lactate 1 mM can decrease mRNA level of genes related to lipid transport and TG synthesis whilst under higher amount of the metabolite the effect is only retained in the mitochondrial FAs uptake. On the other hand, an explanation for less expression of *D-ldh* in the PA-treated hepatocytes with *D-ldh* silencing (Figures 15e and 16e) was not found in the present study. These data could implicate D-lactate dehydrogenase in PA metabolism since there are noticeable alterations in some cases in the *D-ldh* siRNA transfected cells without D-lactate exposure. Indeed, this effect is fairly evident in the qPCR analysis for *D-ldh*, where in the PA condition without D-lactate the mRNA levels of *D-ldh* decreased compared with the siRNA positive and negative control.

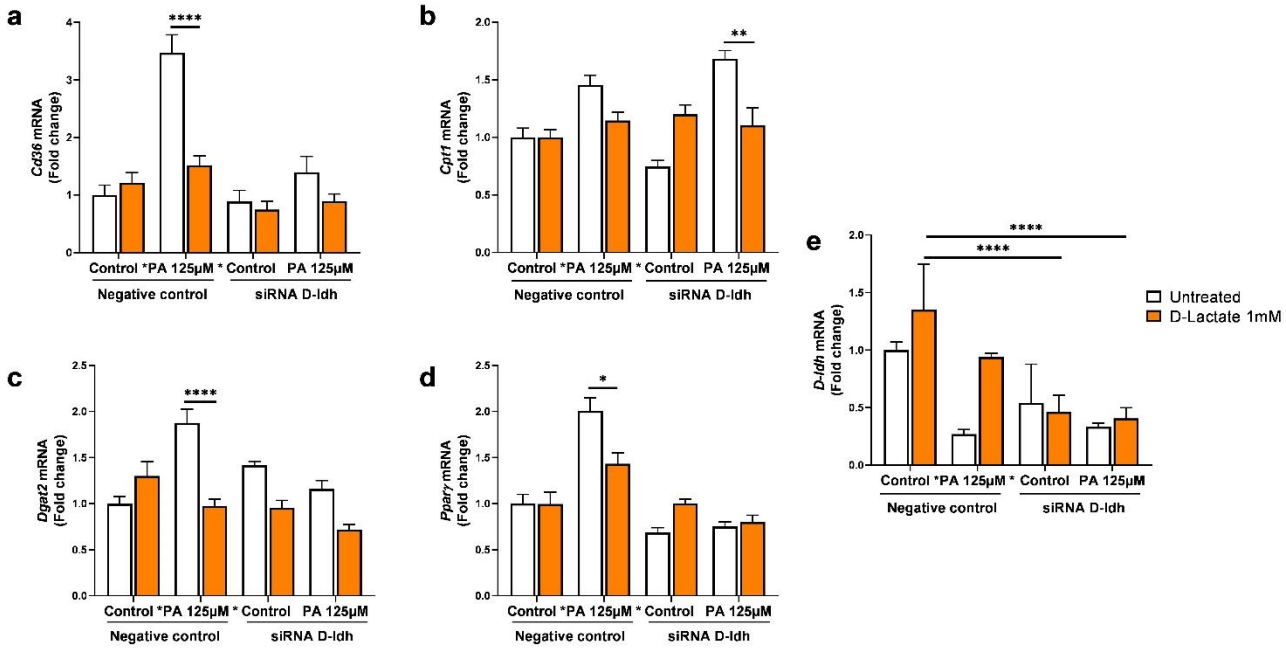

Figure 15. *D-ldh* silencing under D-lactate 1mM treatment. Quantitative RT-PCR analysis of *Cd36* (a), *Cpt1* (b), *Dgat2* (c), *Pparγ* (d), and *D-ldh* (e) in mouse hepatocytes transfected with short interference RNA (siRNA) against *D-ldh* or a siRNA control (Silencer™ Select Negative Control). Mean values were calculated as fold change versus siRNA control untreated with error bars ± SEM of 7 to 8 individual experiments. Statistical analysis was performed with ANOVA Tukey's multiple comparisons test. *$p < 0.05$, **$p < 0.01$ and ****$p < 0.0001$.

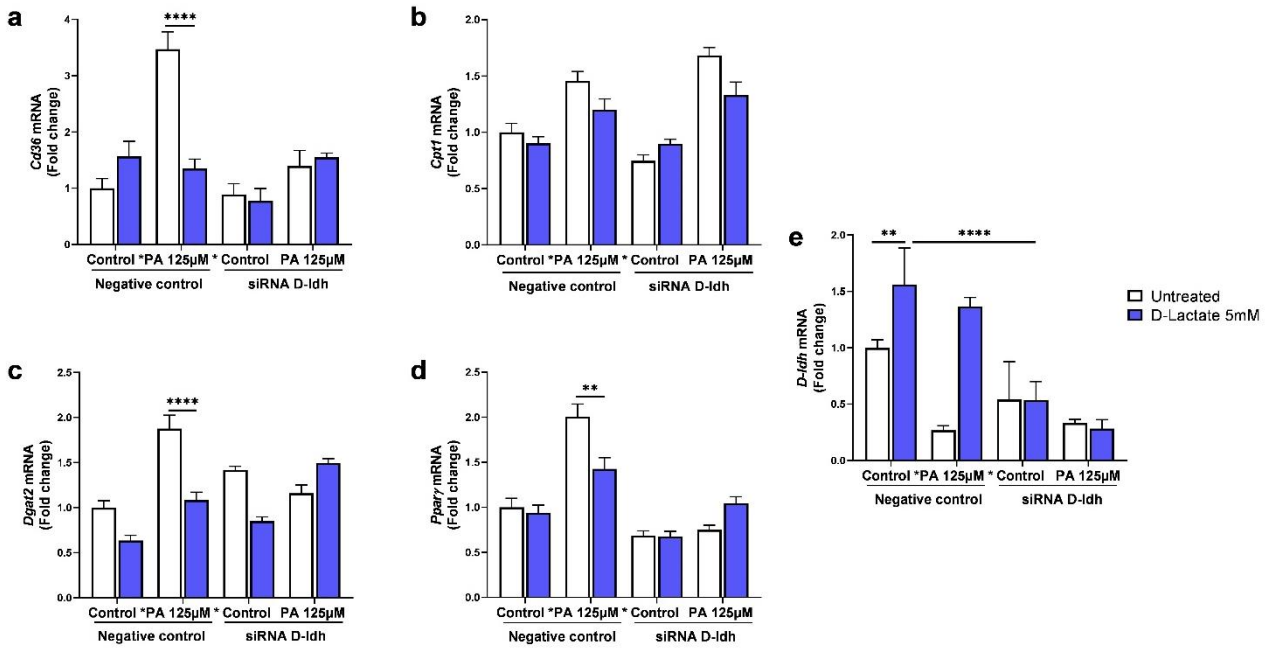

Figure 16. *D-ldh* silencing under D-lactate 5mM treatment. Quantitative RT-PCR analysis of *Cd36* (a), *Cpt1* (b), *Dgat2* (c), *Pparγ* (d), and *D-ldh* (e) in mouse hepatocytes transfected with short interference RNA (siRNA) against *D-ldh* or a siRNA control (Silencer™ Select Negative Control). Mean values were calculated as fold change versus siRNA control untreated with error bars ± SEM of 7 to 8 individual experiments. Statistical analysis was performed with ANOVA Tukey's multiple comparisons test. *$p < 0.05$, **$p < 0.01$ and ****$p < 0.0001$.

These controversial results led us to confirm if the transfection 24h was enough to silence *D-ldh*. For that purpose, we evaluated by Western blot D-LDH protein levels in the conditions of study (Figure 17). We observed that our transfection technique slightly diminished the relative level of D-LDH protein in each condition contrasting with the respective control for each group. The duration and level of knockdown are dependent on the cell type and concentration of siRNA. In addition, it has been suggested that transfections may be repeated to maintain the silencing (Thermo Fisher Scientific). In some cases, repeated siRNA transfection resulted in improved knockdown during selected time points post-transfection. Therefore, for future studies, we propose to set two-time points to repeat the transfection, without changing the concentration of siRNA. For instance, it could be reasonable to re-transfect the monocultures after 24h of the first transfection. Furthermore, to obtain more cues of D-lactate effects in steatosis conditions, we suggest measuring D-lactate levels in the culture medium after the time points selected. Since *D-ldh* is being diminished, it is expected a lower consumption rate of the metabolite. In fact, if the current alterations observed do not change, it could be speculated that D-lactate may act as a signalling molecule.

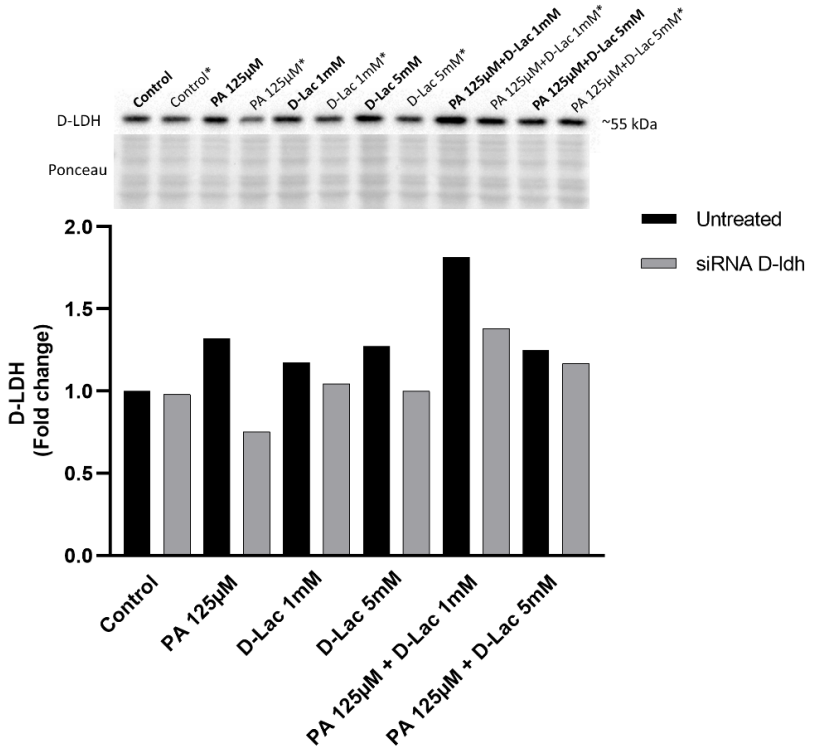

Figure 15. D-lactate dehydrogenase protein levels in mouse hepatocytes transfected with siRNA against *D-ldh*. Immunoblotting of D-LDH in mouse hepatocytes transfected with siRNA against *D-ldh* or siRNA control (Silencer™ Select Negative Control) for 24h. After the transfection period, hepatocytes underwent treatment with palmitic acid (PA) 125µM and D-lactate 1 or 5mM. Western blot of D-LDH was normalized to ponceau.

5.5 Unravelling the mechanisms of D-lactate against fat accumulation

Though D-lactate could provide some of the acetyl-CoA needed for DNL, it is unknown whether D-lactate is essential or the preferred substrate for this function. Therefore, to unravel if D-lactate is the main source of pyruvate production and subsequently acetyl-CoA, we assessed mRNA expression of genes involved in pyruvate or acetyl-CoA generation in steatosis-induced hepatocytes under D-lactate treatment.

Pyruvate is an important intermediate in the central metabolism, being ultimately destined for transport into the mitochondria where is critical for mitochondrial ATP generation and for driving several major biosynthetic pathways intersecting the citric acid cycle (Parlati et al., 2021). Although D-LDH is an enzyme involved in proximal mitochondrial pyruvate metabolism, there are several enzymes that regulate it. For instance, PDK4, which is regulated by the hypoxia inducible factor 1 (HIF1), phosphorylates and inhibits pyruvate dehydrogenase (PDH). As a consequence, pyruvate derived from glucose or lactate cannot be converted into acetyl-CoA for the tricarboxylic acid cycle (TCA) (Gray et al., 2014). In our model, it was evident a similar trend between both *Hif1a* and *Pdk4* mRNA expression (Figure 18 a-b). We observed a significant upregulation in the PA-induced steatotic hepatocytes compared with the control untreated in the two conditions and timepoints. In fact, it has been demonstrated that both genes are overexpressed in NAFLD (Hwang et al., 2009; Mesarwi et al., 2016). In contrast, hepatic *Pdk4* deficiency has been related to diminishing TG accumulation in NASH mice as well as to improving liver regeneration (Y. Zhao et al., 2020). Whereas knockout of *Hif1* showed a protection against the development of liver fibrosis in a mouse model of NAFLD (Mesarwi et al., 2016). Our data indicate that after modulation with D-lactate 1 mM in the PA-treated cells, *Hif1a* mRNA levels were decreased compared with the PA-control. In fact, either after 6h or 24h were reported statistically significant between both groups ($p < 0.0001$) (Figure 18a). This phenomenon was not observed with D-lactate 5 mM. Interestingly, upon 6h treatment D-lactate per se causes a significant upregulation of *Hif1a* compared with the control untreated ($p = 0.0002$ for D-lactate 1 mM; and $p = 0.0024$ for D-lactate 5 mM) (Figure 18a). Nevertheless, after 24h the mRNA levels were similar to the control untreated. This could suggest that D-lactate induces *Hif1a* in an early stage. Contrarily, under steatosis conditions, the metabolite apparently has a role in the reduction of *Hif1a* expression (Figure 18a). In line with the reciprocal HIF1-PDK4 interplay, upon 6h of D-lactate treatment in steatosis-induced hepatocytes also significantly decreased *Pdk4* expression regardless of the lactate concentration, compared with PA control (Figure 18b) ($p = 0.0206$ for D-lactate 1 mM; and $p = 0.059$ for D-lactate 5 mM). However, after 24h this effect was only retained in the condition

with D-lactate 5 mM (p = 0.0002) (Figure 18b). This difference implies that the activation of PDK4 is not exclusively of HIF1 activity. It was difficult to understand whether the decrease caused by D-lactate in these two genes expression is related to the anti-lipogenic effect attributed to it in this study. On the one hand, we could assume that if D-lactate decreases *Hif1a* and *Pdk4* expression, then it may be expected an enhancement in acetyl-CoA production and a possible increase in lipogenesis or epigenetic modifications. Considering this fact, it can easily be seen how PDK4 deficiency might promote FAs synthesis and therefore increase liver TG content. Hence, it would be difficult to speculate that the protective role of D-lactate is via HIF1/PDK4/PDH signalling. Moreover, it is known that PDKs are regulated by allosteric effectors. While pyruvate suppresses PDK activity, acetyl-CoA and NADH activate PDKs (Jeong et al., 2012). In this context, albeit D-lactate may be a substrate for acetyl-CoA production and notably reduces *Pdk4* expression, we can infer that there are no overburden of acetyl-CoA and FAs production via D-lactate due to the allosteric regulation. On the other hand, the downregulation of *Pdk4* caused by D-lactate treatment could be involved in a protective mechanism against glucotoxicity, in order to maintain a lower steady-state concentration of glucose. Lower levels of glucose avoid the overactivation of CHREBP, an inducer of lipogenesis. However, our qPCR results diverge from this hypothesis in the lowest D-lactate concentration after 24h, where a significant upregulation of *Chrebp* was reported in the cells treated with PA and exposed to D-lactate 1 mM, contrasting whit PA control (p = 0.0016) (Figure 11, section 5.3).

In contrast, aligned with the crosstalk between D-lactate and PDK4 signalling in our model, it has been demonstrated that inhibition of PDK4 in mice reduced TG accumulation via AMPK activation, which is an enhancer of β-oxidation (M. Zhang et al., 2018). Likewise, Hwang and colleagues reported that PDK4 deficiency suppressed the increase in lipogenic enzymes in mouse liver caused by long-term high saturated fat diet. This evidence led us to consider the probability of the anti-lipogenic effect of the metabolite D-lactate being indeed linked to PDK4 signalling, likely related to PDK4-AMPK axis. In addition, the suppression of PDK4 was related to the formation of small LDs, whereas the wild-type model showed larger LDs (Hwang et al., 2009). It has been demonstrated that small LDs are associated with an increase in β-oxidation (Eynaudi et al., 2021), which could explain the fade in TG production. Nevertheless, small LDs evoke mitochondrial dysfunction, although it depends on the FA that builds them. Future work should evaluate whether D-lactate alters LDs size.

Furthermore, even though pyruvate can be considered as a major carbon source for lipid biosynthesis, the metabolite acetate is an alternative precursor. Inside the mitochondria, the

enzyme Acetyl- CoA synthetase 1 (ACSS1) catalyses the reaction of acetate and CoA to form acetyl-CoA, which enters the TCA cycle to produce citrate. Citrate is exported to the cytosol and is broken down to acetyl-CoA and OAA by ATP-citrate lyase (ACLY) (Parlati et al., 2021). Additionally, the acetate present in the cytosol can be converted into acetyl-CoA through the enzyme ACSS2 (Batchuluun et al., 2022). Subsequently, the acetyl-CoA produced from both mechanisms might be used for DNL, thereby, upregulation of these pathways may trigger an excess in lipid accumulation. In our study, the quantitative qPCR for *Acss2* showed a significant overexpression in the steatotic hepatocytes in both time points, compared with PA control (p = 0.0414 after 6h; and $p < 0.0001$ after 24h) (Figure 18d). This result is consistent with the evidence of the positive correlation between ACSS2 and NAFLD progression (Z. Huang et al., 2018; Park et al., 2021). Upon D-lactate treatment, only D-lactate 1 mM significantly decreased *Acss2* gene expression after 24h (p = 0.0004) (Figure 18d). This is in accordance with a decrease in FAs synthesis previously observed. Nonetheless, in order to elucidate the acetyl-CoA circuit in steatosis conditions and under the presence of D-lactate, it should be analysed the expression of all the enzymes involved in the signalling, including ACLY, ACSS1, acyl-CoA thioesterase 12 (ACOT12) and ACSS3. Curiously, acetate is becoming recognized as a cellular regulatory molecule with diverse functions beyond the formation of acetyl-CoA for lipogenesis. In fact, it has been reviewed that acetate has alleviation effects on NAFLD, mainly via AMPK activation as well as through epigenetic modifications (Dai et al., 2020). Therefore, it is possible to assume that an augmentation in acetate triggered by D-lactate, in part, could be behind the protective effect that we observed.

Inside the mitochondria, malic enzyme 2 (Me2) can also regenerate pyruvate from malate, which represents one of the main TCA cycle intermediates (Prochownik & Wang, 2021). In the pyruvate-malate cycle, once pyruvate is inside the mitochondria enters the TCA cycle via conversion to oxaloacetate (OAA), which is then converted to malate. Malate can be recycled to pyruvate in the mitochondria trough the enzyme Me2, or can be transported to the cytosol, via the malate-pyruvate shuttle, where can be reconverted to cytosolic pyruvate (Pongratz et al., 2007; Prochownik & Wang, 2021). According to data in figure 18 (c), *Me2* expression was not differentially modulated in steatosis conditions compared with the control untreated. Of note, upon 6h of incubation, *Me2* expression was significantly upregulated in the conditions with sole D-lactate, compared with the control untreated (p =0.0003 for 1 mM and p =0.0006 for 5 mM) (Figure 18c). It is possible to assume that when the cells detect an excess of D-lactate, it is converted into pyruvate which enters to the TCA cycle and rise malate production. Subsequently, malate can be reconverted into pyruvate through the enzyme Me2. However, we

can verify that D-lactate does not alter this signalling pathway under steatosis conditions, otherwise we would expect an increment in *Me2* caused by D-lactate treatment, which would imply that the pyruvate generated from D-lactate would be used to maintain the pyruvate-malate loop and not to enhance lipogenesis.

Since we increased the amount of the normal levels of D-lactate, we south to investigate if the endogenous D-lactate would have a role in the alterations reported. Endogenous D-lactate is produced via the methylglyoxal (MG) detoxification process through the glyoxalase system. The glyoxalase pathway comprises two enzymes, Glyoxalase 1 and 2 (Glo1 and Glo2). In the presence of reduced glutathione (GSH) Glo1 converts MG to S-D-lactoglutathione (SLG), whereas Glo 2 converts SLG to D-lactate and reforms GSH which is consumed in the Glo1-catalysed reaction (Manosalva et al., 2022). Here, we assessed mRNA levels of *Glo1* to investigate if besides the exogenous D-lactate exist an increase in endogenous D-lactate. Our data demonstrate that *Glo1* levels decreased in the presence of D-lactate in the steatosis groups, which indicates that the effect that we identified may be attributed to the exogenous D-lactate (Figure 18e).

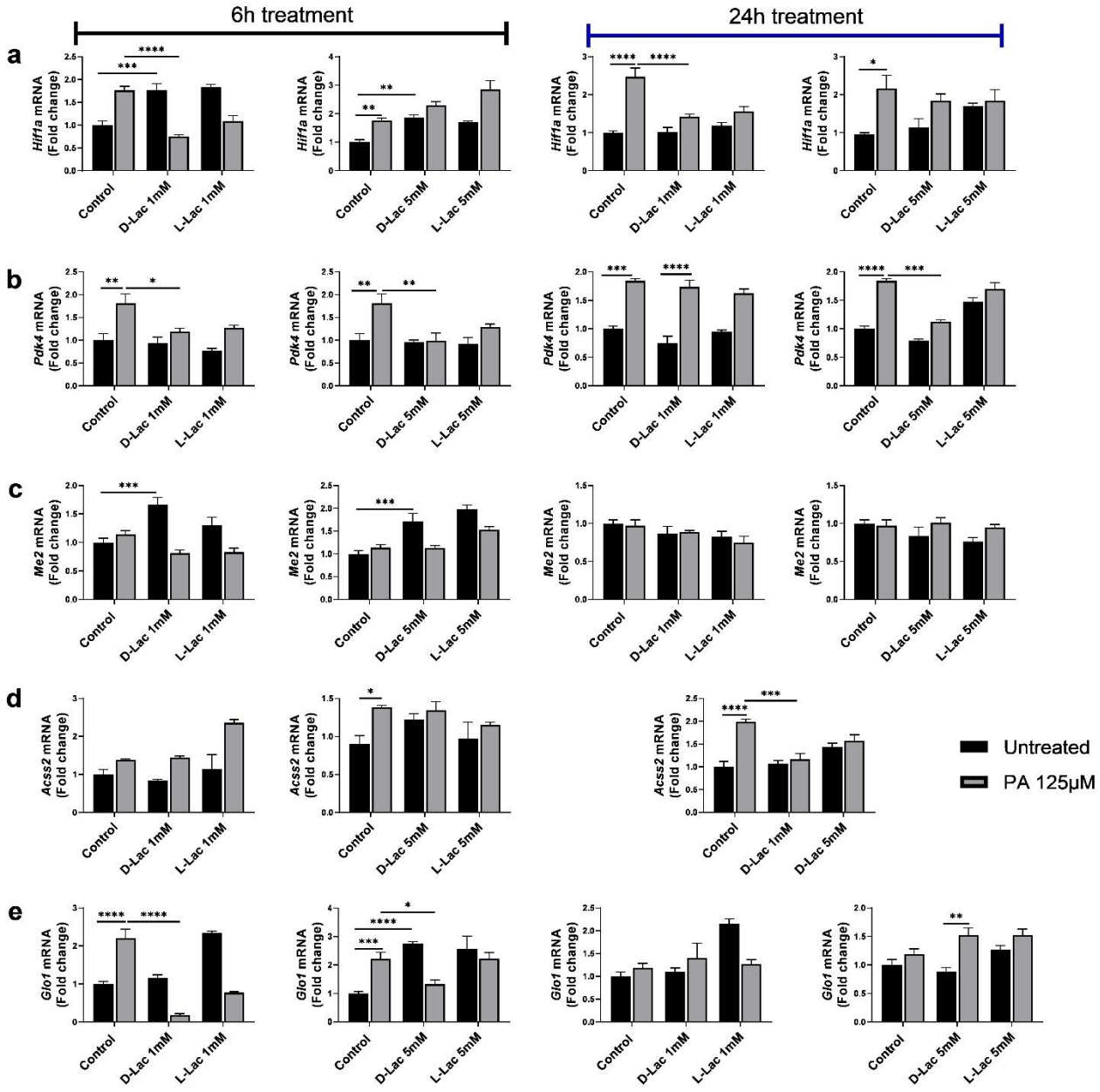

Figure 16. Exogenous D-lactate might alter cytosolic acetate catabolism. Quantitative RT-PCR analysis for (a) *Hif1a*, (b) *Pdk4*, (c) *Me2*, (d) *Acss2*, and (e) *Glo1* in mouse hepatocytes under D or L-lactate treatment. For *Acss2* the conditions with L-lactate after 24h are not present. Mean values were calculated as fold change versus control untreated with error bars ± SEM of 5 to 6 individual experiments. Statistical analysis was performed with ANOVA Tukey's multiple comparisons test. **p* < 0.05, ***p*< 0.01, ****p* < 0.001 and *****p* < 0.0001.

5.6 D-lactate modulates lipid metabolism markers in macrophages and does not alter mitochondria dynamics

Kupffer cells (KCs) and monocyte-derived liver macrophages act as key players in the progression of fatty liver disease (Tran et al., 2020). Therefore, there is a need to elucidate how the alterations in macrophage lipid metabolism coordinate its functions during the pathology

(J. Yan & Horng, 2020). In this study, we aimed to explore whether D-lactate alters lipid metabolism in macrophages under steatosis conditions. Hence, we examined genes related to FA transport and storage in J774A.1 macrophage cell line. Nevertheless, unlike in the AML12 cell line, we only analysed the gene expression after 24h.

Interestingly, unlike the observed in AML12 cells, D-lactate in macrophages did not resemble the same effect neither in mitochondria fission and fusion (Figure 19) nor in lipid metabolism, precluding *Pparγ* (Figure 20). Indeed, only *Pparγ* mRNA levels reported a significant reduction in macrophages that underwent treatment with PA and D-lactate 5 mM, compared with the PA-control (p = 0.0025) (Figure 20d). Curiously, 1 mM D-lactate alone diminished *Pparγ* expression compared with the control untreated (p =0.0094) (Figure 19d). This indicates that D-lactate might have a role in modulating LDs formation in macrophages as in hepatocytes.

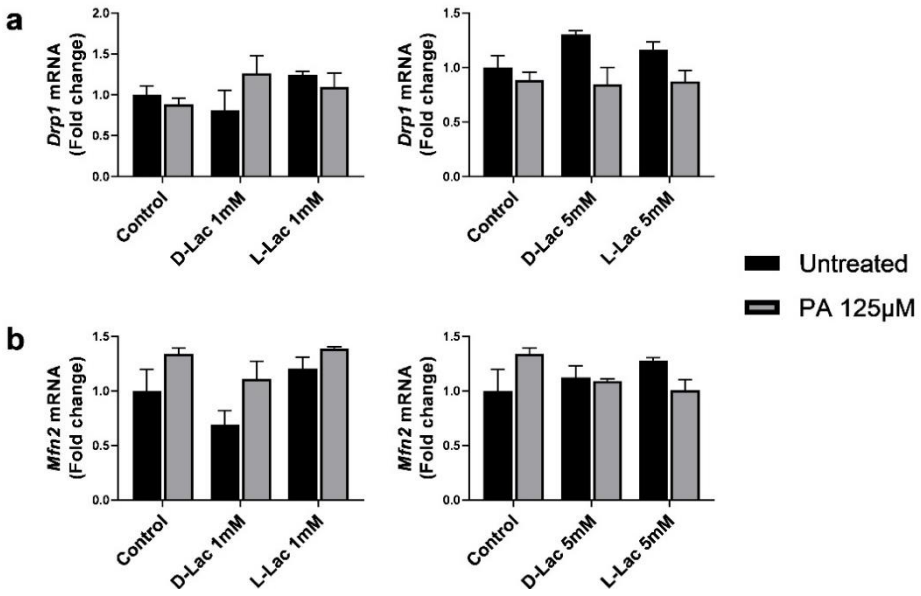

Figure 17. D-lactate does not regulate mitochondria dynamics in J744 macrophages. Quantitative RT-PCR analysis for (a) *Drp1* (Mitochondria fission) and (b) *Mfn2* (Mitochondrial fusion) in murine macrophages under palmitic acid (PA) and D or L-lactate 24h treatment. Mean values were calculated as fold change versus control untreated with error bars ± SEM of 3 individual experiments. Statistical analysis was performed with ANOVA Tukey's multiple comparisons test.

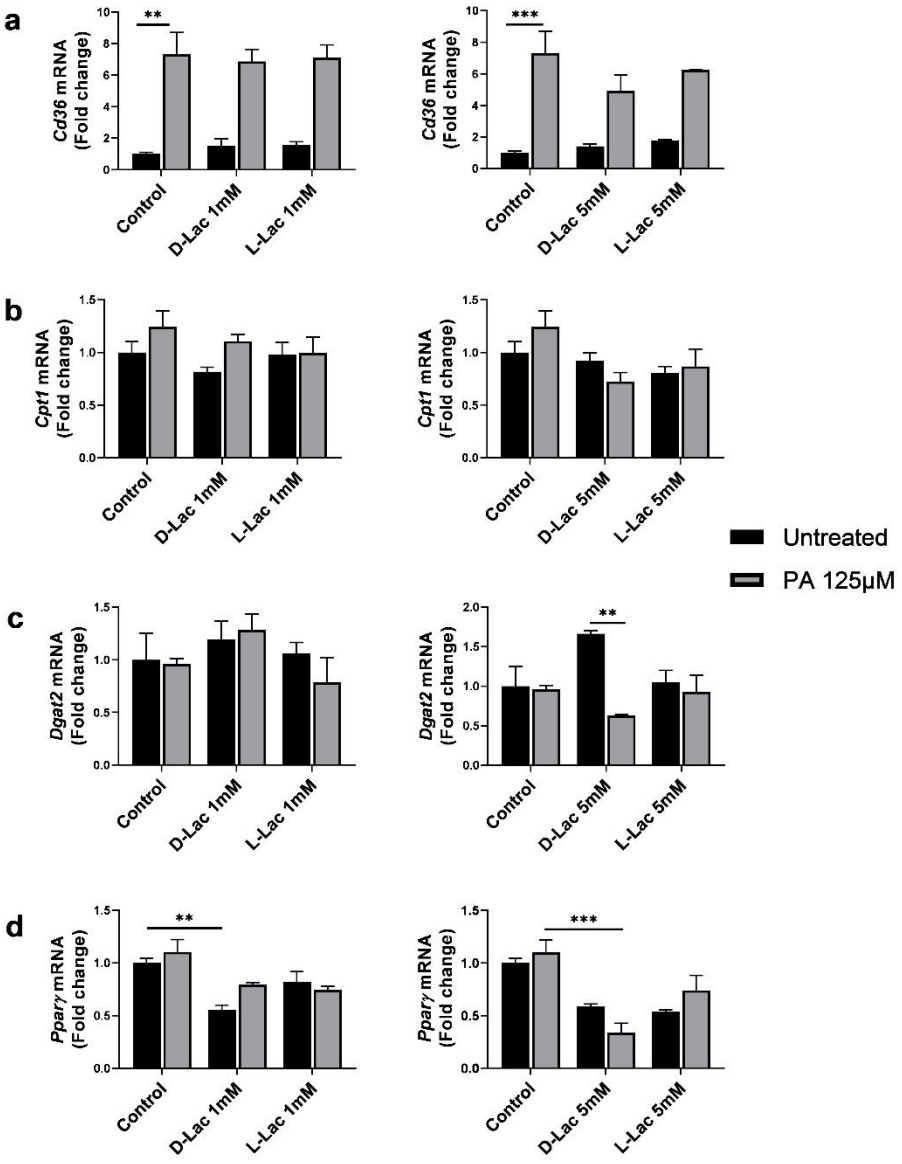

Figure 18. D-lactate alters fatty acid uptake and lipid droplet formation in macrophages. Quantitative RT-PCR analysis for (a) *Cd36,* (b) *Cpt1*, (c) *Dgat2*, and (d) *Pparγ* in murine macrophages under palmitic acid (PA) and D or L-lactate 24h treatment. Mean values were calculated as fold change versus control untreated with error bars ± SEM of 3 individual experiments. Statistical analysis was performed with ANOVA Tukey's multiple comparisons test. $^{**}p < 0.01$ and $^{***}p < 0.001$.

It has been reviewed that after exposure to inflammatory signals, macrophages increase lipid synthesis as well as the uptake of FFAs (J. Yan & Horng, 2020). In agreement with this mechanism, our results demonstrated an increment in FFA uptake which is even higher than in hepatocytes, thus, in the complete NAFLD network may protect the liver. Nonetheless, we could not explain why *Dgat2* and *Pparγ* expression remained unaltered in the PA conditions. Of note, D-lactate 5 mM alone causes a significant increase in *Dgat2* expression rather than in the steatosis condition. This result led us to speculate that under PA stress, FA metabolism

within the cell remains at low rates in the presence of 5 mM D-lactate. Despite this, it can be expected that under lipid-mediated stress, macrophages function as facilitators of FA uptake of hepatic lipid storage as TGs, an adaptation to lipid overload that limits lipid toxicity and might confer tissue protection. However, it can be assumed that although no statistical significance was reported, it seems to tend for D-lactate to have a role in reduce FAs transport and storage in steatotic macrophages, compared with PA controls.

In response to the excessive accumulation of liver fat, hepatocytes are capable of promoting lipid peroxidation that in turn leads to the release of free radicals, hepatocyte injury, and KCs activation (Rada et al., 2020). Then, KCs are able to overproduce inflammatory mediators that can worse the inflammatory scenario. Recently, it was reported that macrophages treated with PA switched towards a pro-inflammatory polarization stage reflected by elevated TNF-α, IL-6, IL-1β and inducible nitric oxide synthase (iNOS) (Rada et al., 2020). Intriguingly, it has been suggested that microbial metabolites, such as L- and D-lactate, may regulate macrophage inflammatory response (Errea et al., 2016; H. cun Zhou et al., 2022). In fact, Hoque and colleagues reported that exposure to high concentrations of lactic acid in the liver hinder inflammation and attenuate organ injury (Hoque et al., 2014). Therefore, we hypothesized that D-lactate might exert and anti-inflammatory effect and decrease mRNA levels of pro-inflammatory markers including *IL-8, Tnf-α* and *Tgf-β,* in macrophages subjected to lipotoxicity. In regard to *IL-8* expression, our results showed a nine to tenfold increase in all the conditions treated with PA in spite of the presence of D-lactate, compared with the controls untreated (Figure 21a). In respect to *Tnf-α* mRNA levels, we observed a significant upregulation in the PA-induced macrophages treated with D-lactate in contrast with the control untreated (p = 0.007 for D-lactate 1 mM; and p = 0.0472 for D-lactate 5 mM) (Figure 21b). These results confirmed the pro-inflammatory signal caused by lipid-mediated stress and not due to the presence of D-lactate, since the increase is similar as the observed in the PA-control groups. On the other hand, *Tgf-β* expression showed an opposite tendency under D-lactate treatment in the macrophages exposed to PA. Apparently, D-lactate can diminish significantly mRNA levels of *Tgf-β* in steatosis conditions compared with the steatosis control (p = 0.039 for D-lactate 5 Mm). An over flux of FA in the liver induces production of *Tgf-β* by KCs, which activates HSCs to produce collagen leading to fibrosis (Wallace et al., 2022). We recently demonstrated in an *in vitro* experiment that D-lactate but not L-lactate can significantly reduce macrophage *Tgf-β* mRNA expression and protein production in the absence of any inflammatory stimuli (Santos et al., 2020). Then, our present study indicates that even in the presence of a pro-

inflammatory stimuli triggered by PA, L and D-lactate can restore mRNA levels of Tgf-*β* which could attenuate liver fibrosis (Figure 21c).

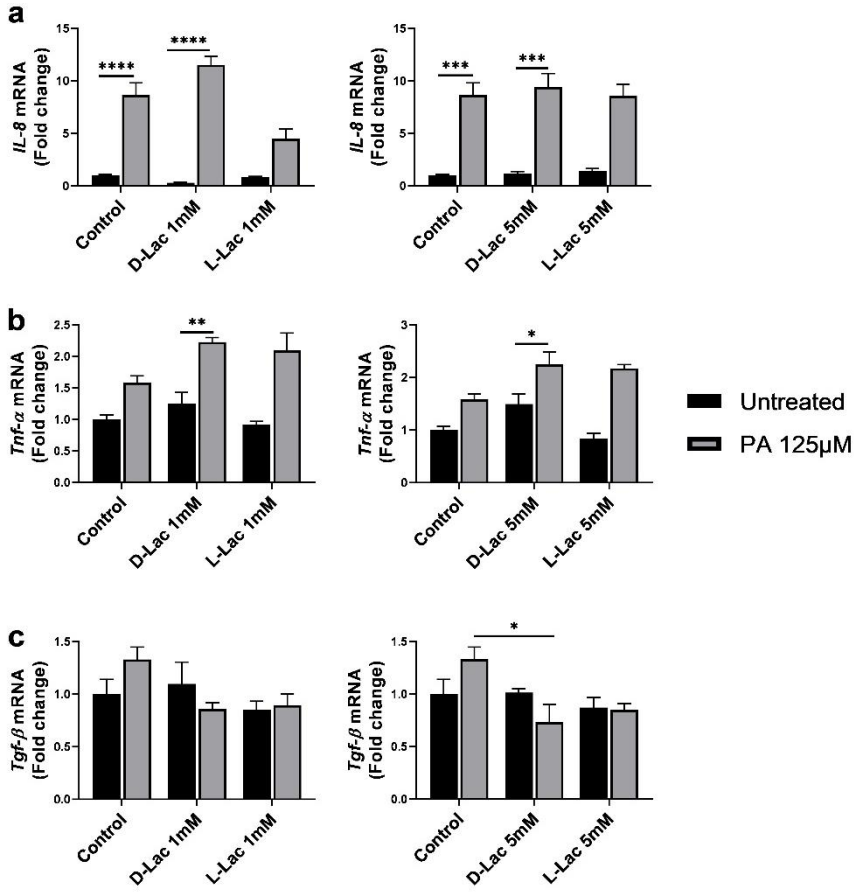

Figure 19. D-lactate does not attenuate the pro-inflammatory response in mouse macrophages. Quantitative RT-PCR analysis for (a) *Il-8,* (b) *Tnf-α,* and (c) *Tgf-β* in murine macrophages under palmitic acid (PA) and D or L-lactate for 24h treatment. Mean values were calculated as fold change versus control untreated with error bars ± SEM of 3 individual experiments. Statistical analysis was performed with ANOVA Tukey's multiple comparisons test.

Controversial results regarding the role of lactate activity in macrophages during inflammation have been described. Lactate may be a metabolite involved in the regulation of the pro- or anti- inflammatory response in macrophages (Manosalva et al., 2022). This effect may depend on the concentration of the metabolite, time of exposure and also be tissue-specific. Also, it was reported that short-term lactate exposure has limited effects on cytokine production, whereas long-term lactate treatment shows strong anti-inflammatory effects in monocytes (Ratter et al., 2018).

Given that macrophages signalling pathways can be mediated by microbial metabolites, continuing research should analyse other mechanisms to disclose the role of D-lactate in the regulation of inflammatory diseases. For instance, it could be explored its possible non-

metabolic functions including its capability of affecting epigenetics via histone lactylation (H. cun Zhou et al., 2022). Indeed, it was reported that exogenous L-lactate triggers an endogenous "lactate clock" in M1 macrophages which induces the M2 phenotype through an increase in histone lactylation. It was found that histone lactylation is not required for the regulation of pro-inflammatory genes. On the contrary, it serves as a mechanism to initiate the expression of genes associated with M2-like macrophages, which may explain the anti-inflammatory effects of L-lactate (D. Zhang et al., 2019). It would be interesting to test whether D-lactate is involved in histone modifications which in turn regulates NAFLD-associated genes. In addition, it is required to assess the target gene panel of the present study in an *in vitro* NASH-like phenotype co-culture with hepatocytes and macrophages subjected to D-lactate treatment, in order to represent the closest model to the real liver interactome.

6 Concluding remarks and future perspectives.

To the best of our knowledge, D-lactate has been classified as a benefit molecule even in the gut-liver axis. On the contrary, several adverse effects have been linked to concentrations in plasma. In the present work, we disentangled a part of the D-lactate effect directly in hepatocyte and macrophage lipid metabolism. Our study provides new insights in the characterization of the role of D-lactate in both hepatocyte and macrophage cell steatosis *in vitro* models. Firstly, we confirmed that our *in vitro* model resembles features of the lipogenic gene profile present in steatosis conditions. Furthermore, our treatment strategy demonstrated a protective effect of D-lactate but not L-lactate against lipid accumulation. Our major hypothesis is that D-lactate might modulate the capability of the cells to transport FFAs from the medium to the cytoplasm. Nonetheless, besides D-LDH, it has been reported that D-lactate can be metabolized by the gut microbiota to produce propionate via the acrylate pathway, through the enzyme Lactoyl CoA dehydratase (LCD) (Balasubramanian & Subramanian, 2019). Although in the Nile red assay we identified D-lactate with a more protective role against fat accumulation rather than L-lactate, we cannot discard the hypothesis that the conversion of D-lactate to other SCFAs can enhance a protective role in the liver against NAFLD in *in vivo* experiments. In fact, the reduction in the hepatocellular vacuolization score in the probiotic-treated mice led us to hypothesized that if D-lactate is sensed as a toxic molecule and then participates as an intermediate in DNL, the hepatocytes then might not uptake FAs in order to maintain lipids pool. In addition, D-lactate metabolism may contribute to the production of ambivalent molecules in lipid storage such as propionate, succinate and butyrate contributing to lipid homeostasis (Sheridan et al., 2022).

Overall, our results suggest that in *in vivo* experiments it would be convenient to establish a regime with 1 mM of D-lactate every 6h instead of ingesting 5 mM per day. It was remarkably that in steatotic hepatocytes D-lactate attenuates the overexpression of genes related to lipogenesis, fatty acid transport, triglycerides synthesis and storage, whereas in macrophages the effect is more noticeable in lipid droplet formation. Even though the small number of protein analysis did not allow us to take strongest conclusions, we assumed that D-lactate might modulate liver mitochondrial activity and ameliorate steatosis in hepatocytes. However, the therapeutic relevance of the findings is currently unclear and the exact regulatory mechanism remains to be further studied. We highlighted cholesterol-related pathways as well as PPARγ signalling as mechanisms that should be examined. Nonetheless, we started to pave the way of the role of D-lactate under lipid-mediated stress. In order to obtain robust results, the present work should be complemented with the analysis of the Nile Red assay, D-lactate rate consumption, siRNA experiment, qPCR and Western blotting for both hepatocytes and macrophages in the missing timepoints and conditions. Additionally, an important complement for the present work would be the measurement of the PA in the culture medium after the incubation period, to confirm what we observed in the Nile Red experiment and to obtain more cues about the role of D-lactate. Moreover, we propose to design an experiment with the use of oleic acid and a mixture of both palmitic and oleic acid, since both fatty acids are the major components of the western diet and have been identified with different roles in the regulation of lipid metabolism and NAFLD progression.

It is noteworthy that our study is focused on a possible option to prevent NAFLD. In our model we added both PA and D or L-lactate at the same time to observe the direct competition between both molecules at cellular levels. Taking into account the results obtained, future work should explore *in vitro* the use of D-lactate under different strategies. Cells can be pre-incubated with D-lactate and after the pre-incubation time it can be induced lipid accumulation. Of note, in a recent study of the protective effects of LAB in hepatic injury and inflammation was used an opposite alternative. Hepatocytes were pre-incubated first with FAs for 24h and after were treated with total cellular fluid of different LAB for 48h (Kanmani & Kim, 2018). Therefore, we could also alter our model by adding an interval between the induction with PA and the D-lactate treatment.

Besides the compelling evidence of the mechanisms by which D-lactate interferes in hepatocyte lipid metabolism, we explored other pathways that could explain, in part, the effect attributed to D-lactate. We propose that the observed alterations may be attributed to the

exogenous D-lactate. The anti-lipogenic effect of the metabolite may be related to the inhibition of PDK4 which would contribute to increased acetate production, a metabolite with protective roles in NAFLD, not as a lipogenesis substrate but as a molecular signal for epigenetic states. Indeed, we postulate that histone lactylation via D-lactate or interactions between D-lactate and other RNA structures might unveil the role of D-lactate in NAFLD. In fact, the silencing of *D-ldh* strengthens the hypothesis of D-lactate acting as a signalling molecule. This theory could elucidate the preliminary *in vivo* results, reinforcing that in addition to the microbiota composition, it is critical to characterize the interactions between microbial metabolites and determine the underlying mechanisms. Importantly, we confirmed that lactate is the main metabolite produced by *L. reuteri*. Nevertheless, we identified other molecules as possible candidates that may, in parallel with lactate, contribute to ameliorating liver disease. Indeed, it is possible that D-lactate supplementation does not improve liver disease outcomes in the same proportions as *L. reuteri*. Therefore, we opened a road future for new studies focused on the synergic relationships between *L. reuteri* metabolites, leading to a better understanding of host-microbiota homeostasis maintenance during NAFLD.

Finally, taking into account the important role of macrophages in the relationship between gut microbiota and inflammation, developing macrophage-targeting approaches in the prevention and therapy of NAFLD is an appealing strategy. Therefore, the molecular signalling mechanisms involved between the microbial metabolites and macrophages will provide new directions for novel probiotics, in which D-lactate- producers and lactic acid-utilizing bacteria hold promise.

7 References

1. Abumrad, N. A., Cabodevilla, A. G., Samovski, D., Pietka, T., Basu, D., & Goldberg, I. J. (2021). Endothelial cell receptors in tissue lipid uptake and metabolism. *Circulation Research*, *128*(3), 433–450. https://doi.org/10.1161/circresaha.120.318003
2. Agus, A., Clément, K., & Sokol, H. (2021). Gut microbiota-derived metabolites as central regulators in metabolic disorders. *Gut*, *70*(6), 1174–1182. https://doi.org/10.1136/gutjnl-2020-323071
3. Ahmadi, S., Wang, S., Nagpal, R., Wang, B., Jain, S., Razazan, A., Mishra, S. P., Zhu, X., Wang, Z., Kavanagh, K., & Yadav, H. (2020). A human-origin probiotic cocktail ameliorates aging-related leaky gut and inflammation via modulating the microbiota/taurine/tight junction axis. *JCI Insight*, *5*(9). https://doi.org/10.1172/jci.insight.132055
4. Albillos, A., de Gottardi, A., & Rescigno, M. (2020). The gut-liver axis in liver disease: Pathophysiological basis for therapy. *Journal of Hepatology*, *72*(3), 558–577. https://doi.org/10.1016/j.jhep.2019.10.003
5. Allaire, J. M., Crowley, S. M., Law, H. T., Chang, S. Y., Ko, H. J., & Vallance, B. A. (2018). The Intestinal Epithelium: Central Coordinator of Mucosal Immunity. *Trends in Immunology*, *39*(9), 677–696. https://doi.org/10.1016/j.it.2018.04.002
6. Aron-Wisnewsky, J., Vigliotti, C., Witjes, J., Le, P., Holleboom, A. G., Verheij, J., Nieuwdorp, M., & Clément, K. (2020). Gut microbiota and human NAFLD: disentangling microbial signatures from metabolic disorders. *Nature Reviews Gastroenterology and Hepatology*, *17*(5), 279–297. https://doi.org/10.1038/s41575-020-0269-9
7. Bajaj, J. S., Ng, S. C., & Schnabl, B. (2022). Promises of microbiome-based therapies. *Journal of Hepatology*, *76*(6), 1379–1391. https://doi.org/10.1016/j.jhep.2021.12.003
8. Balasubramanian, S., & Subramanian, R. (2019). Metabolic perturbation of acrylate pathway in *Lactobacillus plantarum*. *Biocatalysis and Biotransformation*, *37*(4), 310–316. https://doi.org/10.1080/10242422.2019.1606215
9. Batchuluun, B., Pinkosky, S. L., & Steinberg, G. R. (2022). Lipogenesis inhibitors: therapeutic opportunities and challenges. *Nature Reviews Drug Discovery*, *21*(4), 283–305). https://doi.org/10.1038/s41573-021-00367-2
10. Bedi, S., Hines, G. V., Lozada-Fernandez, V. v., Piva, C. D. J., Kaliappan, A., Rider, S. D., & Hostetler, H. A. (2017). Fatty acid binding profile of the liver X receptor α. *Journal of Lipid Research*, *58*(2), 393–402. https://doi.org/10.1194/jlr.M072447
11. Bessone, F., Razori, M. V., & Roma, M. G. (2019). Molecular pathways of nonalcoholic fatty liver disease development and progression. *Cellular and Molecular Life Sciences* *76*(1), 99–128. https://doi.org/10.1007/s00018-018-2947-0
12. Bi, K., Zhang, X., Chen, W., & Diao, H. (2020). Micrornas regulate intestinal immunity and gut microbiota for gastrointestinal health: A comprehensive review. *Genes*, 11(9), 1–17). https://doi.org/10.3390/genes11091075
13. Carvalho, B. M., Guadagnini, D., Tsukumo, D. M. L., Schenka, A. A., Latuf-Filho, P., Vassallo, J., Dias, J. C., Kubota, L. T., Carvalheira, J. B. C., & Saad, M. J. A. (2012). Modulation of gut microbiota by antibiotics improves insulin signalling in high-fat fed mice. *Diabetologia*, *55*(10), 2823–2834. https://doi.org/10.1007/s00125-012-2648-4
14. Chambers, E. S., Byrne, C. S., Rugyendo, A., Morrison, D. J., Preston, T., Tedford, C., Bell, J. D., Thomas, L., Akbar, A. N., Riddell, N. E., Sharma, R., Thursz, M. R.,

Manousou, P., & Frost, G. (2019). The effects of dietary supplementation with inulin and inulin-propionate ester on hepatic steatosis in adults with non-alcoholic fatty liver disease. *Diabetes, Obesity and Metabolism*, *21*(2), 372–376. https://doi.org/10.1111/dom.13500

15. Chávez-Talavera, O., Tailleux, A., Lefebvre, P., & Staels, B. (2017). *Bile acids in meta-inflammatory disorders*. *152*(7), 1679–1694. https://doi.org/10.1053/j.gastro.2017.01.055ï
16. Dai, X., Hou, H., Zhang, W., Liu, T., Li, Y., Wang, S., Wang, B., & Cao, H. (2020). Microbial Metabolites: Critical Regulators in NAFLD. *Frontiers in Microbiology*, *11*(1). https://doi.org/10.3389/fmicb.2020.567654
17. Danne, C., Ryzhakov, G., Martínez-López, M., Ilott, N. E., Franchini, F., Cuskin, F., Lowe, E. C., Bullers, S. J., Arthur, J. S. C., & Powrie, F. (2017). A Large Polysaccharide Produced by Helicobacter hepaticus Induces an Anti-inflammatory Gene Signature in Macrophages. *Cell Host and Microbe*, *22*(6), 733-745.e5. https://doi.org/10.1016/j.chom.2017.11.002
18. Dawson, P. A., & Karpen, S. J. (2015). Intestinal transport and metabolism of bile acids. *Journal of Lipid Research*, *56*(6), 1085–1099. https://doi.org/10.1194/jlr.R054114
19. Errea, A., Cayet, D., Marchetti, P., Tang, C., Kluza, J., Offermanns, S., Sirard, J.-C., & Rumbo, M. (2016). Lactate Inhibits the Pro-Inflammatory Response and Metabolic Reprogramming in Murine Macrophages in a GPR81-Independent Manner. *PLOS ONE*, *11*(11). https://doi.org/10.1371/journal.pone.0163694
20. Estes, C., Anstee, Q. M., Arias-Loste, M. T., Bantel, H., Bellentani, S., Caballeria, J., Colombo, M., Craxi, A., Crespo, J., Day, C. P., Eguchi, Y., Geier, A., Kondili, L. A., Kroy, D. C., Lazarus, J. v., Loomba, R., Manns, M. P., Marchesini, G., Nakajima, A., … Razavi, H. (2018). Modeling NAFLD disease burden in China, France, Germany, Italy, Japan, Spain, United Kingdom, and United States for the period 2016–2030. *Journal of Hepatology*, *69*(4), 896–904. https://doi.org/10.1016/j.jhep.2018.05.036
21. Estes, C., Razavi, H., Loomba, R., Younossi, Z., & Sanyal, A. J. (2018). Modeling the Epidemic of Nonalcoholic Fatty Liver Disease Demonstrates an Exponential Increase in Burden of Disease. *Hepatology*, *67*(1). https://doi.org/10.1002/hep.29466
22. Eynaudi, A., Díaz-Castro, F., Bórquez, J. C., Bravo-Sagua, R., Parra, V., & Troncoso, R. (2021). Differential Effects of Oleic and Palmitic Acids on Lipid Droplet-Mitochondria Interaction in the Hepatic Cell Line HepG2. *Frontiers in Nutrition*, *8*. https://doi.org/10.3389/fnut.2021.775382
23. Fabbrini, E., Tiemann Luecking, C., Love-Gregory, L., Okunade, A. L., Yoshino, M., Fraterrigo, G., Patterson, B. W., & Klein, S. (2016). Physiological Mechanisms of Weight Gain-Induced Steatosis in People with Obesity. *Gastroenterology*, *150*(1), 79-81. https://doi.org/10.1053/j.gastro.2015.09.003
24. Ferguson, D., & Finck, B. N. (2021). Emerging therapeutic approaches for the treatment of NAFLD and type 2 diabetes mellitus. *Nature Reviews Endocrinology*, *17*(8), 484–495. https://doi.org/10.1038/s41574-021-00507-z
25. Fernandez-Cantos, M. V., Garcia-Morena, D., Iannone, V., El-Nezami, H., Kolehmainen, M., & Kuipers, O. P. (2021). Role of microbiota and related metabolites in gastrointestinal tract barrier function in NAFLD. *Tissue Barriers*, *9*(3). https://doi.org/10.1080/21688370.2021.1879719

26. Fernández-Veledo, S., & Vendrell, J. (2019). Gut microbiota-derived succinate: Friend or foe in human metabolic diseases? *Reviews in Endocrine and Metabolic Disorders*, *20*(4), 439–447. https://doi.org/10.1007/s11154-019-09513-z
27. Filali-Mouncef, Y., Hunter, C., Roccio, F., Zagkou, S., Dupont, N., Primard, C., Proikas-Cezanne, T., & Reggiori, F. (2022). The ménage à trois of autophagy, lipid droplets and liver disease. *Autophagy*, *18*(1), 50–72. https://doi.org/10.1080/15548627.2021.1895658
28. Gao, X., Lin, S. H., Ren, F., Li, J. T., Chen, J. J., Yao, C. B., Yang, H. bin, Jiang, S. X., Yan, G. Q., Wang, D., Wang, Y., Liu, Y., Cai, Z., Xu, Y. Y., Chen, J., Yu, W., Yang, P. Y., & Lei, Q. Y. (2016). Acetate functions as an epigenetic metabolite to promote lipid synthesis under hypoxia. *Nature Communications*, *7*. https://doi.org/10.1038/ncomms11960
29. Geier, A., Rinella, M. E., Balp, M. M., McKenna, S. J., Brass, C. A., Przybysz, R., Cai, J., Knight, A., Gavaghan, M., Howe, T., Rosen, D., & Ratziu, V. (2021). Real-World Burden of Nonalcoholic Steatohepatitis. *Clinical Gastroenterology and Hepatology*, *19*(5), 1020-1029. https://doi.org/10.1016/j.cgh.2020.06.064
30. Gerbe, F., & Jay, P. (2016). Intestinal tuft cells: Epithelial sentinels linking luminal cues to the immune system. *Mucosal Immunology*, *9*(6), 1353–1359. https://doi.org/10.1038/mi.2016.68
31. Giacomello, M., Pyakurel, A., Glytsou, C., & Scorrano, L. (2020). The cell biology of mitochondrial membrane dynamics. *Nature Reviews Molecular Cell Biology*, *21*(4), 204–224. https://doi.org/10.1038/s41580-020-0210-7
32. Gillard, J., Clerbaux, L. A., Nachit, M., Sempoux, C., Staels, B., Bindels, L. B., Tailleux, A., & Leclercq, I. A. (2022). Bile acids contribute to the development of non-alcoholic steatohepatitis in mice. *JHEP Reports*, *4*(1). https://doi.org/10.1016/j.jhepr.2021.100387
33. Gray, L. R., Tompkins, S. C., & Taylor, E. B. (2014). Regulation of pyruvate metabolism and human disease. *Cellular and Molecular Life Sciences*, *71*(14), 2577–2604. https://doi.org/10.1007/s00018-013-1539-2
34. Hallsworth, K., & Adams, L. A. (2019). Lifestyle modification in NAFLD/NASH: Facts and figures. *JHEP Reports*, *1*(6), 468–479. https://doi.org/10.1016/j.jhepr.2019.10.008
35. Hassan, M., Moghadamrad, S., Sorribas, M., Muntet, S. G., Kellmann, P., Trentesaux, C., Fraudeau, M., Nanni, P., Wolski, W., Keller, I., Hapfelmeier, S., Shroyer, N. F., Wiest, R., Romagnolo, B., & de Gottardi, A. (2020). Paneth cells promote angiogenesis and regulate portal hypertension in response to microbial signals. *Journal of Hepatology*, *73*(3), 628–639. https://doi.org/10.1016/j.jhep.2020.03.019
36. Heeren, J., & Scheja, L. (2021). Metabolic-associated fatty liver disease and lipoprotein metabolism. *Molecular Metabolism*, *50*. https://doi.org/10.1016/j.molmet.2021.101238
37. Herman, M. A. (2021). Metabolic liver disease — what's in a name? *Nature Reviews Endocrinology*, *17*(2), 79–80. https://doi.org/10.1038/s41574-020-00452-3
38. Hoque, R., Farooq, A., Ghani, A., Gorelick, F., & Mehal, W. Z. (2014). Lactate reduces liver and pancreatic injury in toll-like receptor- and inflammasome-mediated inflammation via gpr81-mediated suppression of innate immunity. *Gastroenterology*, *146*(7), 1763–1774. https://doi.org/10.1053/j.gastro.2014.03.014
39. Huang, D. Q., El-Serag, H. B., & Loomba, R. (2021). Global epidemiology of NAFLD-related HCC: trends, predictions, risk factors and prevention. *Nature Reviews Gastroenterology and Hepatology*, *18*(4), 223–238. https://doi.org/10.1038/s41575-020-00381-6

40. Huang, Z., Zhang, M., Plec, A. A., Estill, S. J., Cai, L., Repa, J. J., McKnight, S. L., & Tu, B. P. (2018). ACSS2 promotes systemic fat storage and utilization through selective regulation of genes involved in lipid metabolism. *Proceedings of the National Academy of Sciences of the United States of America*, *115*(40). https://doi.org/10.1073/pnas.1806635115
41. Huby, T., & Gautier, E. L. (2021). Immune cell-mediated features of non-alcoholic steatohepatitis. *Nature Reviews Immunology*. https://doi.org/10.1038/s41577-021-00639-3
42. Hwang, B., Jeoung, N. H., & Harris, R. A. (2009). Pyruvate dehydrogenase kinase isoenzyme 4 (PDHK4) deficiency attenuates the long-term negative effects of a high-saturated fat diet. *Biochemical Journal*, *423*(2), 243–252. https://doi.org/10.1042/BJ20090390
43. Ipsen, D. H., Lykkesfeldt, J., & Tveden-Nyborg, P. (2018). Molecular mechanisms of hepatic lipid accumulation in non-alcoholic fatty liver disease. *Cellular and Molecular Life Sciences*, *75*(18), 3313–3327. https://doi.org/10.1007/s00018-018-2860-6
44. Jang, H. R., Park, H. J., Kang, D., Chung, H., Nam, M. H., Lee, Y., Park, J. H., & Lee, H. Y. (2019). A protective mechanism of probiotic *Lactobacillus* against hepatic steatosis via reducing host intestinal fatty acid absorption. *Experimental and Molecular Medicine*, *51*(8). https://doi.org/10.1038/s12276-019-0293-4
45. Jeong, J. Y., Jeoung, N. H., Park, K. G., & Lee, I. K. (2012). Transcriptional regulation of pyruvate dehydrogenase kinase. *Diabetes and Metabolism Journal*, *36*(5), 328–335. https://doi.org/10.4093/dmj.2012.36.5.328
46. Jia, Z., Chen, X., Chen, J., Zhang, L., Oprescu, S. N., Luo, N., Xiong, Y., Yue, F., & Kuang, S. (2022). ACSS3 in brown fat drives propionate catabolism and its deficiency leads to autophagy and systemic metabolic dysfunction. *Clinical and Translational Medicine*, *12*(2). https://doi.org/10.1002/ctm2.665
47. Kamada, N., Seo, S. U., Chen, G. Y., & Núñez, G. (2013). Role of the gut microbiota in immunity and inflammatory disease. *Nature Reviews Immunology*, *13*(5), 321–335. https://doi.org/10.1038/nri3430
48. Kanmani, P., & Kim, H. (2018). Protective effects of lactic acid bacteria against TLR4 induced inflammatory response in hepatoma HepG2 cells through modulation of toll-like receptor negative regulators of mitogen-activated protein kinase and NF-κB signaling. *Frontiers in Immunology*, *9*. https://doi.org/10.3389/fimmu.2018.01537
49. Kazankov, K., Jørgensen, S. M. D., Thomsen, K. L., Møller, H. J., Vilstrup, H., George, J., Schuppan, D., & Grønbæk, H. (2019). The role of macrophages in nonalcoholic fatty liver disease and nonalcoholic steatohepatitis. *Nature Reviews Gastroenterology and Hepatology*, *16*(3), 145–159. https://doi.org/10.1038/s41575-018-0082-x
50. Koh, A., de Vadder, F., Kovatcheva-Datchary, P., & Bäckhed, F. (2016). From dietary fiber to host physiology: Short-chain fatty acids as key bacterial metabolites. *Cell*, *165*(6), 1332–1345. https://doi.org/10.1016/j.cell.2016.05.041
51. Kohjima, M., Enjoji, M., Higuchi, N., Kato, M., Kotoh, K., Yoshimoto, T., Fujino, T., Yada, M., Harada, N., Takayanagi, R., & Nakamuta, M. (2007). Re-evaluation of fatty acid metabolism-related gene expression in nonalcoholic fatty liver disease. *Int. J. Mol. Med*, *20*, 351–358). Int. J. Mol. Med. https://doi.org/10.3892/ijmm.20.3.351
52. Korbecki, J., & Bajdak-Rusinek, K. (2019). The effect of palmitic acid on inflammatory response in macrophages: an overview of molecular mechanisms. *Inflammation Research*, *68*(11), 915–932. https://doi.org/10.1007/s00011-019-01273-5

53. Koutnikova, H., Genser, B., Monteiro-Sepulveda, M., Faurie, J. M., Rizkalla, S., Schrezenmeir, J., & Clement, K. (2019). Impact of bacterial probiotics on obesity, diabetes and non-alcoholic fatty liver disease related variables: A systematic review and meta-analysis of randomised controlled trials. *BMJ Open*, *9*(3). https://doi.org/10.1136/bmjopen-2017-017995
54. Kwong, A. K. Y., Wong, S. S. N., Rodenburg, R. J. T., Smeitink, J., Chan, G. C. F., & Fung, C. W. (2021). Human d-lactate dehydrogenase deficiency by LDHD mutation in a patient with neurological manifestations and mitochondrial complex IV deficiency. *JIMD Reports*, *60*(1), 15–22. https://doi.org/10.1002/jmd2.12220
55. Lazarus, J. v., Mark, H. E., Anstee, Q. M., Arab, J. P., Batterham, R. L., Castera, L., Cortez-Pinto, H., Crespo, J., Cusi, K., Dirac, M. A., Francque, S., George, J., Hagström, H., Huang, T. T. K., Ismail, M. H., Kautz, A., Sarin, S. K., Loomba, R., Miller, V., … Zheng, M. H. (2022). Advancing the global public health agenda for NAFLD: a consensus statement. *Nature Reviews Gastroenterology and Hepatology*, *19*(1), 60–78. https://doi.org/10.1038/s41575-021-00523-4
56. Lee, Y. K., Park, J. E., Lee, M., & Hardwick, J. P. (2018). Hepatic lipid homeostasis by peroxisome proliferator-activated receptor gamma 2. *Liver Research*, *2*(4), 209–215. https://doi.org/10.1016/j.livres.2018.12.001
57. Levitt, M. D., & Levitt, D. G. (2020). Quantitative evaluation of d-lactate pathophysiology: new insights into the mechanisms involved and the many areas in need of further investigation. *Clinical and Experimental Gastroenterology*, *13*. 321–337. https://doi.org/10.2147/CEG.S260600
58. Li, B., Zhang, J., Chen, Y., Wang, Q., Yan, L., Wang, R., Wei, Y., You, Z., Li, Y., Miao, Q., Xiao, X., Lian, M., Chen, W., Qiu, D., Fang, J., Gershwin, M. E., Tang, R., & Ma, X. (2021). Alterations in microbiota and their metabolites are associated with beneficial effects of bile acid sequestrant on icteric primary biliary Cholangitis. *Gut Microbes*, *13*(1). https://doi.org/10.1080/19490976.2021.1946366
59. Li, H., Shi, J., Zhao, L., Guan, J., Liu, F., Huo, G., & Li, B. (2021). Lactobacillus plantarum KLDS1.0344 and Lactobacillus acidophilus KLDS1.0901 Mixture Prevents Chronic Alcoholic Liver Injury in Mice by Protecting the Intestinal Barrier and Regulating Gut Microbiota and Liver-Related Pathways. *Journal of Agricultural and Food Chemistry*, *69*(1), 183–197. https://doi.org/10.1021/acs.jafc.0c06346
60. Li, X., & Wang, H. (2020). Multiple organs involved in the pathogenesis of non-alcoholic fatty liver disease. *Cell and Bioscience*, *10*(1). https://doi.org/10.1186/s13578-020-00507-y
61. Linden, A. G., Li, S., Choi, H. Y., Fang, F., Fukasawa, M., Uyeda, K., Hammer, R. E., Horton, J. D., Engelking, L. J., & Liang, G. (2018). Interplay between ChREBP and SREBP-1c coordinates postprandial glycolysis and lipogenesis in livers of mice. *Journal of Lipid Research*, *59*(3), 475–487. https://doi.org/10.1194/jlr.M081836
62. Liu, Y., Beyer, A., & Aebersold, R. (2016). On the Dependency of Cellular Protein Levels on mRNA Abundance. *Cell*, *165*(3), 535–550. https://doi.org/10.1016/j.cell.2016.03.014
63. Liu, Y., Chen, K., Li, F., Gu, Z., Liu, Q., He, L., Shao, T., Song, Q., Zhu, F., Zhang, L., Jiang, M., Zhou, Y., Barve, S., Zhang, X., Mcclain, C. J., & Feng, W. (2020). Probiotic *Lactobacillus rhamnosus* GG Prevents Liver Fibrosis Through Inhibiting Hepatic Bile Acid Synthesis and Enhancing Bile Acid Excretion in Mice. *Hepatology*, *71*(6). https://doi.org/10.1002/hep.30975

64. Lu, Q., Tian, X., Wu, H., Huang, J., Li, M., Mei, Z., Zhou, L., Xie, H., & Zheng, S. (2021). Metabolic Changes of Hepatocytes in NAFLD. *Frontiers in Physiology*, *12*. https://doi.org/10.3389/fphys.2021.710420
65. Manosalva, C., Quiroga, J., Hidalgo, A. I., Alarcón, P., Anseoleaga, N., Hidalgo, M. A., & Burgos, R. A. (2022). Role of Lactate in Inflammatory Processes: Friend or Foe. *Frontiers in Immunology*, *12*. https://doi.org/10.3389/fimmu.2021.808799
66. Maude, H., Sanchez-Cabanillas, C., & Cebola, I. (2021). Epigenetics of Hepatic Insulin Resistance. *Frontiers in Endocrinology*, *12*. https://doi.org/10.3389/fendo.2021.681356
67. McLaren, D. G., Han, S., Murphy, B. A., Wilsie, L., Stout, S. J., Zhou, H., Roddy, T. P., Gorski, J. N., Metzger, D. E., Shin, M. K., Reilly, D. F., Zhou, H. H., Tadin-Strapps, M., Bartz, S. R., Cumiskey, A. M., Graham, T. H., Shen, D. M., Akinsanya, K. O., Previs, S. F., … Pinto, S. (2018). DGAT2 Inhibition Alters Aspects of Triglyceride Metabolism in Rodents but Not in Non-human Primates. *Cell Metabolism*, *27*(6), 1236-1248.e6. https://doi.org/10.1016/j.cmet.2018.04.004
68. Mesarwi, O. A., Shin, M. K., Bevans-Fonti, S., Schlesinger, C., Shaw, J., & Polotsky, V. Y. (2016). Hepatocyte hypoxia inducible factor-1 mediates the development of liver fibrosis in a mouse model of nonalcoholic fatty liver disease. *PLoS ONE*, *11*(12). https://doi.org/10.1371/journal.pone.0168572
69. Monroe, G. R., van Eerde, A. M., Tessadori, F., Duran, K. J., Savelberg, S. M. C., van Alfen, J. C., Terhal, P. A., van der Crabben, S. N., Lichtenbelt, K. D., Fuchs, S. A., Gerrits, J., van Roosmalen, M. J., van Gassen, K. L., van Aalderen, M., Koot, B. G., Oostendorp, M., Duran, M., Visser, G., de Koning, T. J., … Jans, J. J. (2019). Identification of human D lactate dehydrogenase deficiency. *Nature Communications*, *10*(1). https://doi.org/10.1038/s41467-019-09458-6
70. Mu, Q., Tavella, V. J., & Luo, X. M. (2018). Role of Lactobacillus reuteri in human health and diseases. *Frontiers in Microbiology*, *9*. https://doi.org/10.3389/fmicb.2018.00757
71. Nagaya, T., Tanaka, N., Suzuki, T., Sano, K., Horiuchi, A., Komatsu, M., Nakajima, T., Nishizawa, T., Joshita, S., Umemura, T., Ichijo, T., Matsumoto, A., Yoshizawa, K., Nakayama, J., Tanaka, E., & Aoyama, T. (2010). Down-regulation of SREBP-1c is associated with the development of burned-out NASH. *Journal of Hepatology*, *53*(4), 724–731. https://doi.org/10.1016/j.jhep.2010.04.033
72. Nair, B., & Nath, L. R. (2020). Inevitable role of TGF-β1 in progression of nonalcoholic fatty liver disease. *Journal of Receptors and Signal Transduction*, *40*(3), 195–200. https://doi.org/10.1080/10799893.2020.1726952
73. Oh, J. M., Choi, J. M., Lee, J. Y., Oh, S. J., Kim, H. C., Kim, B. H., Ma, J. Y., & Kim, S. K. (2012). Effects of palmitic acid on TNF-α-induced cytotoxicity in SK-Hep-1 cells. *Toxicology in Vitro*, *26*(6), 783–790. https://doi.org/10.1016/j.tiv.2012.05.013
74. Okubo, H., Kushiyama, A., Sakoda, H., Nakatsu, Y., Iizuka, M., Taki, N., Fujishiro, M., Fukushima, T., Kamata, H., Nagamachi, A., Inaba, T., Nishimura, F., Katagiri, H., Asahara, T., Yoshida, Y., Chonan, O., Encinas, J., & Asano, T. (2016). Involvement of resistin-like molecule β in the development of methionine-choline deficient diet-induced non-alcoholic steatohepatitis in mice. *Scientific Reports*, *6*. https://doi.org/10.1038/srep20157
75. Park, G., Jung, S., Wellen, K. E., & Jang, C. (2021). The interaction between the gut microbiota and dietary carbohydrates in nonalcoholic fatty liver disease. *Experimental and Molecular Medicine*, *53*(5), 809–822). https://doi.org/10.1038/s12276-021-00614-x

76. Parlati, L., Régnier, M., Guillou, H., & Postic, C. (2021). New targets for NAFLD. *JHEP Reports*, *3*(6). https://doi.org/10.1016/j.jhepr.2021.100346
77. Pettinelli, P., & Videla, L. A. (2011). Up-regulation of PPAR-γ mRNA expression in the liver of obese patients: An additional reinforcing lipogenic mechanism to SREBP-1c induction. *Journal of Clinical Endocrinology and Metabolism*, *96*(5), 1424–1430. https://doi.org/10.1210/jc.2010-2129
78. Pongratz, R. L., Kibbey, R. G., Shulman, G. I., & Cline, G. W. (2007). Cytosolic and mitochondrial malic enzyme isoforms differentially control insulin secretion. *Journal of Biological Chemistry*, *282*(1), 200–207. https://doi.org/10.1074/jbc.M602954200
79. Prins, G. H., Rios-Morales, M., Gerding, A., Reijngoud, D. J., Olinga, P., & Bakker, B. M. (2021). The effects of butyrate on induced metabolic-associated fatty liver disease in precision-cut liver slices. *Nutrients*, *13*(12), 4203. https://doi.org/10.3390/nu13124203
80. Prochownik, E. v., & Wang, H. (2021). Review the metabolic fates of pyruvate in normal and neoplastic cells. *Cells*, *10*(4). https://doi.org/10.3390/cells10040762
81. Rada, P., González-Rodríguez, Á., García-Monzón, C., & Valverde, Á. M. (2020). Understanding lipotoxicity in NAFLD pathogenesis: is CD36 a key driver? *Cell Death and Disease*, *11*(9). https://doi.org/10.1038/s41419-020-03003-w
82. Ranganathan, P., Shanmugam, A., Swafford, D., Suryawanshi, A., Bhattacharjee, P., Hussein, M. S., Koni, P. A., Prasad, P. D., Kurago, Z. B., Thangaraju, M., Ganapathy, V., & Manicassamy, S. (2018). GPR81, a Cell-Surface Receptor for Lactate, Regulates Intestinal Homeostasis and Protects Mice from Experimental Colitis. *The Journal of Immunology*, ji1700604. https://doi.org/10.4049/jimmunol.1700604
83. Ratter, J. M., Rooijackers, H. M. M., Hooiveld, G. J., Hijmans, A. G. M., de Galan, B. E., Tack, C. J., & Stienstra, R. (2018). In vitro and in vivo Effects of Lactate on Metabolism and Cytokine Production of Human Primary PBMCs and Monocytes. *Frontiers in Immunology*, *9*, 2564. https://doi.org/10.3389/fimmu.2018.02564
84. Ritze, Y., Bárdos, G., Claus, A., Ehrmann, V., Bergheim, I., Schwiertz, A., & Bischoff, S. C. (2014). Lactobacillus rhamnosus GG Protects against non-alcoholic fatty liver disease in mice. *PLoS ONE*, *9*(1), e80169. https://doi.org/10.1371/journal.pone.0080169
85. Sabnis, R. W. (2021). Novel Diacylglycerol Acetyltransferase 2 Inhibitors for Treating Liver Diseases. *ACS Medicinal Chemistry Letters*, *12*(7), 1073–1074. https://doi.org/10.1021/acsmedchemlett.1c00319
86. Safari, Z., & Gérard, P. (2019). The links between the gut microbiome and non-alcoholic fatty liver disease (NAFLD). *Cellular and Molecular Life Sciences*, *76*(8), 1541–1558. https://doi.org/10.1007/s00018-019-03011-w
87. Sakurai, Y., Kubota, N., Yamauchi, T., & Kadowaki, T. (2021). Role of insulin resistance in mafld. *International Journal of Molecular Sciences*, *22*(8), 4156. https://doi.org/10.3390/ijms22084156
88. Salminen, S., Collado, M. C., Endo, A., Hill, C., Lebeer, S., Quigley, E. M. M., Sanders, M. E., Shamir, R., Swann, J. R., Szajewska, H., & Vinderola, G. (2021). The International Scientific Association of Probiotics and Prebiotics (ISAPP) consensus statement on the definition and scope of postbiotics. *Nature Reviews Gastroenterology and Hepatology*, *18*(9), 649–667. https://doi.org/10.1038/s41575-021-00440-6
89. Santos, A. A., Afonso, M. B., Ramiro, R. S., Pires, D., Pimentel, M., Castro, R. E., & Rodrigues, C. M. P. (2020). Host miRNA-21 promotes liver dysfunction by targeting small intestinal *Lactobacillus* in mice. *Gut Microbes*, *12*(1), 1–18. https://doi.org/10.1080/19490976.2020.1840766

90. Scheijen, J. L. J. M., Hanssen, N. M. J., van de Waarenburg, M. P. H., Jonkers, D. M. A. E., Stehouwer, C. D. A., & Schalkwijk, C. G. (2012). L (+) and D (-) lactate are increased in plasma and urine samples of type 2 diabetes as measured by a simultaneous quantification of L (+) and D (-) lactate by reversed-phase liquid chromatography tandem mass spectrometry. *Experimental Diabetes Research*, *2012*, 1-10. https://doi.org/10.1155/2012/234812
91. Schulman, I. G. (2017). Liver X receptors link lipid metabolism and inflammation. *FEBS Letters*, *591*(19), 2978–2991). Wiley Blackwell. https://doi.org/10.1002/1873-3468.12702
92. Schulthess, J., Pandey, S., Capitani, M., Rue-Albrecht, K. C., Arnold, I., Franchini, F., Chomka, A., Ilott, N. E., Johnston, D. G. W., Pires, E., McCullagh, J., Sansom, S. N., Arancibia-Cárcamo, C. v., Uhlig, H. H., & Powrie, F. (2019). The Short Chain Fatty Acid Butyrate Imprints an Antimicrobial Program in Macrophages. *Immunity*, *50*(2), 432-445. https://doi.org/10.1016/j.immuni.2018.12.018
93. Seo, S. U., Kamada, N., Muñoz-Planillo, R., Kim, Y. G., Kim, D., Koizumi, Y., Hasegawa, M., Himpsl, S. D., Browne, H. P., Lawley, T. D., Mobley, H. L. T., Inohara, N., & Núñez, G. (2015). Distinct Commensals Induce Interleukin-1β via NLRP3 Inflammasome in Inflammatory Monocytes to Promote Intestinal Inflammation in Response to Injury. *Immunity*, *42*(4), 744–755. https://doi.org/10.1016/j.immuni.2015.03.004
94. Sharpton, S. R., Schnabl, B., Knight, R., & Loomba, R. (2021). Current Concepts, Opportunities, and Challenges of Gut Microbiome-Based Personalized Medicine in Nonalcoholic Fatty Liver Disease. *Cell Metabolism*, *33*(1), 21–32. https://doi.org/10.1016/j.cmet.2020.11.010
95. Sheridan, P. O., Louis, P., Tsompanidou, E., Shaw, S., Harmsen, H. J., Duncan, S. H., Flint, H. J., & Walker, A. W. (2022). Distribution, organization and expression of genes concerned with anaerobic lactate utilization in human intestinal bacteria. *Microbial Genomics*, *8*(1). https://doi.org/10.1099/mgen.0.000739
96. Shin, E., Bae, J. S., Han, J. Y., Lee, J., Jeong, Y. S., Lee, H. J., Ahn, Y. H., & Cha, J. Y. (2016). Hepatic DGAT2 gene expression is regulated by the synergistic action of ChREBP and SP1 in HepG2 cells. *Animal Cells and Systems*, *20*(1), 7–14. https://doi.org/10.1080/19768354.2015.1131738
97. Suez, J., Zmora, N., Segal, E., & Elinav, E. (2019). The pros, cons, and many unknowns of probiotics. *Nature Medicine*, *25*(5), 716–729. https://doi.org/10.1038/s41591-019-0439-x
98. Thoo, L., Noti, M., & Krebs, P. (2019). Keep calm: the intestinal barrier at the interface of peace and war. *Cell Death and Disease*, *10*(11). https://doi.org/10.1038/s41419-019-2086-z
99. Tiegs, G., & Horst, A. K. (2022). TNF in the liver: targeting a central player in inflammation. *Seminars in Immunopathology*, *44*(4), 445-459. https://doi.org/10.1007/s00281-022-00910-2
100. Tran, S., Baba, I., Poupel, L., Dussaud, S., Moreau, M., Gélineau, A., Marcelin, G., Magréau-Davy, E., Ouhachi, M., Lesnik, P., Boissonnas, A., le Goff, W., Clausen, B. E., Yvan-Charvet, L., Sennlaub, F., Huby, T., & Gautier, E. L. (2020). Impaired Kupffer Cell Self-Renewal Alters the Liver Response to Lipid Overload during Non-alcoholic Steatohepatitis. *Immunity*, *53*(3), 627-640.https://doi.org/10.1016/j.immuni.2020.06.003

101. Trefts, E., Gannon, M., & Wasserman, D. H. (2017). The liver. *Current Biology*, *27*(21), R1147–R1151. https://doi.org/10.1016/j.cub.2017.09.019
102. Tripathi, A., Debelius, J., Brenner, D. A., Karin, M., Loomba, R., Schnabl, B., & Knight, R. (2018). The gut-liver axis and the intersection with the microbiome. *Nature Reviews Gastroenterology and Hepatology*, *15*(7), 397–411. https://doi.org/10.1038/s41575-018-0011-z
103. Troisi, J., Cavallo, P., Colucci, A., Pierri, L., Scala, G., Symes, S., Jones, C., & Richards, S. (2020). Metabolomics in genetic testing. *Advances in Clinical Chemistry*, *94*, 85–153.https://doi.org/10.1016/bs.acc.2019.07.009
104. Vancamelbeke, M., & Vermeire, S. (2017). The intestinal barrier: a fundamental role in health and disease. *Expert Review of Gastroenterology and Hepatology*, *11*(9), 821–834. https://doi.org/10.1080/17474124.2017.1343143
105. Vitetta, L., Coulson, S., Thomsen, M., Nguyen, T., & Hall, S. (2017). Probiotics, D–Lactic acidosis, oxidative stress and strain specificity. *Gut Microbes*, *8*(4), 311–322. https://doi.org/10.1080/19490976.2017.1279379
106. Wallace, S. J., Tacke, F., Schwabe, R. F., & Henderson, N. C. (2022). Understanding the cellular interactome of non-alcoholic fatty liver disease. *JHEP Reports*, *4*(8), 100524. https://doi.org/10.1016/j.jhepr.2022.100524
107. Wang, H., Mehal, W., Nagy, L. E., & Rotman, Y. (2021). Immunological mechanisms and therapeutic targets of fatty liver diseases. *Cellular and Molecular Immunology*, *18*(1), 73–91. https://doi.org/10.1038/s41423-020-00579-3
108. Wang, J., Chen, W. D., & Wang, Y. D. (2020). The Relationship Between Gut Microbiota and Inflammatory Diseases: The Role of Macrophages. *Frontiers in Microbiology*, *11*. https://doi.org/10.3389/fmicb.2020.01065
109. Wang, K., Liao, M., Zhou, N., Bao, L., Ma, K., Zheng, Z., Wang, Y., Liu, C., Wang, W., Wang, J., Liu, S. J., & Liu, H. (2019). *Parabacteroides distasonis* Alleviates Obesity and Metabolic Dysfunctions via Production of Succinate and Secondary Bile Acids. *Cell Reports*, *26*(1), 222-235. https://doi.org/10.1016/j.celrep.2018.12.028
110. Wang, R., Tang, R., Li, B., Ma, X., Schnabl, B., & Tilg, H. (2021). Gut microbiome, liver immunology, and liver diseases. *Cellular and Molecular Immunology*, *18*(1), 4–17. https://doi.org/10.1038/s41423-020-00592-6
111. Wang, T., & Ma, C. (2021). The hepatic macrophage pool in NASH. In *Cellular and Molecular Immunology*, *18*(8), 2059–2060.https://doi.org/10.1038/s41423-021-00690-z
112. Wculek, S. K., Dunphy, G., Heras-Murillo, I., Mastrangelo, A., & Sancho, D. (2021). Metabolism of tissue macrophages in homeostasis and pathology. *Cellular & Molecular Immunology*. 1-25. https://doi.org/10.1038/s41423-021-00791-9
113. Wu, J., Wang, K., Wang, X., Pang, Y., & Jiang, C. (2021). The role of the gut microbiome and its metabolites in metabolic diseases. *Protein and Cell*, *12*(5), 360–373. https://doi.org/10.1007/s13238-020-00814-7
114. Wu, K., Yuan, Y., Yu, H., Dai, X., Wang, S., Sun, Z., Wang, F., Fei, H., Lin, Q., Jiang, H., & Chen, T. (2020). The gut microbial metabolite trimethylamine N-oxide aggravates GVHD by inducing M1 macrophage polarization in mice. *Blood*, *136*(4), 501-515. https://doi.org/10.1182/blood.2019003990
115. Xu, X., Sun, S., Liang, L., Lou, C., He, Q., Ran, M., Zhang, L., Zhang, J., Yan, C., Yuan, H., Zhou, L., Chen, X., Dai, X., Wang, B., Zhang, J., & Zhao, J. (2021). Role of the Aryl Hydrocarbon Receptor and Gut Microbiota-Derived Metabolites Indole-3-

Acetic Acid in Sulforaphane Alleviates Hepatic Steatosis in Mice. *Frontiers in Nutrition*, *8*. https://doi.org/10.3389/fnut.2021.756565

116. Yan, J., & Horng, T. (2020). Lipid Metabolism in Regulation of Macrophage Functions. *Trends in Cell Biology*, *30*(12), 979–989. https://doi.org/10.1016/j.tcb.2020.09.006
117. Yan, R., Wang, K., Wang, Q., Jiang, H., Lu, Y., Chen, X., Zhang, H., Su, X., Du, Y., Chen, L., Li, L., & Lv, L. (2021). Probiotic *Lactobacillus casei Shirota* prevents acute liver injury by reshaping the gut microbiota to alleviate excessive inflammation and metabolic disorders. *Microbial Biotechnology*, 15(1), 247–261. https://doi.org/10.1111/1751-7915.13750
118. Yang, J. D., Hainaut, P., Gores, G. J., Amadou, A., Plymoth, A., & Roberts, L. R. (2019). A global view of hepatocellular carcinoma: trends, risk, prevention and management. *Nature Reviews Gastroenterology and Hepatology*, *16*(10), 589–604. https://doi.org/10.1038/s41575-019-0186-y
119. Yang, M., Khoukaz, L., Qi, X., Kimchi, E. T., Staveley-O'Carroll, K. F., & Li, G. (2021). Diet and Gut Microbiota Interaction-Derived Metabolites and Intrahepatic Immune Response in NAFLD Development and Treatment. *Biomedicines*, *9*(12), 1893. https://doi.org/10.3390/biomedicines9121893
120. Yao, L., Wang, C., Zhang, X., Peng, L., Liu, W., Zhang, X., Liu, Y., He, J., Jiang, C., Ai, D., & Zhu, Y. (2016). Hyperhomocysteinemia Activates the Aryl Hydrocarbon Receptor/CD36 Pathway to Promote Hepatic Steatosis in Mice. *Hepatology*, *64*(1), 92-105. https://doi.org/10.1002/hep.28518
121. Yao, M., Qv, L., Lu, Y., Wang, B., Berglund, B., & Li, L. (2021). An Update on the Efficacy and Functionality of Probiotics for the Treatment of Non-Alcoholic Fatty Liver Disease. *Engineering*. https://doi.org/10.1016/j.eng.2020.01.017
122. Yoon, Y., Kim, G., Noh, M. giun, Park, J. hyeon, Jang, M., Fang, S., & Park, H. (2020). *Lactobacillus fermentum* promotes adipose tissue oxidative phosphorylation to protect against diet-induced obesity. *Experimental and Molecular Medicine*, *52*(9), 1574–1586. https://doi.org/10.1038/s12276-020-00502-w
123. Yoshimura, Y., Araki, A., Maruta, H., Takahashi, Y., & Yamashita, H. (2017). Molecular cloning of rat acss3 and characterization of mammalian propionyl-CoA synthetase in the liver mitochondrial matrix. *Journal of Biochemistry*, *161*(3), 279–289. https://doi.org/10.1093/jb/mvw067
124. Younossi, Z. M., Tampi, R., Priyadarshini, M., Nader, F., Younossi, I. M., & Racila, A. (2019). Burden of Illness and Economic Model for Patients with Nonalcoholic Steatohepatitis in the United States. *Hepatology*, *69*(2), 564–572. https://doi.org/10.1002/hep.30254
125. Zhang, D., Tang, Z., Huang, H., Zhou, G., Cui, C., Weng, Y., Liu, W., Kim, S., Lee, S., Perez-Neut, M., Ding, J., Czyz, D., Hu, R., Ye, Z., He, M., Zheng, Y. G., Shuman, H. A., Dai, L., Ren, B., … Zhao, Y. (2019). Metabolic regulation of gene expression by histone lactylation. *Nature*, *574*(7779), 575–580. https://doi.org/10.1038/s41586-019-1678-1
126. Zhang, M., Zhao, Y., Li, Z., & Wang, C. (2018). Pyruvate dehydrogenase kinase 4 mediates lipogenesis and contributes to the pathogenesis of nonalcoholic steatohepatitis. *Biochemical and Biophysical Research Communications*, *495*(1), 582–586. https://doi.org/10.1016/j.bbrc.2017.11.054
127. Zhang, X., Coker, O. O., Chu, E. S. H., Fu, K., Lau, H. C. H., Wang, Y. X., Chan, A. W. H., Wei, H., Yang, X., Sung, J. J. Y., & Yu, J. (2021). Dietary cholesterol drives fatty

liver-associated liver cancer by modulating gut microbiota and metabolites. *Gut*, *70*(4), 761–774. https://doi.org/10.1136/gutjnl-2019-319664

128. Zhao, S., Jang, C., Liu, J., Uehara, K., Gilbert, M., Izzo, L., Zeng, X., Trefely, S., Fernandez, S., Carrer, A., Miller, K. D., Schug, Z. T., Snyder, N. W., Gade, T. P., Titchenell, P. M., Rabinowitz, J. D., & Wellen, K. E. (2020). Dietary fructose feeds hepatic lipogenesis via microbiota-derived acetate. *Nature*, *579*(7800), 586–591. https://doi.org/10.1038/s41586-020-2101-7
129. Zhao, Y., Tran, M., Wang, L., Shin, D.-J., & Wu, J. (2020). PDK4-Deficiency Reprograms Intrahepatic Glucose and Lipid Metabolism to Facilitate Liver Regeneration in Mice. *Hepatology Communications*, *4*(4), 504.517. https://doi.org/10.1002/hep4.1484
130. Zhao, Z. H., Wang, Z. X., Zhou, D., Han, Y., Ma, F., Hu, Z., Xin, F. Z., Liu, X. L., Ren, T. Y., Zhang, F., Xue, Y., Cui, A., Liu, Z., Bai, J., Liu, Y., Cai, G., Su, W., Dai, X., Shen, F., … Fan, J. G. (2021). Sodium Butyrate Supplementation Inhibits Hepatic Steatosis by Stimulating Liver Kinase B1 and Insulin-Induced Gene. *CMGH*, *12*(3), 857–871. https://doi.org/10.1016/j.jcmgh.2021.05.006
131. Zheng, D., Liwinski, T., & Elinav, E. (2020). Interaction between microbiota and immunity in health and disease. *Cell Research*, *30*(6), 492–506. https://doi.org/10.1038/s41422-020-0332-7
132. Zhou, D., Chen, Y. W., Zhao, Z. H., Yang, R. X., Xin, F. Z., Liu, X. L., Pan, Q., Zhou, H., & Fan, J. G. (2018). Sodium butyrate reduces high-fat diet-induced non-alcoholic steatohepatitis through upregulation of hepatic GLP-1R expression. *Experimental and Molecular Medicine*, *50*(12), 157. https://doi.org/10.1038/s12276-018-0183-1
133. Zhou, D., Pan, Q., Xin, F. Z., Zhang, R. N., He, C. X., Chen, G. Y., Liu, C., Chen, Y. W., & Fan, J. G. (2017). Sodium butyrate attenuates high-fat diet-induced steatohepatitis in mice by improving gut microbiota and gastrointestinal barrier. *World Journal of Gastroenterology*, *23*(1), 60–75. https://doi.org/10.3748/wjg.v23.i1.60
134. Zhou, H. cun, Yan, X. yan Y., Yu, W. wen, Liang, X. qin, Du, X. yan, Liu, Z. chang, Long, J. ping, Zhao, G. hui, & Liu, H. bin. (2022). Lactic acid in macrophage polarization: The significant role in inflammation and cancer. *International Reviews of Immunology*, 41(1), 4–18. https://doi.org/10.1080/08830185.2021.1955876
135. Zhou, H., Du, W., Li, Y., Shi, C., Hu, N., Ma, S., Wang, W., & Ren, J. (2018). Effects of melatonin on fatty liver disease: The role of NR4A1/DNA-PKcs/p53 pathway, mitochondrial fission, and mitophagy. *Journal of Pineal Research*, *64*(1). https://doi.org/10.1111/jpi.12450
136. Zhu, Y., Han, X. Q., Sun, X. J., Yang, R., Ma, W. Q., & Liu, N. F. (2020). Lactate accelerates vascular calcification through NR4A1-regulated mitochondrial fission and BNIP3-related mitophagy. *Apoptosis*, *25*(5–6), 321–340. https://doi.org/10.1007/s10495-020-01592-7

8 Annexes

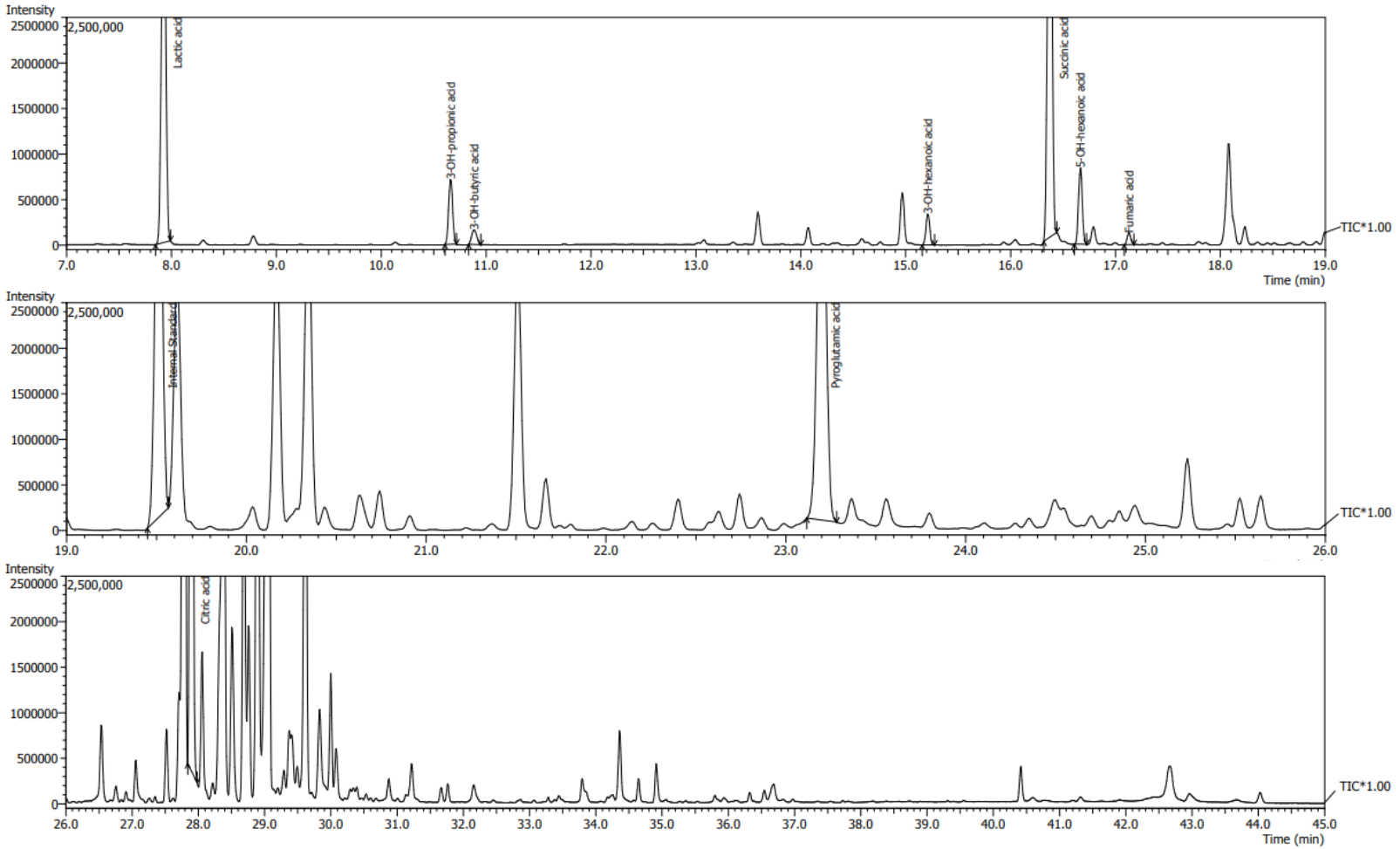

1a. Chromatogram of MRS broth (control). Time course of the detection of culture medium metabolites (control) derived from incubation for 48h at 37°C, detected by GC-MS. The X-Axis shows the retention time and the Y-Axis the intensity counts.

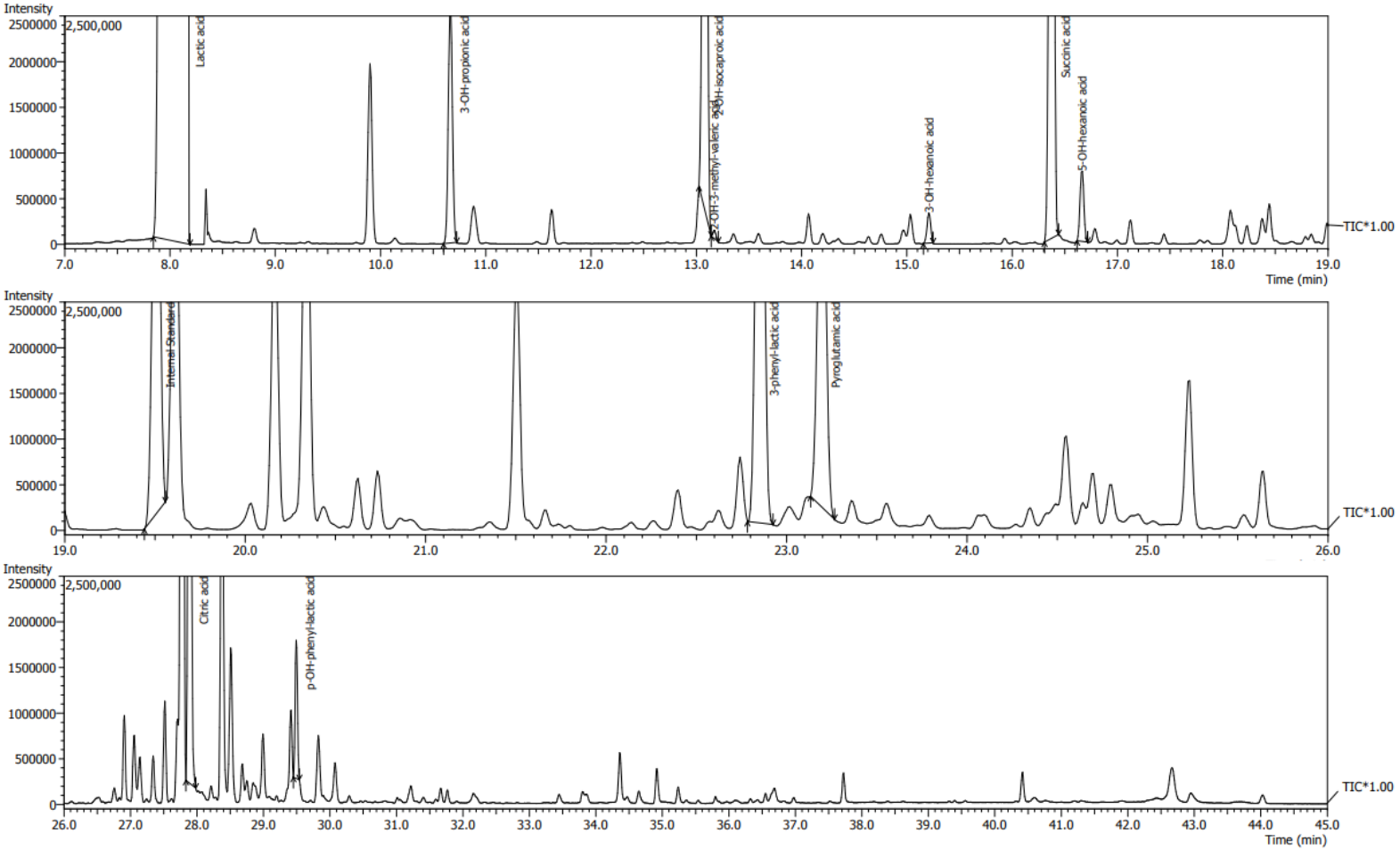

1b. Chromatogram of *L. reuteri* ATCC 6475 supernatant. Time course of the detection of *L. reuteri* ATCC 6475 metabolites (control) derived from incubation for 48h at 37°C, detected by GC-MS. The X-Axis shows the retention time and the Y-Axis the intensity counts.

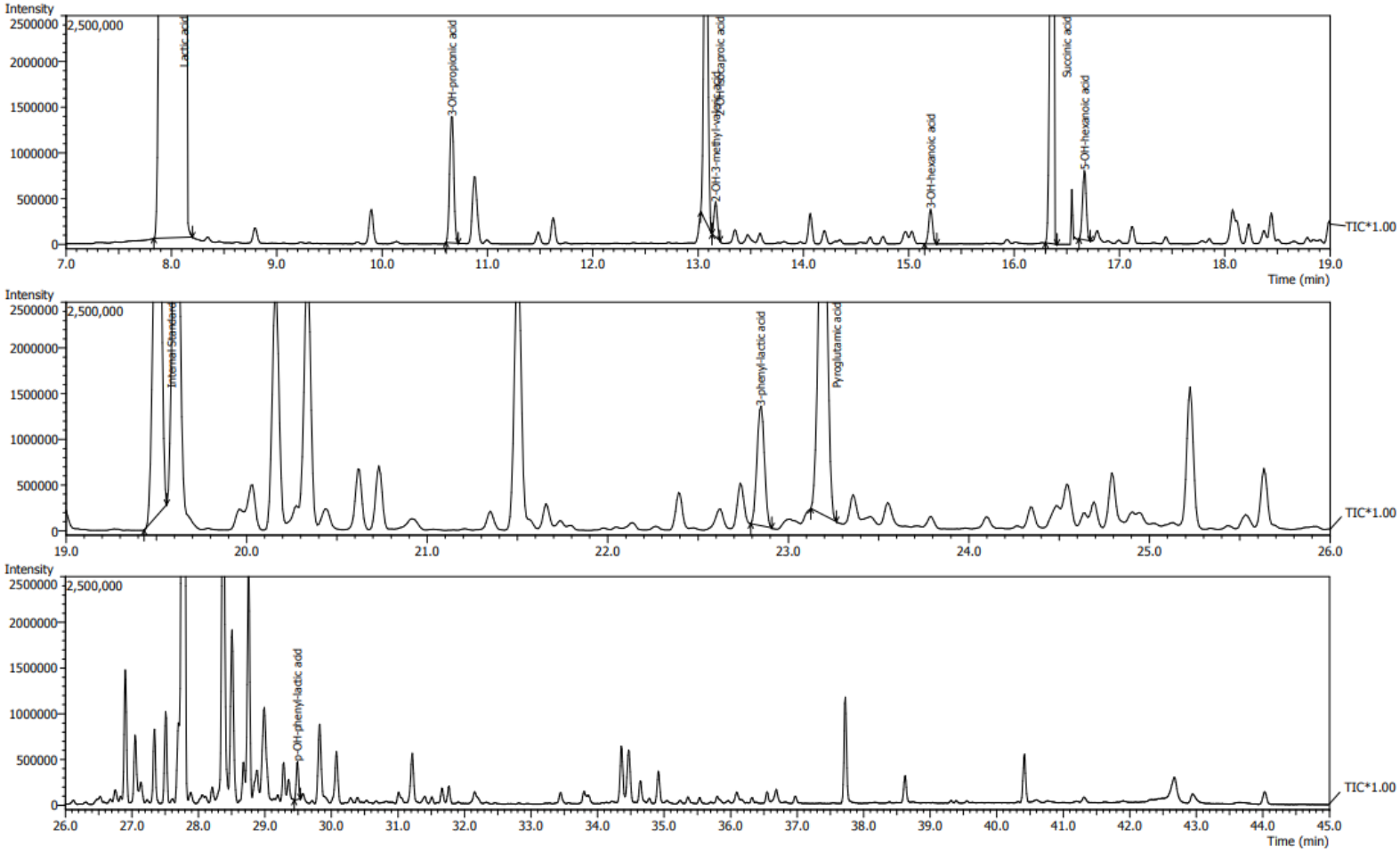

1c. Chromatogram of *L. reuteri* DSM 17938 supernatant. Time course of the detection of Apoptoses *L. reuteri* DSM 17938 metabolites (control) derived from incubation for 48h at 37°C, detected by GC-MS. The X-Axis shows the retention time and the Y-Axis the intensity counts.

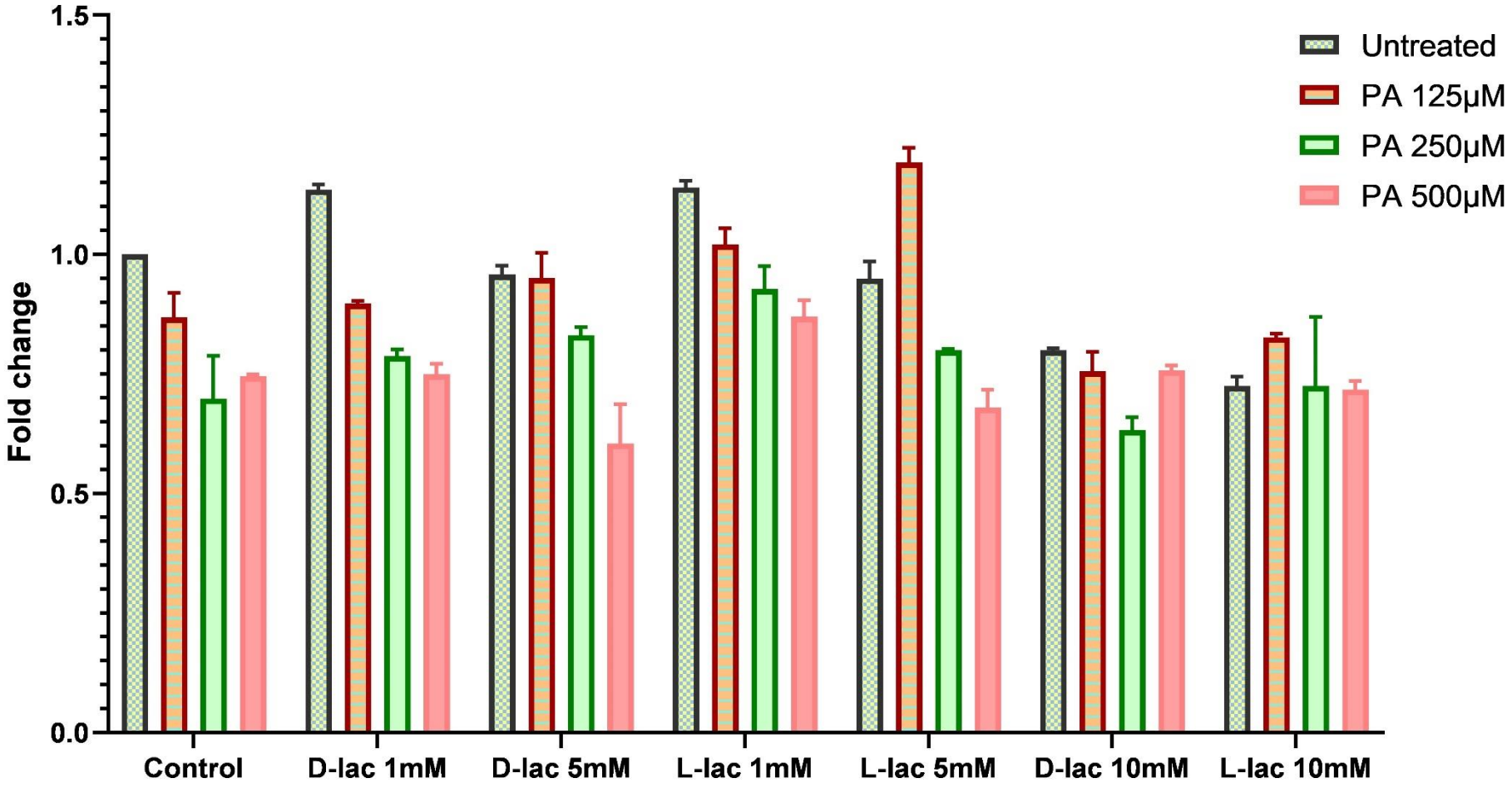

1d. MTS assay. Hepatocytes subjected to D- or L-lactate 1, 5 or 10mM and palmitic acid (PA) 125, 250 and 500µM for 24h, after 48h of confluency. For the assay were performed 4 individual experiments.